

https://dspace.org/

Recombinant production and activity assessment of growth stimulatory proteins in the resuscitation of mycobacterium tuberculosis

Campbell, Lisa

2020
https://hdl.handle.net/10539/29996

Downloaded from a DSpace repository. https://dspace.org/

Recombinant production and activity assessment of growth stimulatory proteins in the resuscitation of *Mycobacterium tuberculosis*



Lisa Campbell

(808632)

Supervisors: Prof Bavesh Kana & Dr Julian Peters

A dissertation submitted to the Faculty of Health Sciences, University of the Witwatersrand, Johannesburg, in fulfilment of the degree of Master of Science in Medicine
March 2020

Declaration

I, Lisa Campbell, declare that this dissertation is my own unaided work. It is being submitted for the degree of Maser of Science in Medicine at the University of the Witwatersrand, Johannesburg. It has not been submitted before for any degree or examination at any other university.



03 June 2020

Presentations arising from this study

Campbell, L, Peters, J & Kana, B. Recombinant RipA and RpfB proteins enhance the time to detection of model *Mycobacterium tuberculosis*. Oral presentation at the Molecular Biosciences Trust Postgraduate Research Day, 28 November 2019.

Abstract

Mycobacterium tuberculosis (*Mtb*) is able to enter a non-culturable, dormant-like, state under stressful conditions to evade eradication. When growth permissive conditions resume, *Mtb* can exit this non-culturable state and resume active replication. Non-culturable populations are of great interest in clinical settings as they can contribute to misdiagnoses and inaccurate treatment monitoring. Resuscitation promoting factors (Rpfs) have been implicated as stimulatory growth factors for resuscitation from the non-culturable state, together with their interacting partner, Rpf-interacting protein A (RipA). In this study the resuscitation capabilities of Resuscitation promoting factor B (RpfB) and RipA against *Mtb* were evaluated. The catalytic regions of RipA and RpfB were expressed and purified and their muralytic activity was assesed using four protein activity assays. The resuscitation capabilities of RipA and RpfB in Mycobacterial growth indicator tube (MGIT) assays was evaluated using carbon starvation-derived non-culturable *Mtb* from the laboratory strain (H37Rv). It was observed that RipA and RpfB supplementation was able to stimulate the resuscitation of non-culturable, carbon-starved H37Rv, significantly decreasing its time-to-positivity (TTP) in MGIT assays compared to un-supplemented MGIT media. Upon investigating clinical strains of *Mtb*, no significant reduction in TTP of non-culturable, carbon-starved Beijing and LAM isolates was reported. Supplementation of RipA and RpfB in MGIT assays to improve the detection of clinical isolates of *Mtb* and enhance their TTP was evaluated using a South African cohort of 30 sputum specimens. Overall RipA and RpfB supplementation yielded no significant improvements to MGIT TTP, regardless of initial colony forming units, patient gender, immunology or diagnostic data; however, 20% of individual specimens did benefit from the supplementation, yielding improved TTP when compared to un-supplemented MGITs. No significant adverse effects were observed during supplementation and given the positive yield in some specimens, it is suggested that the addition of RipA and RpfB could improve the detection of *Mtb* in clinical specimens.

Acknowledgments

I would like to thank my supervisors, Prof Bavesh Kana and Dr Julian Peters, and the CBTBR team for their support and guidance throughout this project.

My thanks to the funding bodies, the University of the Witwatersrand, the National Research Foundation and the German Academic Exchange Service (DAAD) for their contributions and financial support throughout this research.

Finally, to my family and friends, the sincerest thank you will not suffice in expressing my gratitude for the support and patience during these last 2 years. You have my appreciation and love always.

Table of Contents

Declaration i

Presentations arising from this study ii

Abstract iii

Acknowledgments iv

Table of Contents v

List of Figures x

List of Tables xii

1. Introduction 1

1.1. Tuberculosis 1

1.1.1. The global epidemic 1

1.1.2. Drug treatment 1

1.1.3. Vaccination 2

1.1.4. Drug resistant TB 2

1.2. TB Pathogenesis 3

1.2.1. Transmission and immune pathogenesis 3

1.2.2. Outcomes of TB transmission 4

1.2.2.1. Active TB disease 4

1.2.2.2. Elimination 6

1.2.2.3. Latent TB infection 6

1.2.2.4. Incipient TB 7

1.2.2.5. Subclinical TB 7

1.3. Detection and Diagnosis 7

1.3.1. Detection of active TB 7

1.3.1.1. Smear microscopy 8

1.3.1.2. Culture 8

1.3.1.3. Molecular tools 9

1.3.2. Detection of latent TB....10
1.4. Bacterial culturability, persistence and resuscitation....10
1.4.1. Different culturable states....10
1.4.2. Differentially culturable tubercle bacilli (DCTB)....12
1.5. Resuscitation promoting factors and their interacting partners....13
1.6. The knowledge gap....15
2. Methods....17
2.1. Strains and culturing conditions....17
2.2. DNA extraction and clean up....18
2.2.1. Plasmid mini-prep – QIAprep Miniprep kit....18
2.2.2. Plasmid maxi-prep – Nucelobond Xtra Maxi kit....18
2.2.3. Ethanol precipitation....19
2.3. Restriction digests....20
2.4. Nucleic acid quantification and visualisation....20
2.4.1. Nanodrop quantification of nucleic acids (and protein)....20
2.4.2. Agarose gel electrophoresis....20
2.5. Transformation of *E. coli* – Calcium chloride method....20
2.6. Protein expression and extraction....21
2.6.1. Protein Induction....21
2.6.2. Small scale protein extraction – Bacterial Protein Extraction Reagent (B-PER)....21
2.6.3. Cell lysis by French press....22
2.6.4. Tag removal – TEV-digestion....22
2.6.5. Dialysis buffer exchange....22
2.6.6. Small scale protein purification – Zymo His-Ppin Protein Mini Prep Kit....22
2.6.7. Small scale protein purification – Qiagen Ni-NTA Spin kit....23
2.6.8. Small scale protein purification – His-Select Nickel Affinity Gel....23
2.6.9. Large scale protein purification – His-Select Nickle Affinity Gel....24

2.6.10. High salt wash 25
2.6.11. Sodium dodecyl sulphate-polyacrylamide electrophoresis gels (SDS-PAGE) 25
2.6.12. SDS-PAGE gel visualisation – Coomasie R250 staining 26
2.6.13. Western blot – Biorad Transblot system 27
2.7. Protein activity assays 27
2.7.1. MUF-triNAG activity assay 27
2.7.2. FITC activity assay 28
2.7.2.1. *M. smegmatis* peptidoglycan extraction 28
2.7.2.2. Peptidoglycan labelling with FITC 28
2.7.2.3. FITC-Peptidoglycan cleavage assay 29
2.7.3. Remazol brilliant blue dye release assay 29
2.7.3.1. Cell wall labelling with remazol brilliant blue dye 29
2.7.3.2. Remazol brilliant blue-cell wall cleavage assay 29
2.7.4. Zymography 29
2.8. Carbon starvation assay 30
2.9. *In vitro* resuscitation assays 30
2.9.1. Most-probable number assays (MPN assays) 30
2.9.2. Colony forming units assay (CFU assays) 31
2.9.3. Mycobacterial growth indicator tube assays (MGIT assays) 31
2.9.3.1. Media supplementation of MGIT cultures 31
2.10. Ethical considerations 32
3. Results 33
3.1. Confirmation of the pETM20_RipA$_{332-472}$ and pETM11_RpfB$_{280-362}$ vectors 33
3.2. Confirmation of the presence of His-affinity tags 33
3.2.1. Western blots to confirm the presence of His-affinity tags 33
3.2.2. Small scale purification using the His-affinity tags 36
3.3. Optimization of the conditions for RipA expression and purification 36

3.3.1. pH optimization 36
3.3.2. Imidazole optimization 39
3.3.3. Small scale RipA purification at the optimised conditions 40
3.4. Batch expression of RipA 41
3.4.1. Purification binding at pH 7.6 and eluting at pH 8.6 41
3.4.2. Salt wash to remove non-specific binding proteins and aggregates 42
3.4.3. Affinity tag removal 42
3.4.4. Purification of tagless-RipA 43
3.5. Optimization of the conditions for RpfB protein expression and purification 44
3.5.1. pH optimisation 44
3.5.2. Imidazole optimization 45
3.5.3. Small scale RpfB purification at the optimised conditions 46
3.6. Batch expression of RpfB 48
3.6.1. Purification binding and eluting at pH 8.0 48
3.6.2. Salt wash to remove non-specific binding proteins and aggregates 49
3.6.3. Affinity tag removal 49
3.6.4. Purification of tagless RpfB 50
3.7. Protein activity assays 51
3.7.1. MUF-triNAG assay 51
3.7.2. FITC assay 52
3.7.3. Remazol brilliant blue dye release assay 54
3.7.4. Zymography 54
3.8. *In vitro* assays 56
3.8.1. Resuscitation of starved H37Rv in liquid media with recombinant RipA and RpfB 56
3.8.2. Resuscitation of starved H37Rv on solid media with recombinant RipA and RpfB 57
3.8.3. Resuscitation of starved H37RV, Beijing and LAM strains with recombinant RipA and RpfB 57

3.8.4. Resuscitation of clinical *Mtb* strains with recombinant RipA and RpfB.....58

4. Discussion.....63

4.1. Conclusion 69

5. Supplementary Figures.....70

Appendix A: Ethics clearance certificate.....75

6. References 76

List of Figures

Figure 1.1. The spectrum of clinical TB presentations.

Figure 1.2. The spectrum of culturability.

Figure 1.3. RipA and RpfB are lytic enzymes which act on the peptidoglycan layer of the bacterial cell wall.

Figure 3.1. Confirmation of pETM20_RipA332-472 and pETM11_RpfB280-362 vectors by restriction digest.

Figure 3.2. Time-course induction of his-tagged RipA (25 kDa) and his-tagged RpfB (12 kDa) protein expression.

Figure 3.3. The small-scale purification of his-tagged RipA and his-tagged RpfB from the soluble lysate of RipA and RpfB strains.

Figure 3.4. The pH optimisation of tagged-RipA purification on his-select nickel affinity gel.

Figure 3.5. Imidazole concentration optimization for his tagged-RipA purification on his-select nickel affinity gel.

Figure 3.6. Small scale purification if his-tagged RipA on his-select nickel affinity gel at optimal pH and imidazole concentration.

Figure 3.7. Batch purification of his-tagged RipA on his-select nickel affinity gel, binding at pH 7.6 and eluting at pH 8.6.

Figure 3.8. High salt wash of his-tagged RipA purification elutions to minimise non-specific binding proteins and aggregates

Figure 3.9. Time course digestion of his-tagged RipA by TEV protease at 37°C for the removal of the TxA-His tag.

Figure 3.10. The purification of tagless-RipA on his-select nickel affinity gel.

Figure 3.11. The pH optimisation of tagged-RpfB purification on his-select nickel affinity gel.

Figure 3.12. Imidazole concentration optimization for tagged-RpfB purification on his-select nickel affinity gel.

Figure 3.13. Small scale purification of his-tagged RpfB on his-select nickel affinity gel at optimal pH and imidazole concentration.

Figure 3.14. Batch purification of his-tagged RpfB on his-select nickel affinity gel, binding and eluting at pH 8.0.

Figure 3.15. High salt wash of his-tagged RpfB purification elutions to minimise non-specific binding proteins and aggregates.

Figure 3.16. Time course digestion of his-tagged RipA by TEV protease at 37°C for the removal of the his-tag.
Figure 3.17. The purification of tagless-RpfB on his-select nickel affinity gel.
Figure 3.18. MUF-triNAG assay was inconclusive in establishing recombinant RipA and RpfB muralytic activity.
Figure 3.19. Recombinant RipA and RpfB synergistic muralytic activity was established by FITC assay.
Figure 3.20. Recombinant RipA and RpfB display antagonistic muralytic activity in the remazol brilliant blue protein activity assay.
Figure 3.21. Zymogram demonstrating the lytic activity of recombinant RipA.
Figure 3.22. Supplementation of recombinant RipA and RpfB to MGIT cultures increased the time to positivity of starved H37Rv.
Figure 3.23. Supplementation of recombinant RipA and RpfB did not increase the number of resuscitated H37Rv bacilli on solid media.
Figure 3.24. Improved resuscitation of carbon-starved *Mtb* in MGIT assays with recombinant RipA and RpfB supplementation is strain dependent.
Figure 3.25. Supplementation of recombinant RipA and RpfB to MGIT cultures had no significant effect on the time to positivity of clinical isolates of *Mtb*.
Figure 3.26. Supplementation of MGIT assays with recombinant RipA and RpfB had no significant effect on MGIT time-to-positivity regardless of specimen demographics, immunology and diagnostic data.

List of Tables

Table 1. Culturing conditions for the various strain types utilised in this study

Table 2. List of strain used in this study

Table 3. SDS-PAGE gel recipes for two gels

Table 4. The demographics, immunology and original diagnostic data of the 30 clinical specimens utilised in this study, categorised by HIV status and CD4 cell count.

1. Introduction

1.1. Tuberculosis

1.1.1. The global epidemic

Tuberculosis (TB), caused by members of the *Mycobacterium tuberculosis* complex (MTBC), is a leading cause of death from a single infectious agent worldwide, claiming approximately 1.45 million lives in 2018 alone (WHO, 2019a). The TB epidemic is most rampant across Southeast Asia, Africa and the Western Pacific, where more than 50 % of the estimated 10 million total global incidence cases are found (WHO, 2019a). South Africa is particularly severely affected with approximately 300 000 incidence cases being reported in 2018 (WHO, 2019a). A significant gap is seen between the number of estimated incidences of TB and the number of reported cases, which has been attributed to underreporting of cases, as well as misdiagnosis. The control of TB infections is hindered by many factors, including complex clinical presentations, delayed diagnosis, poor treatment adherence and drug resistance (Millet *et al.*, 2013). It is currently believed that TB is grossly under-diagnosed and massive efforts from the stop-TB partnerships, as well as the WHO, are being directed towards finding the missing cases. Bacteriological confirmation of diagnosed TB is an important aim for the control of TB disease as it guarantees accurate diagnosis and simultaneously confirms phenotypic drug susceptibility, by so doing ensuring the start of effective treatment regimens. The increasing emergence of drug resistant TB and the continually spreading global epidemic has created a need for new treatment strategies as well as faster and more accurate diagnostic tools for diagnosis and treatment monitoring.

1.1.2. Drug treatment

Treatment of TB is complex and dependent on bacteriological results of drug resistance. Drug susceptible TB is treated through a six month first-line treatment regimen. This regimen consists of a combination therapy approach of four drugs for the first two months, which include rifampicin (RIF), isoniazid (INH), ethambutol (EMB) and pyrazinamide (PZA). The remaining four months of treatment known as the sterilization phase, involves the administration of only two drugs (RIF and INH). In general, standard first-line treatment outcomes worldwide are good with an 85% success rate being reported in 2018. This high success rate is also observed in South Africa, with 77% of the treated cases recording a favourable outcome (Kerantzas and Jacobs, 2017; WHO, 2019a). Despite the first-line

regimen being considered a short regimen, six month treatments are lengthy for patients thus making adherence a significant concern and risk factor for treatment failure. The introduction of directly observed therapy short-term (DOTS) as the standard for treatment in 1995 was proposed as a solution to poor adherence throughout treatment; however, no advantage over self-administration has been observed (Volmink and Garner, 2007; Karumbi and Garner, 2015).

1.1.3. Vaccination

To date only one vaccine exists to protect against TB: Bacillus Calmette Guerin (BCG). BCG, an attenuated form of *Mycobacterium bovis*, is one of the most widely distributed vaccines worldwide (McShane, 2011). The vaccine provides immunity against severe forms of childhood TB, including TB meningitis, but protection is limited and often only lasts ten years. Some studies now suggest that protection may surpass this, protecting for up to twenty years; however, further investigation, particularly in higher burdened TB countries is necessary (Aronson *et al.*, 2004; Barreto *et al.*, 2005; Abubakar *et al.*, 2013; Mangtani *et al.*, 2014, 2018; Nguipdop-Djomo *et al.*, 2015). BCG has been shown to be ineffective in protecting against adult pulmonary TB and is ineffective in *Mycobacterium* sensitised individuals, hence negating its use as a booster to increase immunity (Brandt *et al.*, 2002; Trunz, Fine and Dye, 2006; Aagaard *et al.*, 2009; Kagina *et al.*, 2009). Novel strategies for protection against TB, are desperately needed, especially in high burden areas, to curb the spread of infection.

1.1.4. Drug resistant TB

Resistance to first- and second-line TB treatments poses a considerable challenge for TB treatment and disease surveillance. Multi-drug resistant TB (MDR-TB) strains are resistant to the most effective first-line drugs, RIF and INH, and require second-line therapy for control and elimination of the disease. In recent years, an increase in the detection of mono-RIF resistance has also been observed due to the simultaneous detection of TB and RIF-resistance using the Xpert MTB/RIF diagnosis platform (WHO, 2019a). MDR-TB is typically treated through DOTS-plus regimen, involving eight months of intensive treatment with four drugs, followed by continuation treatment phase for 18-20 months (WHO, 2019b). Modifications to the recommended guidelines for MDR-TB treatment were made by the WHO in March 2019 to eliminate the use of injectables, including kanamycin and capreomycin. Currently, a fully oral second-line regimen containing a fluoroquinolone (either moxifloxacin or levofloxacin),

bedaquiline, linezolid and one other effective agent is recommended (WHO, 2019b). Other effective second-line agents often utilised include clofozamine, cycloserine, ethambutol, delamanid, pyrazinamide, meropenem, ethionamide and P-aminosalicylic acid (WHO, 2019b). The success rates of DOTS-plus worldwide is only 56%, and drops even lower in South Africa to 54% (WHO, 2019a). The poor success rate as well as the cost and adverse effects associated with treatment of MDR-TB constitute a need for extensive further study and innovative solutions. An alternative shorter regimen of nine to 12 months for MDR-TB can be recommended for some patients; however, this regimen contains an injectable drug, amikacin, and is known to be less effective in regions where resistance to drugs in the regimen is common, including Southern Africa (Dheda *et al.*, 2017; WHO, 2019b).

Extensive-drug resistance (XDR-TB) is resistance to RIF, INH, as well as a fluoroquinolone and an injectable. The emergence of XDR-TB is growing worldwide and South Africa is one of the top five counties for XDR-TB incidence (WHO, 2019a). Treatment of XDR-TB is highly specific and considers drug susceptibility on an individual patient basis, taking into consideration each patient's history to create a personalised treatment plan. Despite these efforts, treatment success is still very poor, especially in South Africa where only 39% of patients undergoing XDR-TB treatment have a positive outcome (WHO, 2019b).

1.2. TB Pathogenesis

1.2.1. Transmission and immune pathogenesis

Mtb is transmitted in aerosolized particles, called droplet nuclei (Churchyard *et al.*, 2017). These 1 to 5 µm particles enter susceptible individuals by inhalation and are translocated to the alveoli, where they are engulfed by alveolar macrophages. *Mtb* can disrupt macrophage maturation and fusion with the lysosome thus preventing elimination of the bacteria. The exact mechanisms behind this are still obscure (Smith, 2003; Russel, 2011); however, recent studies have attributed this phenomenon to *Mtb* nucleoside diphosphate kinase (Ndk) which exhibits GTPase activating protein (GAP) activity towards Rab5 and Rab7, resulting in the lack of recruitment of their respective effectors EEA1 (early endosome antigen 1) and RILP (Rab7-interacting lysosomal protein) (Sun *et al.*, 2010). Another mycobacterial protein that has been implicated in phagosome-lysozyme arrest is SapM, a monoester alkaline phosphatase that dephosphorylates PI3P9, a central player in phagosomal maturation (Fernandez-Soto *et al.*, 2019). Other immune response cells are then recruited by cytokines

and chemokines that are produced by the infected macrophages, resulting in formation of the granuloma, which is the hallmark of TB infection. The granuloma prevents dissemination of the bacteria and the spread of infection, but can also create a protective niche for bacterial replication (Ramakrishnan, 2012). Most TB infections result in rapid elimination of the bacteria within the granuloma; however, if the infection persists, the onset of active disease can occur.

1.2.2. Outcomes of TB transmission

Five major outcomes of transmission are experienced in TB infections: elimination, latency, incipient TB, subclinical TB and active disease. These outcomes exist as a dynamic spectrum of disease states, in which infected individuals can alternate presentation depending on host immunity and concurrent conditions (Pai *et al.*, 2016; Drain *et al.*, 2018). The disease outcome is dependent on the immune response initiated by the bacterium. This response is spatially organised within the granuloma, with pro-inflammatory responses contained toward the centre of the granuloma, surrounded by anti-inflammatory response cells. Not only does the immune response vary within the granuloma, it also varies between granulomas of the same lung (Marakalala *et al.*, 2016). This variation within and between granulomas effects control of TB infections, disease progression and the presentation of disease (Marakalala *et al.*, 2016). The five outcomes and their characterising features are summarised in figure 1.1 below.

1.2.2.1. Active TB disease

Active disease occurs if the immune system is unable to eradicate or control the TB infection, resulting in the clinical presentation of the disease. The bacteria survive the stress of the granuloma and continue to replicate thus resulting in the rupturing of the granuloma. The released bacilli are then exposed to neighbouring macrophages which they then infect, and by so doing, propagate infection within the host. Active disease manifestations are associated with classical clinical symptoms of TB, including a persistent cough, weight-loss, fatigue and night sweats (Hunter *et al.*, 2014; Pai *et al.*, 2016). The most common manifestation of active TB occurs in the lung (pulmonary TB) in 85% of *Mtb* infections; however, disease can manifest elsewhere in the body (extra-pulmonary TB) (Farer, Lowell and Meador, 1979). Other commonly reported manifestations include lymphatic, pleural, skeletal, central nervous system, ocular, pancreatic, genitourinary, milliary and cerebral TB (Kandola and Meena, 2014; Ramirez-Lapausa, Menendez-Saldana and Noguerado-Asensio, 2015). In the active

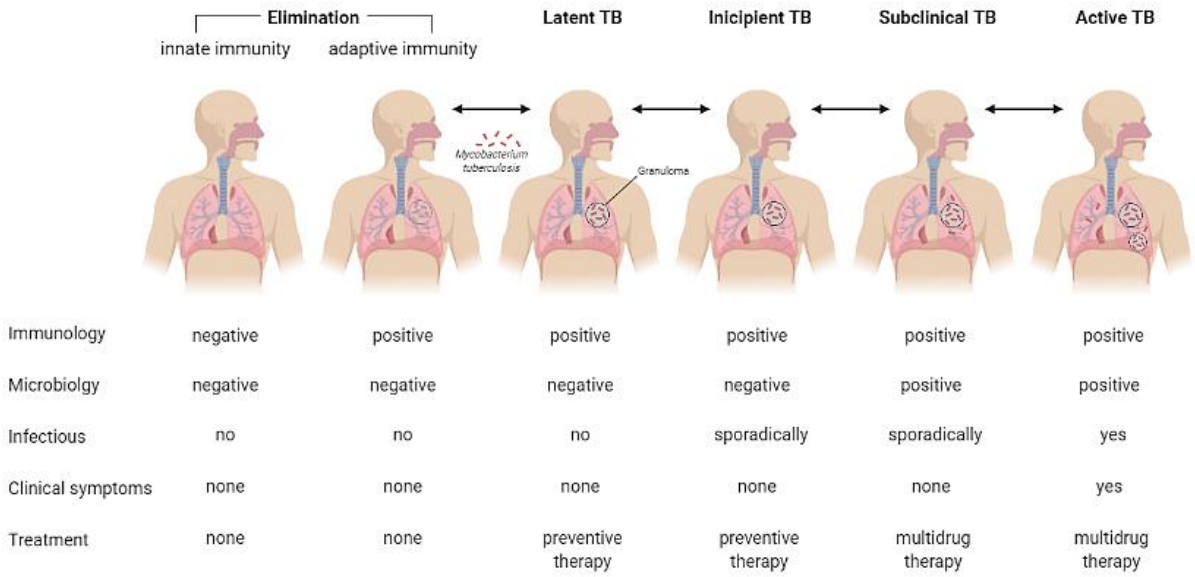


Figure 1.1. The spectrum of clinical TB presentations. The outcomes of TB transmission exist as a spectrum of manifestations, ranging from early elimination, latent infection, incipient TB, subclinical TB and active TB disease. Elimination of the TB infection can occur due to the innate or adaptive immune system, resulting in no microbiological detection of the infection. Eliminated TB cannot be transmitted and displays no clinical symptoms. The innate and adaptive response to TB infection is distinguished by immunological positivity in diagnostic tests. Latent TB infections are not microbiologically positive but can be detected by immunological tests. These infections have the potential for progression on the spectrum toward incipient, subclinical or active disease. Subclinical and incipient TB both manifest asymptomatically but vary in their propensity to progress to active disease. Incipient TB is not likely to progress in the near future and is microbiologically negative, while subclinical TB presents microbiologically positive disease, which is likely to progress to active disease in the near future. Active TB disease is both immunologically and microbiologically positive and can be transmitted. Active TB presents with various clinical symptoms and requires multidrug therapy. Adapted from Pai et al. (2016).

state, TB is transmittable through aerosolized droplets, which are expelled to the environment during expectoration (Churchyard *et al.*, 2017). Active TB can be separated into two classes, primary and secondary disease, based on the time elapsed between the initial infection and the onset of active disease. Primary active disease occurs in naïve patients that progress to active disease within five years of the initial infection. Primary infections often have favourable outcomes (Vynnycky and Fine, 1997; Palomino, Leao and Ritacco, 2007). During primary disease, patients are often asymptomatic and require detection by immunological methods; however, due to low bacterial loads, diagnosis is difficult (Palomino, Leao and Ritacco, 2007). Secondary active disease occurs in individuals who have been previously exposed, by reactivation of latent TB infections or by re-infection with new bacilli (Palomino, Leao and Ritacco, 2007). Clinical manifestations of secondary infections are more severe than those in primary infections, displaying the expected symptoms mentioned previously (Hunter *et al.*, 2014).

1.2.2.2. Elimination

It has been demonstrated that a number of host factors play a critical role in the resistance to TB infection thus preventing the establishment of infection and leaving no trace of exposure. These individuals, termed innate resistors, do not establish infection due to bacterial eradication at the site of infection by the innate immune system, without the initiation of an acquired immune response (Simmons *et al.*, 2018). However, once infection has been established, elimination can occur if the bacteria are eradicated by either the host immune system or with anti-tuberculosis drugs. Complete eradication of the bacteria occurs within two to eight weeks of infection due to the development of an effective cell-mediated immune response. This causes the granuloma to become caseating and necrotic. Most bacilli are unable to survive this necrotic environment and are eliminated (Schluger and Rom, 1998; Frieden *et al.*, 2003; Ahmad, 2011). Individuals who have cleared the infection are still immunologically positive and can be identified through skin tuberculin tests (Frieden *et al.*, 2003; Ahmad, 2011).

1.2.2.3. Latent TB infection

Latent TB infection (LTBI) occurs if the infection does not progress to active disease and a balance between the host and pathogen is achieved. No clinical or microbiological symptoms of active disease are observed, therefore diagnosis of LTBI is reliant on immunological tests (Dheda, Barry and Maartens, 2016; Drain *et al.*, 2018). The physiology of the bacteria during LTBI is still unknown. Individuals who are latently infected have a 5 to 15% risk of progressing to active disease within their lifetime. Many risk factors can influence the progression from latency to active disease, including HIV-co-infection, silicosis, close contact with TB-infected individuals, malnutrition, smoking, diabetes, aging, immune suppression therapy and therapy with tumor-necrosis factor alpha blockers (Lönnroth *et al.*, 2010; Ai *et al.*, 2016). Research to identify specific biomarkers of higher risk individuals is of great interest and would benefit the detection of cases that need preventative therapy. A sixteen gene transcriptome risk signature from whole blood was identified by Zak et al. to distinguish individuals that were progressing to active disease up to two years before they were diagnosed (Zak *et al.*, 2017). This risk signature was further validated in a recent study which identified whole blood transcriptional changes, plasma protein changes, and changes in the peripheral blood cell subsets prior to progression to active disease (Scriba *et al.*, 2017). Monitoring of these biomarkers in high risk areas and in individuals with close contact to TB-

infected individuals may assist in early identification of active TB infections, allowing for faster treatment initiation and better disease outcomes.

1.2.2.4. Incipient TB

Incipient TB disease occurs if the infection does not progress to active disease but is expected to progress in the near future. Similarly to LTBI, no clinical or microbiological symptoms of active disease are observed in incipient disease. The bacteria in this state are thought to be metabolically active, indicative of the impending progression to active disease and replication (Drain *et al.*, 2018). Incipient TB can be detected using immunological tests; however, these tests cannot provide any indication of the risk of progression to active disease (Rangaka *et al.*, 2014). In these cases, radiological detection may be a useful tool in monitoring the progression to active disease.

1.2.2.5. Subclinical TB

Subclinical TB disease occurs if the infection does not progress to active disease or present any symptoms of active TB, but does induce other abnormalities that can be detected microbiologically (Drain *et al.*, 2018). Subclinical disease is defined as asymptomatic disease associated with either radiological or microbiological confirmation of TB. The bacilli are metabolically active and induce an immune response, and therefore can be detected using similar immunological tests to active TB, despite discrepancies in the sensitivity of these tests. It is unclear whether sub-clinical TB also mimics active disease in infectiousness, as TB in this state can possibly lead to the formation of infectious aerosols (Dowdy, Basu and Andrews, 2013). It is believed that TB disease can alternate back and forth between subclinical disease, incipient disease and LTBI states many times before finally progressing fully to active TB disease (Drain *et al.*, 2018).

1.3. Detection and Diagnosis

1.3.1. Detection of active TB

Active TB is detected and diagnosed by X-rays, PET/CT imaging scans, smear, culture and molecular microbiological tests, including the widely used GeneXpert tool. Imaging tests are often used for screening, and microbiological tests for confirmation of infection (Pai *et al.*, 2016).

1.3.1.1. Smear microscopy

Smear microscopy is one of the most common diagnostic tools utilised in low- and middle-income countries for the detection of TB, due to its low cost, fast turnaround time and ease of use (Hänscheid *et al.*, 2007; Ryu, 2015; Caulfield and Wengenack, 2016). Microscopy has low sensitivity as a diagnostic tool, requiring a minimum of 5000 to 10000 bacilli per ml of specimen for a positive result. This is a significant disadvantage for individuals with low bacterial loads, including HIV-infected individuals, where false negative diagnoses are a risk (Getahun *et al.*, 2007; Palomino, Leao and Ritacco, 2007). The most common techniques used for smear microscopy are conventional Ziehl-Neelson microscopy and fluorescent auramine microscopy. Variable sensitivity of smear microscopy has been reported as a limitation of this technique in diagnostic settings; however, this can be improved with decontamination and concentration of the specimen (Gomes, Saad and Stirbulov, 2003; Getahun *et al.*, 2007; Palaci *et al.*, 2007).

1.3.1.2. Culture

Culture based diagnostics are the gold standard for TB diagnosis. Culture is more sensitive than smear microscopy and requires a minimum of ten to 100 viable bacilli per ml of specimen for a positive result (Colebunders and Bastian, 2000; van Zyl-Smit *et al.*, 2011). The major limitation of culture is the lengthy turnaround time of up to eight weeks, due to the slow growing nature of *Mtb* (Ryu, 2015). The lengthy time to diagnosis is worsened in HIV-positive individuals where bacterial loads are generally low (Johnson *et al.*, 1998). Culturing was traditionally performed on solid media, either Lowenstein-Jensen or Middelbrook 7H10/7H11; however, automated liquid culturing systems are now commonly used and provide convenience, greater ease of use and minimise human error in the interpretation of results. These automated systems detect changes in gas pressure, carbon dioxide production and oxygen consumption during bacterial growth. An example of one such system is the BACTEC MGIT 960 system (Becton Dickinson Diagnostic Systems), which utilises an oxygen-quenched fluorochrome for the detection of active growth. As oxygen is utilised during growth, inhibition of the fluorochrome is removed, resulting in a detectable fluorescent signal. Automated culturing systems can now also be adapted for drug-susceptibility testing by the addition of known concentrations of trial drugs and monitoring growth under these conditions (Said *et al.*, 2012; Siddiqi *et al.*, 2012; Isaeva *et al.*, 2013; Kim *et al.*, 2013; Zhao *et al.*, 2014). A drawback of these automated culturing systems, including BACTEC MGIT 960, is their inability to distinguish *Mtb* from other aerobic organisms.

Culturing therefore needs to be used in conjunction with molecular tests which allow for speciation (Pfyffer and Edition, 2015; Caulfield and Wengenack, 2016).

1.3.1.3. Molecular tools

Molecular tests are able to detect *Mtb* DNA, metabolites and cell wall products for the diagnosis of TB without necessarily isolating the whole organism. These include nucleic acid hybridization probes, line probe assays, DNA sequencing and mass-spectrometry (Anochie *et al.*, 2012; Ceyssens *et al.*, 2017). Molecular tests have a faster turnaround time compared to culture-based tests because they can be performed directly on sputum specimens; however, they cannot distinguish between living or dead bacilli and are therefore not useful for treatment monitoring (Moore, Guzman and Mikhail, 2005). Molecular diagnostic tests also allow for the detection of genetic mutations inferring phenotypic resistance to first-line antibiotics. Some common molecular tests include the Hain MTBDRplus line probe assay (Hain Lifescience), GeneXpert (Cepheid) and the amplified *Mtb* direct test (Hologenic Gen-Probe). GeneXpert is the most common molecular test that is used as a point-of-care diagnostic in South Africa. GeneXpert performs DNA extraction and amplification by polymerase chain reaction inside a closed cartridge in a semi-quantitative manner, in conjunction with the detection of rifampicin resistance through *rpoB* gene mutations (Boehme *et al.*, 2010; Helb *et al.*, 2010). The closed system minimises contamination and is simple to perform with a rapid turn-around time of 2 hours. The sensitivity of GeneXpert is good, requiring 131 bacilli per ml for detection (Helb *et al.*, 2010; Theron *et al.*, 2011). The sensitivity of GeneXpert in the detection of *Mtb* in smear negative specimens varies, with studies reporting contradictory results of 70% and 28% (Boehme *et al.*, 2010; Lawn and Nicol, 2011; Sohn *et al.*, 2014). In recent years, the introduction of the GeneXpert Ultra cartridge has allowed for greater sensitivity and accuracy in the detection of TB and RIF resistance (Chakravorty, Simmons, *et al.*, 2017). South Africa is currently the only high burden country utilising this improved tool for the initial diagnosis of TB (WHO, 2019a). Despite its success as a diagnostic tool worldwide, GeneXpert cannot completely replace culturing as the gold-standard for TB diagnosis as it does not determine bacterial viability and currently only detects genetic resistance to RIF. PCR-based assays for the detection of multiple drug resistance genes are being investigated and will likely be similar to the assay developed by Chakravorty et al., which detects mutations which infer resistance to INH, fluoroquinolones and amikacin (Chakravorty, Roh, *et al.*, 2017). Culturing and molecular

tests each provide important information regarding detection, drug susceptibility and resistance, and treatment response, and are therefore used in conjunction for diagnosis.

1.3.2. Detection of latent TB

LTBI is diagnosed by ruling out active TB infections, as immunological tests are unable to distinguish between these two states (Pai *et al.*, 2016). Active TB is excluded based on the absence of clinical symptoms in adult and paediatric patients, as well as negative bacteriological results for adult patients. LTBI is commonly detected using two immunological tests: tuberculin skin tests (TSTs) and interferon gamma release assays (IGRAs). TSTs are the most commonly used screening test which assess pre-sensitization to a purified protein derivative of *Mtb* known as tuberculin. Skin tests are low cost and simple to administer; however, cross-reactivity with BCG vaccinations can occur, resulting in false positive results (Farhat *et al.*, 2006; Mahomed *et al.*, 2011; Nayak and Acharjya, 2012). IGRAs are *in vitro* blood tests which assess the response to *Mtb* antigens by measuring interferon-gamma levels (Pai *et al.*, 2014). Despite the improved specificity over TSTs, IGRAs are less commonly used due to higher costs and the expertise required to perform the test. A significant challenge in the diagnosis of LTBI is the lack of knowledge surrounding the physiology of bacteria in this state. It is believed that latent bacteria are differentially culturable and do not replicate as active TB populations do, making these populations difficult to detect.

1.4. Bacterial culturability, persistence and resuscitation

1.4.1. Different culturable states

Bacteria encounter various adverse environments which do not favour growth, including extreme temperatures, desiccation, non-optimal pH and salinity, radiation, nutrient deprivation and synthetic antimicrobial exposure (Dworkin and Shah, 2010; Lennon and Jones, 2011; Setlow, 2014). To survive these stresses, bacteria can enter a reversible non-replicative state that is characterised by reduced metabolism, often termed dormancy. This state allows bacteria to be less susceptible to these stresses while conserving energy for the resumption of more favourable environmental conditions, where they can reactivate and continue replicative growth (Kell and Young, 2000; Jones and Lennon, 2010; Lennon and Jones, 2011). Bacteria are also able to enter these non-replicative states spontaneously, as a safeguard against stochastic stresses (Avery, 2006; Gardner, West and Griffin, 2007). In sporulating bacteria, such as *Bacillus* and *Clostridium* species, dormant states are achieved

through asymmetrical division to produce an inactive daughter cell, termed a spore. This spore is biologically resilient and has a distinct hardy protective coat of glycoproteins which protects it from various environmental stress (Setlow, 2007; Dworkin and Shah, 2010). In non-sporulating bacteria, such as *Mycobacterium* species, dormant states are less morphologically distinct. Two dormant-like states in mycobacteria have been identified: persisters and viable but not culturable (VBNC) cells (Li *et al.*, 2014; Maisonneuve and Gerdes, 2014).

Persisters are bacteria which have an increased tolerance for antimicrobials without any identifiable genetic resistance mechanisms (Lewis, 2007, 2010). Persister populations form a small percentage of the total bacterial population. During antibiotic stress, the susceptible portion of the population is eradicated, but the tolerant persister population survive and restore the population once the antibiotic is removed (Lewis, 2007, 2010; Lennon and Jones, 2011). VBNC cells, also called quiescent cells, are similar to persisters in also having no identifiable genetic mechanisms of resistance but display reduced culturability under standard laboratory conditions. The distinguishing characteristic between these dormant-like populations is how they re-emerge from the dormant-like, non-culturable state. Persisters are able to spontaneously emerge after a stress has been removed, while VBNC cells require additional time and supplementation to regain culturability (Ayrapetyan *et al.*, 2015; Ayrapetyan, Williams and Oliver, 2015). It has been suggested that due to the similarity of these two states, they may not be distinct from each other but rather form a spectrum of non-replicating states (figure 1.2) (Ayrapetyan *et al.*, 2015; Ayrapetyan, Williams and Oliver, 2015).

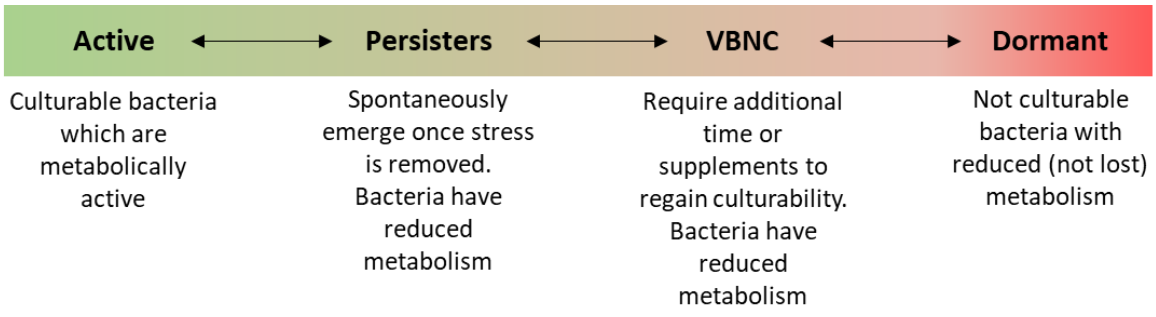


Figure 1.2. The spectrum of culturability. Under stressful conditions, bacteria are able to enter a reversible, dormant state in which they are less susceptible to stress and able to survive. Once growth permissive conditions resume, bacteria can regain culturability and resume active growth. Bacteria can alternatively enter intermediate dormant-like culturability states, acting as Persisters or viable but not culturable (VBNC) cells. Persister cells can spontaneously resume active growth after a stress is removed, while VBNC cells take longer periods of time to resume growth and often require supplements.

Non-culturable, non-replicating, dormant-like cells can exit this state and regain culturability spontaneously or in response to environmental cues in a manner similar to quorum sensing (Lennon and Jones, 2011). The most popular theory for reactivation is the scout cell hypothesis (Epstein, 2009; Buerger *et al.*, 2012b, 2012a). It is hypothesised that bacterial populations consist of both dormant-like and replicating cells; however, dormant-like cells dominate the population. A few of these non-replicating cells will spontaneously resuscitate from the dormant-like state and become scouts for favourable environmental conditions. If conditions are unfavourable for growth, the scout will die and the population will remain predominantly dormant-like, but if conditions are growth permissive, the scout will signal the dormant population to resuscitate and proliferate, which will transition the population to predominately actively replicating cells (Epstein, 2009; Buerger *et al.*, 2012a, 2012b; Gengenbacher and Kaufmann, 2012). A portion of the population will still remain in the dormant-like state as persisters, regardless of the conditions permitting. These tolerant persister populations have been identified in specimens from individuals with active TB disease, and may be major contributors to LTBI and recurrent infections (Lewis, 2007, 2010).

1.4.2. Differentially culturable tubercle bacilli (DCTB)

VBNC cells have been identified in *Mtb* sputum populations and were termed differentially culturable tubercle bacilli (DCTB) (Chengalroyen *et al.*, 2016). These bacilli are unable to grow under standard laboratory conditions without supplementation with additional growth factors; however, they are able to emerge in the presence of a myriad of documented growth supplements, including culture filtrates (CFs) from growing bacteria, recombinant resuscitation promoting factors (Rpfs), free fatty acids and cell wall hydrolysis products (Sun and Zhang, 1999; Shleeva et al., 2002, 2013; Wu et al., 2008; Mukamolova et al., 2010; Huang et al., 2014; Kolwijck et al., 2014; Nikitushkin et al., 2015; O'Connor et al., 2015; Chengalroyen et al., 2016). These populations have been identified in specimens from individuals with active TB disease prior to the initiation of treatment, with dependency on different supplements varying between bacterial populations (Shleeva *et al.*, 2002; Mukamolova *et al.*, 2010; Chengalroyen *et al.*, 2016). DCTB populations are of great interest as they are thought to be key players in drug tolerance, LTBI and relapse (Ayrapetyan, Williams and Oliver, 2015). The reduced culturability of DCTB populations under standard laboratory conditions creates a challenge for diagnostics and may result in a gross underestimation of the extent of infection and over-estimation of the success of treatment. Promoting the resuscitation of DCTB in diagnostic culturing assays may shorten the

turnaround time for culture diagnostic tests, as well as allow for the detection of previously unobserved populations.

1.5. Resuscitation promoting factors and their interacting partners

Rpfs are muralytic enzymes that were first identified in *Micrococcus luteus,* and demonstrated the ability to stimulate the resuscitation of non-culturable bacteria (Mukamolova *et al.*, 1998). The single Rpf in *Mi. luteus* displays activity similar to that of lysozyme and is believed to have dual biological activity as a growth cytokine and resuscitation-stimulatory molecule. *Mi. luteus* Rpf has a 75 amino acid residue N-terminal domain, termed the 'Rpf domain" which contains a c-type lysozyme fold thus hinting at the mechanism of action of this protein (Cohen-Gonsaud *et al.*, 2004). This Rpf, which is essential for growth *in vitro*, can resuscitate non-culturable *Mi. luteus*, as well as several mycobacterial species, including *Mtb*, *M. avium*, *M. bovis* and *M. kansasii* (Mukamolova *et al.*, 1998). Following this work in *Mi. luteus*, Rpfs have been identified, by sequence homology, in other Actinobacteria, including *M. tuberculosis*, *Mycobacterium smegmatis*, and several *Streptomyces* species. The 75 residue catalytic-Rpf region has been highly conserved across all these species. (Mukamolova *et al.*, 1998; Cohen-Gonsaud *et al.*, 2004). Despite its c-type lysozyme fold, *Mi. luteus* Rpf, lacks the critical asparagine residue for c-type lysozyme activity and is thought to act as lytic transglycosylase (Nikitushkin *et al.*, 2015).

Mtb encodes five Rpfs: RpfA, RpfB, RpfC, RpfD and RpfE. These enzymes have all been shown to be dispensable for growth *in vitro* both individually and in combination (Downing *et al.*, 2004, 2005; Tufariello, Jacobs and Chan, 2004; Kana *et al.*, 2008). All five Rpfs are expressed at different levels at different growth phases and are regulated independently of each other (Mukamolova, Turapov, Young, *et al.*, 2002; Gupta, Srivastava and Srivastava, 2010). Each Rpf can be distinguished from its family members by its respective amino- and carboxy-terminal regions. The functional impact of the different regions however requires further investigation (Mukamolova, Turapov, Young, *et al.*, 2002). A functional hierarchy is observed in this family of enzymes, with RpfB and RpfE ranking above the other enzymes (Kana *et al.*, 2008). *Mtb* lacking both RpfB and RpfE display delayed colony formation, increased sensitivity to SDS, a cell wall damaging agent, and decreased growth and persistence during mouse infections (Downing *et al.*, 2005; Kana *et al.*, 2008). These effects can be corrected by the reintroduction of either RpfB or RpfE. This hierarchy of Rpfs appears

to not be maintained in other mycobacterial species, evidenced by the higher ranking of RpfA and RpfB in *M. smegmatis* (Ealand *et al.*, 2018). *M. smegmatis* strains lacking both RpfA and RpfB display altered colony morphology and biofilm formation, as well as increased sensitivity to RIF, vancomycin and SDS, which can be corrected by the complementation of these genes (Ealand *et al.*, 2018).

RpfB from *Mtb* in particular has been identified as important for reactivation from dormancy and non-culturable states, as well as in virulence and survival during mouse infection (Tufariello, Jacobs and Chan, 2004; Kana and Mizrahi, 2010). RpfB displays structural similarity to soluble lytic transglycosylases (SLTs) in *Escherichia coli*, despite its c-type lysozyme fold, and is therefore likely to perform a similar function to lytic transglycosylases (Cohen-Gonsaud *et al.*, 2004). It has been shown that RpfB cleaves the glycosidic bond between *N*-acteyl-muramic acid and *N*-actyl-glucosamine in the sugar backbone of peptidoglycan (figure 3.1.) (Cohen-Gonsaud *et al.*, 2005; Ruggiero *et al.*, 2009). RpfB does not act alone and has been shown to interact with a partner *L,D*-endopeptidase, Rpf-interacting protein A (RipA). RipA possesses a c-terminal domain homologous to the p60 family of hydrolases and cleaves within the peptidoglycan stem peptide, between the *D*-glutanyl-meso-diaminopimelic acid residues (figure 1.3.) (Brennan, 2003; Hett *et al.*, 2007, 2008). Homologues of RipA have been identified in *Streptomyces, Corynebacterium, Nocardia, Frankia*, *Rhodococcus* and *Clostridium* species, all of which conserve the catalytic c-terminal domain (Hett *et al.*, 2007). RipA has also been shown to act on peptidoglycan from various organisms, including *Mi. luteus*, *E. coli*, *M. smegmatis* and *Streptomyces* (Anantharaman and Aravind, 2003; Pilgrim *et al.*, 2003; Sassetti, Boyd and Rubin, 2003). This protein also localises to the septum and cell poles during bacterial growth and division (Hett *et al.*, 2007). RipA and RpfB have been shown to hydrolyse peptidoglycan and by so doing signal the resuscitation of non-culturable *M. smegmatis* (Nikitushkin *et al.*, 2015). It is suggested that the interaction of RipA and RpfB may result in structural changes in RipA that activate the enzyme for its hydrolytic function (Ruggiero, Marasco, *et al.*, 2010; Ruggiero, Squeglia, *et al.*, 2010). The product of RipA and RpfB joint hydrolysis is *N*-acetylglucosaminyl-*β*-*N*-acetyl-1,6-anhydromuramoyl-*L*-ananyl-*D*-isoglutamate (anhydro-GMDP) which has also been observed to possess resuscitation capabilities in *M. smegmatis* (Nikitushkin *et al.*, 2015).

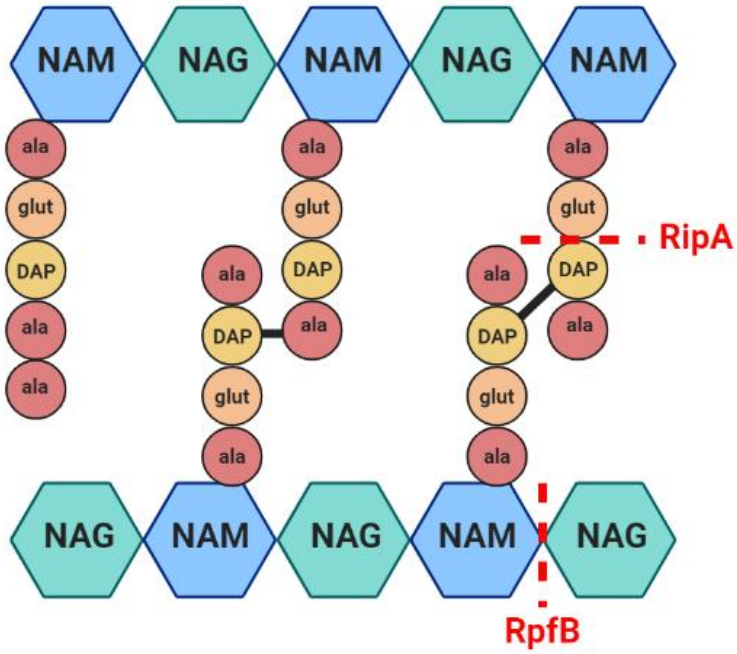


Figure 1.3. Function of RipA and RpfB as lytic enzymes that cleave the peptidoglycan layer of the bacterial cell wall. Peptidoglycan consists of alternating sugars, *N*-acetyl-glucosamine (NAG) and *N*-acetyl-muramic acid (NAM), cross-linked by stem peptides. Stem peptides are built from alanine (ala), meso-diaminopimalate (DAP) and glutamine (glu) residues. Peptidoglycan is cross-linked by 3-3 and 3-4 crosslinks between two DAP residues or between DAP at position 3 and Ala at position 4 of the stem peptide. Rpfs cleave between the sugar residues of the backbone, while RipA cleaves within the stem peptide.

1.6. The knowledge gap

The resuscitation capabilities of RipA and RpfB on *M. smegmatis* have been investigated previously; however, the capabilities of these enzymes to resuscitate *M. tuberculosis* in combination requires further investigation. Several studies have investigated methods of resuscitation in routine diagnostic tests with the intention of improving the diagnostic turn-around time by shortening the time to detection and also allowing for the detection of non-culturable organisms. These studies have shown that supplementation with CF from actively growing *Mtb*, as well as recombinant Rpfs, allows for increased detection of *Mtb* in sputum (Sun and Zhang, 1999; Wu *et al.*, 2008; Mukamolova *et al.*, 2010; Huang *et al.*, 2014; Kolwijck *et al.*, 2014; O'Connor *et al.*, 2015). No work to date has investigated the effect of RipA and RpfB supplementation in combination on the time-to-detection of *Mtb* in MGIT diagnostic assays specifically. This MSc aims to fill this gap and evaluate whether supplementation with recombinant RipA and RpfB could stimulate the resuscitation of non-culturable *Mtb* and reduce the time to detection. It was hypothesised that the supplementation of recombinant RipA and RpfB would stimulate resuscitation and promote the growth of *Mtb* from the non-culturable state, thereby shortening the time to detection in MGIT assays.

The specific objectives were to:

- Optimise the expression and purification of recombinant RipA and recombinant RpfB on small and large scale
- Assess the muralytic activity of recombinant RipA and RpfB in *in vitro* protein activity assays
- Generate non-culturable *Mtb* in an *in vitro* nutrient starvation model
- Assess the resuscitation capabilities of recombinant RipA and RpfB on *in vitro* generated model non-culturable *Mtb* in MGIT assays
- Assess the resuscitation capabilities of recombinant RipA and RpfB on Beijing and LAM strains of *Mtb* passaged from patient specimens in MGIT assays
- Assess the resuscitation capabilities of recombinant RipA and RpfB on *Mtb* in patient specimens in MGIT assays

2. Methods

2.1. Strains and culturing conditions

Various *E. coli*, *M. smegmatis* and *Mtb* strains were utilised in this study. The culturing conditions used to grow each strain are listed in table 1. below. All the strains utilised in this study are listed in Table 2 below.

Table 1. Culturing conditions for the various strain types utilised in this study

Organism	Culture media	Culture conditions
E. coli	Luria-Bertani broth (LB) and Luria-Bertani Agar solid media (LA) (Sigma)	37°C for all cultures, shaking at 100 rpm for liquid cultures
M. smegmatis	Difco 7H9 liquid media (BD) supplemented with glucose salts and Tween 80 and BBL 7H10 solid media (BD) supplemented with glucose salts	37°C for all cultures, shaking at 100 rpm for liquid cultures
Mtb	Difco 7H9 liquid media (BD) supplemented with OADC and Tween 80, Dfico 7H9 (BD) supplemented with 13.5 g noble agar (Sigma) per litre, and BBL 7H11 solid media (BD) supplemented with OADC	37°C, without shaking, for all cultures

Table 2. List of strain used in this study

Strain name	Organism	Description
DH5α	*E. coli*	*E. coli* strain with multiple mutations for increased transformation efficiency
DH5α_RipA	*E. coli*	DH5α containing the pETM120_RipA vector
DH5α_RpfB	*E. coli*	DH5α containing the pETM11_RpfB vector
BL21 DE3	*E. coli*	*E. coli* strain with multiple mutations for increased protein expression
RipA	*E. coli*	BL21 DE3 strain containing the pETM20_RipA vector
RpfB	*E. coli*	BL21 DE3 containing the pETM11_RpfB vector
Mc^2155	*M. smegmatis*	*M. smegmatis* laboratory strain mutated for high frequency transformations
H37Rv	*Mtb*	*Mtb* laboratory strain
Beijing	*Mtb*	*Mtb* strains isolated from clinical sputum samples and passaged in the lab, confirmed as Beijing strain by spoligotyping
LAM	*Mtb*	*Mtb* strains isolated from clinical sputum samples and passaged in the lab, confirmed as LAM family strain by spoligotyping

2.2. DNA extraction and clean up

2.2.1. Plasmid mini-prep – QIAprep Miniprep kit

The QIAquick Miniprep kit (Qiagen) was used for small-scale extraction of plasmid DNA from *E. coli*. A single colony of the desired strain was harvested from a LA plate and inoculated into 5 ml of LB broth. This culture was grown overnight at 37°C with shaking at 100 rpm. The 5 ml culture was used for the plasmid DNA extraction, as per the manufacturer's instructions. All the steps were performed at room temperature. Briefly, cells from 5 ml of culture were centrifuged at 6 800 x g for 3 minutes. Cells were then re-suspended in 250 µl Buffer P1 (50 mM Tris-HCl pH 8.0, 10 mM ethylenediaminetetraacetic acid (EDTA), 100 µg/ml RNAse A) and transferred to a 1.5 ml eppendorf tube. To the cell suspension, 250 µl of Buffer P2 (200 mM sodium hydroxide, 1% (w/v) sodium-dodecyl sulphate (SDS), Lyseblue pH indicator) was added and the tube was inverted five times to mix, turning the suspension blue in colour. To neutralise the reaction, 350 µl of Buffer N3 (proprietary and confidential) was added and the tube was inverted five times to mix, turning the suspension colourless. To separate the soluble cell lysate from cellular debris, the suspension was centrifuged at 12 470 x g for 10 minutes. To extract the DNA, 800 µl of the soluble lysate was applied to the QIAprep 2.0 spin column. The column was centrifuged at 12 470 x g for 1 minute, allowing the DNA to bind to the column, and the remaining lysate was discarded as flow through. The DNA-bound column was washed with 500 µl Buffer PB (proprietary and confidential), centrifuged at 12 470 x g for 1 minute and the flow through discarded. A second wash was performed by adding 750 µl of Buffer PE (proprietary and confidential) to the column followed by centrifugation at 12 470 x g for 1 minute and discarding of the wash flow through. The column membrane was then dried by centrifugation at 12 470 x g for 1 minute before placing into a clean 1.5 ml eppendorf tube for DNA elution. A volume of 50 µl of warmed Buffer EB (10 mM Tris-HCl pH 8.5) was placed onto the column membrane, incubated for 1 minute and centrifuged at 12 470 x g at for 1 minute. Eluted plasmid DNA was visualised and quantitated as described in section 2.4.

2.2.2. Plasmid maxi-prep – Nucelobond Xtra Maxi kit

The Nucleobond Xtra Midi kit (Machery-Nagel) was used for large-scale extraction of plasmid DNA from *E. coli*. A single colony was inoculated into 5 ml of LB and grown overnight at 37°C with shaking at 100 rpm. This pre-culture was used to inoculate into 50 ml of LB broth, which was incubated at 37°C until it reached an OD_{600} of approximately 0.8.

The DNA extraction was performed as per the manufacturer's instructions, with the following modifications. Briefly, cells were harvested by centrifugation at 4 000 x g for 10 minutes at 4°C. Cells were then re-suspended in 8 ml resuspension buffer (50 mM Tris, 10 mM EDTA, 100 µg/ml RNAse A) and mixed with an equal volume of lysis buffer (200 mM sodium hydroxide, 1% (w/v) sodium-dodecyl sulphate) to lyse the cells. This was gently inverted to mix, followed by incubation at room temperature for 5 minutes. The lysis reaction was neutralised by adding 8 ml of neutralisation buffer (2.8 M potassium acetate, pH 5.1) and inverting to mix. The soluble cell lysate was partially cleared and separated from the insoluble fraction by centrifugation at 4 000 x g for 10 minutes at 4°C. The soluble lysate was then loaded onto a pre-equilibrated nucleobond column filter. The column was washed with 5 ml of equilibration buffer (100 mM Tris, 15% (v/v) ethanol, 900 mM potassium chloride, 0.15% Trixon X-100 (v/v), pH 6.3) by gravity filtration and the column filter was discarded. The remaining column membrane was washed with 8 ml wash buffer (10 mM Tris, 15% ethanol (v/v), 1.15 M potassium chloride, pH 6.3) by gravity filtration. Plasmid DNA was eluted off the membrane with 5 ml of elution buffer (100 mM Tris, 15% ethanol (v/v), 1 M potassium chloride, pH 8.5) by gravity filtration. Plasmid DNA was then precipitated with 3.5 ml isopropanol, aliquoted into eight 1.5 ml eppendorf tubes and centrifuged at 15 000 x g for 30 minutes at room temperature. The DNA pellet was washed with 300 µl of 70% (v/v) ethanol and centrifuged at 15 000 x g for 5 minutes at room temperature. The DNA was then dried at 65°C in a speed vacuum for 15 minutes. Each aliquot was reconstituted in 50 µl of TE buffer (10 mM Tris-HCl, 10 mM EDTA, pH 8.0) and the aliquots were pooled together. Plasmid DNA was visualised and quantitated as described in section 2.4.

2.2.3. Ethanol precipitation

Ethanol precipitation was performed to concentrate DNA and remove any residual salts. A tenth volume of 3 M sodium acetate pH 5.2 and three volumes of 100% ethanol were added to the DNA. DNA was incubated at 4°C for 20 minutes and harvested by centrifugation at 12 470 x g for 15 minutes at room temperature. The DNA was washed with 1 ml of 70% (v/v) ethanol and harvested by centrifugation at 12 470 x g for 5 minutes at room temperature. The DNA pellet was dried at 65°C in a speed vacuum for 15 minutes and reconstituted in 100 µl of distilled water. DNA was quantified and visualised as described in section 2.4.

2.3. Restriction digests

Restriction digests were performed to map vectors prior to transformations. A microgram of plasmid DNA was digested by 1 unit of enzyme at 37°C for 1 hour. Digested DNA was visualised on 1% (w/v) agarose gels, as described in section 2.4.2.

2.4. Nucleic acid quantification and visualisation

2.4.1. Nanodrop quantification of nucleic acids (and protein)

DNA and protein were quantified using the Nanodrop ND1000 (ThermoScientific). Nucleic acids were quantified at 260 nm and their quality was assessed automatically using the same instrument at a wavelength of 230nm and 325 nm. An A260/A280 ratio of 1.8 was indicative of pure DNA. Protein concentration was measured at 280 nm. The Nanodrop machine was calibrated with 2 µl of the appropriate media and 2 µl of the nucleic acid or protein sample of interest measured at the appropriate wavelength.

2.4.2. Agarose gel electrophoresis

The visualisation of nucleic acids was performed by agarose gel electrophoresis. One percent agarose gels were prepared by dissolving 0.5 g of agarose powder in 50 ml of 1x TAE buffer (40 mM Tris-acetate, 1 mM EDTA, pH 8.0) per gel. The volume of reagents was adjusted accordingly for the number of gels needed. The appropriate amount of agarose powder was weighed and mixed with the appropriate volume of 1x TAE buffer. The gel mixture was boiled in a microwave in 30 second intervals until the agarose powder was completely dissolved. The molten gel was left to cool to approximately 55°C before adding 2 µl of ethidium bromide per 50 ml of gel. This was swirled gently to evenly distribute the ethidium bromide in solution. The gel was then poured into a casting tray with a comb and allowed to solidify at room temperature for approximately 30 minutes. The comb was removed from the solidified gel and the gel was transferred to a running tank and covered with 1x TAE buffer. Nucleic acid samples were mixed with loading dye at a 5:1 ratio prior to loading into the wells of the gel. Loaded gels were run at 80 V until the dye front had migrated an appropriate distance. This was followed by visualisation of the DNA in the gel using SynGene Gbox and Snapgene version 7.12 acquisition software.

2.5. Transformation of *E. coli* – Calcium chloride method

The calcium chloride method was used to make chemically competent *E. coli* for transformations. A single colony of the desired strain to be transformed was inoculated into a

5 ml pre-culture and grown overnight at 37°C with shaking at 100 rpm. This pre-culture was then used to inoculate a 100 ml culture, which was grown at 37°C with shaking at 100 rpm to an approximate OD_{600nm} of 0.5. Cells were chilled on ice for 10 minutes before harvesting by centrifugation at 3 000 x g for 10 minutes at 4°C. Cells were re-suspended in 10 ml of cold 0.1 M magnesium chloride by gentle swirling and incubated on ice for 20 minutes. Cells were harvested by centrifugation at 3 000 x g for 10 minutes at 4°C and washed in 0.1 M calcium chloride. The calcium chloride wash was repeated until cells started to stick to the sides of the falcon tube used for centrifugation. Cells were re-suspended in 0.1 M calcium chloride to the desired volume. For each transformation reaction, 100 µl of competent cells was used. For the transformation step, 1 µg of clean DNA was added to 100 µl of competent cells and incubated on ice for 15 minutes before heat shock at 42°C for 90 seconds. Cells were then incubated on ice for 3 minutes and rescued with 800 µl of SOC media at 37°C for 1 hour. Successful clones, which had taken up the DNA and appropriate antibiotic resistance markers, were selected for growth on LA plates with the appropriate antibiotics.

2.6. Protein expression and extraction

2.6.1. Protein Induction

Protein expression was induced overnight at 22°C with 1 mM isopropyl *β-D*-1-thiogalactopyranoside (IPTG). A single colony of the desired protein expressing strain, generated in section 2.5, was grown overnight in a 5 ml pre-culture at 37°C with shaking at 100 rpm. This pre-culture was used to inoculate a 50 ml or 1 L culture and grown for 3 to 5 hours at 37°C with shaking at 100 rpm. A 1 ml aliquot of this uninduced culture was collected and centrifuged at 12 470 x g for 5 minutes at room temperature to harvest the cells. The cells were then re-suspended in 300 µl B-PER (bacterial protein extraction reagent) and frozen overnight at -20°C. The remaining culture was induced with 1 mM IPTG and incubated overnight at 22°C with shaking at 100 rpm.

2.6.2. Small scale protein extraction – Bacterial Protein Extraction Reagent (B-PER)

For small scale protein extractions, B-PER was used. To prevent protease digestion during cell lysis, complete protease inhibitor cocktail (Roche) was added to B-PER (1 tablet per 10 ml B-PER). The desired volume of culture for extraction (maximum 20 ml) was harvested by centrifugation at 4 000 x g for 10 minutes at room temperature. Cells were re-suspended in a

500 µl B-PER and incubated at room temperature for 10 minutes. Centrifugation at 12 470 x g at for 20 minutes room temperature was used to separate the cell lysate into the soluble and insoluble protein fractions. The soluble cell lysate fraction was used for small scale protein purifications, as described in sections 2.6.6, 2.6.7 and 2.6.8.

2.6.3. Cell lysis by French press

High pressure disruption in the French press was used to lyse large culture volumes (more than 30 ml). Cells from the desired culture volume were harvested by centrifugation at 4 000 x g for 15 minutes at 4°C and re-suspended in 15 ml cold protein wash buffer (Buffer D – 50 mM Tris-HCl, 150 mM sodium chloride, 5 mM imidazole, 5% (v/v) glycerol). The cell suspension was lysed in the French press at 1.9 kBar in batches of 5 ml to 8 ml at a time. The cell lysate was collected and centrifuged at 4 000 x g for 10 minutes at 4°C to harvest the insoluble cell lysate fraction and any intact cells. The insoluble fraction was re-suspended in 1 ml of B-PER reagent.

2.6.4. Tag removal – TEV-digestion

His-tag removal was performed by TEV digestion to minimise the interference of the tag on protein activity. The digestion reaction was set up as per the manufacturer's instructions. Briefly, 1 U of AcTEV enzyme was used to digest 3 µg of protein in 1x AcTEV reaction buffer (50 mM Tris-HCl, 500 µM EDTA) in the presence of 1 mM dithiothreitol (DTT) at 30°C overnight.

2.6.5. Dialysis buffer exchange

Dialysis buffer exchange was performed to remove the DTT and EDTA from the protein mixture post-TEV digestion. Dialysis was performed using Spectra/Por molecularporous membrane tubing (Spectrum) with a molecular weight cut off of 6 000 to 8000 kDa. The digestion reaction was encapsulated in the membrane tubing and placed inside a beaker of dialysis buffer (50 mM Tris-HCl, 150 mM sodium chloride, 5% (v/v) glycerol, pH 8.0) overnight at 4°C with mixing on a stirring block. The dialysed protein inside the membrane capsule was purified as described in section 2.6.8.

2.6.6. Small scale protein purification – Zymo His-Spin Protein Mini Prep Kit

The Zymo His-Spin Protein Mini Prep kit (Zymo) was used to purify small volumes of his-tagged proteins from B-PER protein extractions (Section 2.6.2). The procedure was carried out as per the manufacturer's instructions. Briefly, 250 µl of his-affinity resin was transferred

to a column which was placed inside a collection tube and centrifuged at 15 000 x g for 10 seconds at room temperature. To the prepared resin, 300 µl of his-tagged protein sample was added and mixed by gently tapping the column. Unbound protein (not his-tagged) was collected in the flow through by centrifugation at 15 000 x g for 10 seconds at room temperature. The resin was washed twice with 250 µl his-wash buffer (50 mM sodium phosphate pH 7.7, 300 mM sodium chloride, 50 mM imidazole, 0.03% (v/v) Trixon X-100) and the flow through was collected by centrifugation at 15 000 x g for 10 seconds at room temperature. The his-affinity column was transferred to a new 1.5 ml eppendorf tube for elution. His-tagged proteins were eluted off the resin with 150 µl of his-elution buffer (50 mM sodium phosphate buffer pH 7.7, 300 mM sodium chloride, 250 mM imidazole) by gentle tapping to re-suspend. The eluted protein was collected by centrifugation at 15 000 x g for 10 seconds at room temperature. Eluted protein was visualised on an SDS-PAGE gel, as described in sections 2.6.11 and 2.6.12.

2.6.7. Small scale protein purification – Qiagen Ni-NTA Spin kit

The Qiagen Ni-NTA spin kit (Qiagen) was used as an alternative method for the purification of small volumes of his-tagged proteins from B-PER protein extractions (Section 2.6.2). This kit relies on changes in pH for the binding and elution of the protein of interest. Briefly, the column membrane was equilibrated with 600 µl of Qiagen Buffer B (7 M urea, pH 8.0). The flow through was collected by centrifugation at 890 x g for 2 minutes at room temperature with the column lid open. To the equilibrated column, 600 µl of soluble lysate was added and the unbound flow through was collected by centrifugation at 270 x g for 5 minutes at room temperature. The column was washed twice with 600 µl of Qiagen Buffer C (8 M urea, pH 6.3) followed by collecting of the flow through at 890 x g for 2 minutes at room temperature. The his-tagged protein was eluted off the column membrane with two consecutive elutions using 200 µl of Qiagen Buffer E (8 M urea, pH 4.5), followed by centrifugation at 890 x g for 2 minutes at room temperature. The soluble lysate, flow through, wash flow through and elutions were visualised on an SDS-PAGE gel, as described in sections 2.6.11 and 2.6.12.

2.6.8. Small scale protein purification – His-Select Nickel Affinity Gel

His-select Nickel Affinity Gel (Sigma) was used for the purification of small volumes of his-tagged proteins from B-PER protein extraction (Section 2.6.2) and for the purification of cleaved, dialysed proteins (Section 2.6.5). The purification was performed as per the manufacturer's instructions. All of the steps were performed at room temperature. Briefly, 50

µl of his-select gel was harvested by centrifugation at 5 000 x g for 30 seconds. The gel was washed twice with distilled water, centrifuging at 5 000 x g for 30 seconds. The gel was equilibrated with 250 µl equilibration/wash buffer (50 mM sodium phosphate, 300 mM sodium chloride, pH 8.0), mixed well by tapping and collected by centrifugation at 5 000 x g for 30 seconds. To purify his-select proteins, 100 µl of soluble lysate was mixed with the equilibrated gel for 1 minute and the flow through was collected at 5 000 x g for 30 seconds. The gel was washed twice with 500 µl equilibration/wash buffer and centrifuged at 5 000 x g for 30 seconds. The his-tagged proteins were eluted off the gel with 50 µl elution buffer (50 mM sodium phosphate, 300 mM sodium chloride, 250 mM imidazole, pH 8.0), by mixing the elution buffer and gel and centrifuging at 5 000 x g for 30 seconds. For the purification of dialysed proteins, Buffer D (50 mM Tris-HCl, 150 mM sodium chloride, 5 mM imidazole, 5% (v/v) glycerol) was used as the equilibration/wash buffer and Buffer C (50 mM Tris-HCl, 150 mM sodium chloride, 500 mM imidazole, 5% (v/v) glycerol) as the elution buffer. The soluble lysate, flow through, washes and elution were visualised on an SDS-PAGE gel, as described in sections 2.6.11 and 2.6.12.

2.6.9. Large scale protein purification – His-Select Nickle Affinity Gel

His-select Nickel Affinity Gel (Sigma) was also used for large scale protein purification of his-tagged proteins. Cells were lysed by French press and the soluble lysate collected by centrifugation, as described in Section 2.6.3. Large scale purification was carried out using an 8 ml his-select nickel affinity gel column connected to a Biologic LP system (Biorad). The nickel affinity column was equilibrated by washing with 30 ml of Buffer D (50 mM Tris-HCl, 150 mM sodium chloride, 5 mM imidazole, 5% (v/v) glycerol), charging with 30 ml of 50 mM nickel chloride and washing again with 60 ml of Buffer D, all at a flowrate of 1 ml/minute. A large 1 L culture of the desired protein expressing strain was grown at 37°C with shaking at 100 rpm and induced overnight at 22°C using 1 mM IPTG, as described in section 2.6.1. Cultures were centrifuged at 4 000 x g for 15 minutes at 4°C to harvest the cells and the collected cells were lysed in the French press, as described in section 2.6.3. The soluble lysate was loaded onto the equilibrated his-select nickel affinity gel column at a flowrate of 1 ml/minute. Flow through containing any unbound protein was collected in 1 ml aliquots after 10 and 15 minutes. The column was washed with 60 ml of Buffer D at a flowrate of 1 ml/minute and three 1 ml aliquots of the wash were collected after 15, 30 and 45 minutes respectively. The desired his-tagged protein was eluted off the column with a 30 ml gradient of 250 to 500 mM imidazole (Buffer C – 50 mM Tris-HCl, 150 mM sodium

chloride, 500 mM imidazole, 5% (v/v) glycerol), at a flow rate of 1 ml/minute. The elution was collected in 3 ml fractions and quantified on the Nanodrop ND100 at 280 nm, as described in section 2.4.1. Peaks from the quantification where visualised on an SDS-PAGE gel, as described in section 2.6.11 and 2.6.12. Imidazole and pH optimisations were performed as described in section 3.3.1, 3.3.2, 3.5.1 and 3.5.2. These optimised variables were used for the large scale purifications, i.e. pH 7.6 for RipA binding, pH 8.6 for RipA eluting, pH 8.0 for RpfB binding and eluting and an imidazole concentration of 20 mM in the wash buffer (Buffer D).

2.6.10. High salt wash

A high salt wash was used to clean protein elutions and to minimise non-specific binding of proteins to the his-select nickel affinity gel. Elutions to be cleaned were pooled together and loaded onto 8 ml of pre-equilibrated his-select nickel affinity gel column at a flow rate of 1 ml/minute. The column was equilibrated by washing with 30 ml of Buffer D, charging with 30 ml 50 mM of nickel chloride, followed by a subsequent wash using 60 ml Buffer D, all at a flow rate of 1 ml/minute. The protein loaded his-select nickel column was washed using 60 ml high salt wash buffer (Buffer E – 50 mM Tris-HCl, 300 mM sodium chloride, 5 mM imidazole, 5% (v/v) glycerol, pH 8.0). The wash was batch collected in a 50 ml falcon tube. Protein was re-eluted off the his-select nickel column using 20 ml of a 250 to 500 mM imidazole gradient (Buffer C) at a flow rate of 1 ml/minute. The elution was collected in 4 ml fractions and quantitated on the Nanodrop ND100 at 280 nm, as described in section 2.4.1. The pooled elutions, pooled wash and re-eluted fractions were visualised on an SDS-PAGE gel, as described in section 2.6.11. and 2.6.12.

2.6.11. Sodium dodecyl sulphate-polyacrylamide electrophoresis gels (SDS-PAGE)

SDS-PAGE gels were used to visualise protein fractions and cell lysates. SDS-PAGE gels of the desired concentration were prepared by combining Tris-HCl buffer, 40% (w/v) bis-acrylamide, 10% (w/v) SDS, 10% (w/v) ammonium persulfate (APS) and TEMED to a final concentration of 0.125 M Tris-HCl, 0.1% (w/v) SDS, 0.1% (w/v) APS and 0.1% (v/v) TEMED, as described in Table 2 below. The resolving gel was cast first in the Biorad casting system and levelled off using a small volume of isopropanol. The gel was allowed to solidify at room temperature for 30 minutes. The isopropanol was poured off the gel and the stacking gel was prepared and poured on top of the resolving gel in the casting system. The well comb was inserted, and the stacking gel was left to solidify at room temperature for 30 minutes.

The gels were placed in the running tank, filled with 1x SDS-PAGE running buffer (25 mM Tris, 200 mM glycine, 0.1% (w/v) SDS), and the combs were removed to allow sample loading. Protein samples to be analysed were mixed with an equal volume of 5x SDS-PAGE loading dye (62.5 mM Tris-HCl, 10% (v/v) glycerol, 2% (w/v) SDS, 5% (v/v) β-mercaptoethanol, 5% (w/v) bromophenol blue) and boiled at 95°C for 5 minutes. The boiled protein sample was then loaded into the wells of the stacking gel. For size determination, 5 µl of PAGE-Plus pre-stained protein ladder (Thermo Scientific) was loaded into the first well of the SDS-PAGE gel. SDS-PAGE gels were run at 85 V at room temperature until the dye front had migrated far enough in the gel (approximately 2 hours). SDS-PAGE gels were either stained with Coomassie R250 dye for visualisation (Section 2.6.12) or used for western blots (Section 2.6.13).

Table 3. SDS-PAGE gel recipes for two gels

	4% stacking gel	**12% resolving gel**	**15% resolving gel**
Distilled water	3.15 ml	6.9 ml	5.7 ml
40% (w/v) bis-acrylamide	0.5 ml	4.8 ml	6 ml
0.5 M Tris-HCl pH 6.8 (stacking)/0.5 M Tris-HCl pH 8.8 (resolving)	1.25 ml	4 ml	4 ml
10% (w/v) SDS	50 µl	160 µl	160 µl
10% (w/v) APS	50 µl	160 µl	160 µl
TEMED	5 µl	16 µl	16 µl

2.6.12. SDS-PAGE gel visualisation – Coomasie R250 staining

Coomasie R250 stain (0.1% (w/v) Coomasie R250, 40% (v/v) methanol and 10% (v/v) acetic acid) was used to visualise SDS-PAGE gels. Gels were removed from the gel casting plates, rinsed briefly in distilled water and stained overnight at room temperature in Coomasie R250 stain. The stain was poured off and stored for repeated usage. The gel was de-stained at room temperature in destaining solution (40% (v/v) methanol and 10% (v/v) acetic acid) with gentle agitation, until the bands of the protein samples were visible. For faster de-staining, the destaining solution was poured off and fresh destaining solution was added frequently.

2.6.13. Western blot – Biorad Transblot system

Western blot with an anti-his conjugate antibody (Sigma) was used to verify the expression of his-tagged proteins. Duplicate SDS-PAGE gels were run, as described in section 2.6.11. One gel was stained for band visualisation as described in section 2.6.12 and the other gel was used for western blotting. The western blot gel was rinsed in distilled water and layered with a methanol-equilibrated PVDF membrane (Biorad) in the transblot transfer cassette (Biorad), as per the manufacturer's instructions. Proteins from the SDS-PAGE gel were transferred to the PVDF membrane at 2.5 A for 10 minutes. The PVDF membrane was incubated in blocking solution (5% (w/v) skim milk powder, 20 mM Tris, 140 mM sodium chloride, 0.1% (v/v) Tween 20, pH 7.6) overnight at 4°C. The anti-his conjugate antibody was added to the blocking solution in a 1:25 000 antibody to blocking solution ratio and incubated at room temperature for 30 minutes to allow antibody binding. To wash away any unbound antibody, the membrane was washed three times in TBST wash buffer (20 mM Tris, 140 mM sodium chloride, 0.1% (v/v) Tween 20, pH 7.6) for 5 minutes on a rocking platform at room temperature. The washed membrane was transferred to a hybridization bag and 1 ml of freshly prepared chemiluminescent peroxidase substrate 1 (Sigma) was added. The substrate was dispersed so that it evenly covered the membrane without any bubbles, and this was incubated at room temperature for 10 minutes. Excess substrate was squeezed from the hybridization bag and the bag sealed. In the dark, the membrane was exposed to x-ray film for 30 seconds to 2 minutes. The x-ray film was developed manually by washing in x-ray film developer (Axim) for 1 minute followed by distilled water for 1 minute. The x-ray film was then incubated in fixative (Axim) for 1 minute and rinsed in distilled water for 1 minute. X-ray films were air dried prior to analysis.

2.7. Protein activity assays

2.7.1. MUF-triNAG activity assay

The muralytic activity of the recombinant proteins was evaluated by testing their ability to cleave a fluorescent peptidoglycan homologue, 4-methylumbelliferyl-*β*-*N'*,*N''*,*N'''*-triacetylchitotrioside (MUF-triNAG). This method was adapted from (Mukamolova *et al.*, 2006; Telkov *et al.*, 2006) and is based on the principle of fluorescent dye release upon cleavage of the substrate. Briefly, the enzyme to be tested was incubated with 8 mM MUF-triNAG substrate in 50 mM citrate buffer pH 6.0 (41 mM sodium citrate, 9 mM citric acid) and 5 mM magnesium sulphate at 37°C for 3 hours. The release of the fluorescent molecule

was measured at an excitation wavelength of 360 nm and emission wavelength of 450 nm on the Spectramax Gemini Plate reader (Spectramax).

2.7.2. FITC activity assay

The muralytic activity of the recombinant proteins was alternatively evaluated using the FITC assay. This assay measures the release of fluorescein isothiocyanate (FITC) during the enzymatic cleavage of FITC-labelled peptidoglycan.

2.7.2.1. *M. smegmatis* peptidoglycan extraction

M. smegmatis cell wall was used for peptidoglycan extraction. This method was adapted from (Rezwan *et al.*, 2007). A 100 ml culture of *M. smegmatis* was grown at 37°C to an OD_{600} of 0.8. The cells were harvested by centrifugation at 3 500 x g for 10 minutes at room temperature and re-suspend in cell fractionation buffer (0.05 M potassium phosphate, 0.022% (v/v) β-mercaptoethanol, pH 6.5). The cells were lysed through three rounds of sonication on ice for 20 minutes. Un-lysed cells were harvested by centrifugation at 1 000 x g for 10 minutes at room temperature. The lysate was centrifuged in the Optima max ultracentrifuge (Beckman) at 27 000 x g at 4°C for 200 minutes, to harvest the cell wall material. The cell wall pellet was re-suspended in fractionation buffer and sonicated on ice for 20 minutes. The lysate was centrifuged at 27 000 x g for 40 minutes at 4°C to collect the peptidoglycan. The peptidoglycan was air dried, weighed and stored at 4°C until use.

2.7.2.2. Peptidoglycan labelling with FITC

The extracted peptidoglycan was labelled with FITC (Invitrogen) according to the manufacturer's instructions. Briefly, dried peptidoglycan was dissolved in 100 mM sodium carbonate buffer pH 8.5 to a final concentration of 2 mg/ml. The FITC dye was solubilised in dimethyl sulfoxide (DMSO) to a concentration of 10 mg/ml. To the solubilised peptidoglycan, 100 µl of solubilised FITC dye was added and mixed. The mixture was incubated overnight in the dark with shaking at room temperature. The labelled peptidoglycan was collected by centrifugation at 13 000 x g for 10 minutes at room temperature. Any unbound dye was washed off with distilled water, followed by harvesting of the labelled peptidoglycan by centrifugation at 13 000 x g for 10 minutes at room temperature between washes, until the wash was completely clear. The labelled peptidoglycan was re-suspended in 50 mM monosodium phosphate pH 6.0 and stored at -20°C until use.

2.7.2.3. FITC-Peptidoglycan cleavage assay

The cleaving capabilities of RipA and RpfB were evaluated by incubating 25 µg of each protein with 50 µg of FITC-labelled peptidoglycan at 37°C for 3 to 5 days in the dark. Each reaction was centrifuged after 5 days at 13 000 x g for 10 minutes at room temperature to collect the peptidoglycan. Fluorescence resulting from the cleavage of the FITC-labelled peptidoglycan was measured in the supernatant at an excitation wavelength of 492 nm and an emission wavelength of 515 nm using the Spectramax Gemini plate reader (Spectramax).

2.7.3. Remazol brilliant blue dye release assay

The remazol blue dye release assay was performed as an alternative muralytic activity assay for the recombinant proteins. This assay measures the release of remazol blue dye from cell wall material via enzymatic cleavage.

2.7.3.1. Cell wall labelling with remazol brilliant blue dye

Mi. luteus cells were labelled with remazol brilliant blue dye as previously described (Zhou, Chen and Recsei, 1988). Briefly, lyophilised cell wall from *Mi. luteus* (Sigma) was incubated in 0.25 M sodium hydroxide with 0.02 M remazol brilliant blue dye at 37°C for six hours. This was followed by incubation at 4°C for 12 hours. The labelled cell wall was washed repeatedly with distilled water to remove any unbound dye until the supernatant was colourless.

2.7.3.2. Remazol brilliant blue-cell wall cleavage assay

The cleavage capabilities of RipA and RpfB were evaluated by incubating 25 µg of each protein with 50 µg remazol brilliant blue labelled-cell wall in 1x cleavage reaction buffer (12.5 M Tris, 2.5 M magnesium chloride, 12.5 M potassium chloride, 0.5 M manganese chloride, 0.0025% (v/v) Tween 20, 25 mM potassium dihydrogen phosphate, pH 5.75) for 3 to 5 days at 37°C. The reactions were centrifuged at 13 000 x g for 10 minutes at room temperature to collect the cell wall. Optical density of the supernatant was measured at 595 nm on the Spectramax Plus 384 plate reader (Spectramax).

2.7.4. Zymography

Zymography was used as an alternative, non-fluorescent assay to test the lytic activity of recombinant RipA and RpfB. This assay measured lytic ability based on the digestion of peptidoglycan embedded in an SDS-PAGE gel. To prepare the gel, freshly extracted peptidoglycan, prepared as described in section 2.7.2.1, was added to the resolving SDS-

PAGE gel before the gel was cast. The proteins of interest were analysed on the peptidoglycan-SDS-PAGE gel, as described in section 2.6.11. After protein separation by SDS-PAGE, the gel was washed by shaking at room temperature in zymography renaturation buffer (25 mM Tris, 1% (v/v) Tween 20, pH 6.5) for 30 minutes. Fresh buffer was added to the gel, followed by incubation at 37°C overnight, with gentle agitation. Lytic regions were visualised by viewing the gel on the SynGene Gbox with Snapgene version 7.12 acquisition software. During incubation, active recombinant proteins in the peptidoglycan-SDS-PAGE gel are expected to digest the surrounding peptidoglycan thus creating a zone of clearance in the gel.

2.8. Carbon starvation assay

Non-culturable cells were generated by the carbon starvation assay, adapted from (Saito *et al.*, 2017) by a colleague in our lab (Padarath, K, unpublished). Briefly, *Mtb* cells were cultured in 7H9 supplemented with OADC and 0.05% (v/v) Tween 80 at 37°C to an OD_{600} between 0.4 and 0.8. The culture was split into two equal volumes and harvested by centrifugation at 3 800 x g from 10 minutes at room temperature. One half of the culture was washed twice in 25 ml phosphate buffered saline (PBS) and the other in 25 ml 7H9 media, followed by centrifugation at 3 800 x g for 10 minutes at room temperature to harvest the cells after each wash. The cells were re-suspended in 25 ml of PBS and 7H9 respectively and centrifuged at 200 x g to remove large clumps of cells and obtain a single cell suspension. The single cell suspension was aspirated out of the falcon tube, leaving approximately 5 ml behind which contained clumped cells. The single cell suspension in PBS was diluted to an OD_{600} of 0.1 in PBS and starved at 37°C for a minimum of two weeks. The control single cell suspension in 7H9 media was used to enumerate the initial bacterial load by colony forming units (CFUs) and most probable number assay, as described in sections 2.9.1 and 2.9.2.

2.9. *In vitro* resuscitation assays

2.9.1. Most-probable number assays (MPN assays)

Most probable number assays were performed to enumerate bacterial cells in liquid media using the Poisson distribution based calculation (McCrady, 1915). For MPN assays carried out in 48-well microtitre plates, 450 µl of media was inoculated with 50 µl of inoculum for each dilution. For MPN assays carried out in a 96-well microtitre plates, 20 µl of the inoculum was inoculated into 180 µl of media for each dilution. Microtitre plates were sealed with biohazard tape and incubated at 37°C for 3 to 5 weeks, before plates were visually

scored. Data from scored plates was analysed in the MPN calculator programme version 2 (United States Environmental Protection Agency) for enumeration of the bacteria by Poisson distribution.

2.9.2. Colony forming units assay (CFU assays)

CFU assays were used to enumerate bacteria on solid media. The necessary 10-fold dilutions from the MPN microtitre plate (Section 2.10.1) were spread onto BBL 7H11 solid agar plates or noble agar plates (Difco) supplemented with recombinant Rpfs. For full plates (~ 25 ml), 100 µl of the MPN dilution were plated and for quarter plates (~ 7.5 ml), 25 µl of the MPN dilution were plated. Agar plates were incubated at 37°C for 5 weeks and manually scored. The CFUs/ml were manually calculated using the following equation:

$$\textbf{CFUs/ml} = \frac{\textbf{number of colonies} \times \textbf{dilution factor}}{\textbf{volume plated in ml}}$$

2.9.3. Mycobacterial growth indicator tube assays (MGIT assays)

Mycobacterial growth indicator tube (MGIT) assays were used to detect the growth of mycobacteria. This automated liquid media assay measures oxygen depletion during bacterial growth via an oxygen-quenched fluorochrome. The time to positivity (TTP) of the fluorochrome provides an indication of bacterial growth. Each MGIT tube was supplemented with 800 µl freshly prepared OADC/PANTA supplement (BD), as per the manufacturer's instruction, and inoculated with 400 µl decontaminated sputum or axenic culture. MGIT tubes were scanned and incubated in the BACTEC MGIT 960 machine at 37°C for 42 days to determine the TTP.

2.9.3.1. Media supplementation of MGIT cultures

In this study, MGIT tubes were supplemented with either CF, an endogenous source of Rpfs and growth factors, or recombinant Rpfs. CF was prepared by growing a culture of H37Rv to exponential phase (approximate OD_{600} of 0.8) and centrifugation at 3 800 x g to harvest the cells. The supernatant, containing all secreted molecules including Rpfs, was filtered through a 0.2 µm filter (Merck-Millipore) to remove any remaining cells. CF was added in a 1:1 ratio to media for *in vitro* assays. For recombinant protein supplementation, recombinant RipA and RpfB were added to 7H9 liquid media or MGIT media to a final concentration of 20 or 50 ng/ml.

2.10. Ethical considerations

Decontaminated sputum specimens utilised in this study were collected and stored for a larger study entitled the SNT study. The ethical clearance certificate for the collection and use of these specimens, M200164, can be seen in appendix A.

3. Results

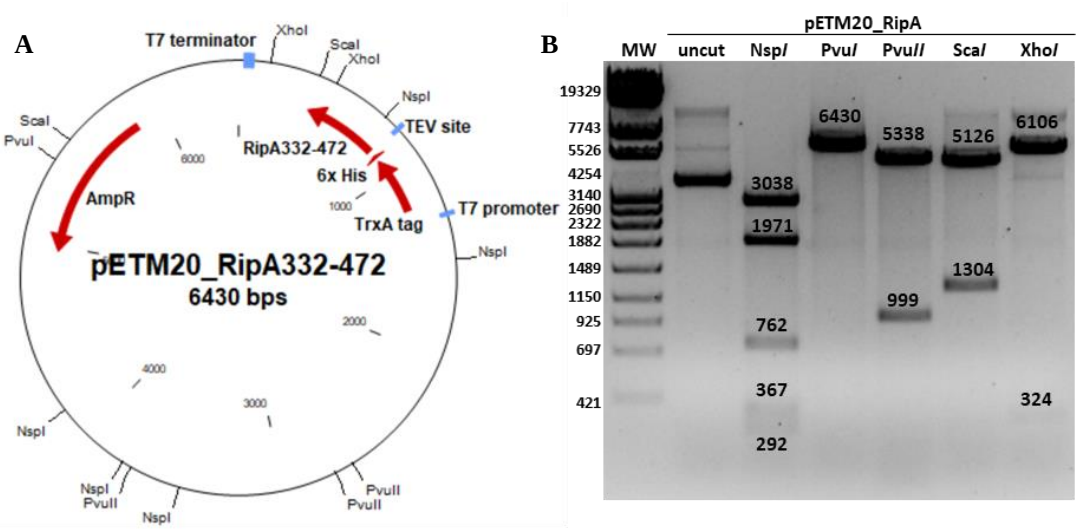
3.1. Confirmation of the pETM20_RipA$_{332-472}$ and pETM11_RpfB$_{280-362}$ vectors

The first objective of this study was to express and purify the catalytic regions of RipA and RpfB. Two vectors encoding the respective catalytic regions, pETM20_RipA$_{332-472}$ and pETM11_RpfB$_{280-362}$, were obtained from Alessia Ruggiero (University of Naples Federico II)(Ruggiero, Marasco, *et al.*, 2010; Squeglia *et al.*, 2013). These vectors were transformed into DH5α for amplification, as described in section 2.5. The respective plasmids were isolated using the Nucleobond Plasmid Extraction Kit (Machery-Nagel), as described in section 2.2.2. Each vector was profiled by restriction mapping, as described in section 2.3. (Figure 3.1). Restriction enzymes for mapping were chosen based on cleavage position to ensure the correct orientation of the respective gene segment and antibiotic resistance gene. Sequencing of each vector was also performed to confirm the absence of frame-shift mutations which would result in non-functional proteins (data not shown). Both vectors mapped correctly, producing the expected band sizes (Figure 3.1) and could be used for expression of their respective proteins. Each vector was transformed into BL21 (DE3) for expression as described in section 2.5. This strain was selected due to its expression of the T7 RNA polymerase, which binds to the T7 promoter found in both pETM11 and pETM20 vectors, thus allowing for the expression of the downstream gene of interest. Both transformations were successful and yielded efficiencies of 64 670 transformants per µg DNA and 65 000 transformants per µg DNA respectively.

3.2. Confirmation of the presence of His-affinity tags

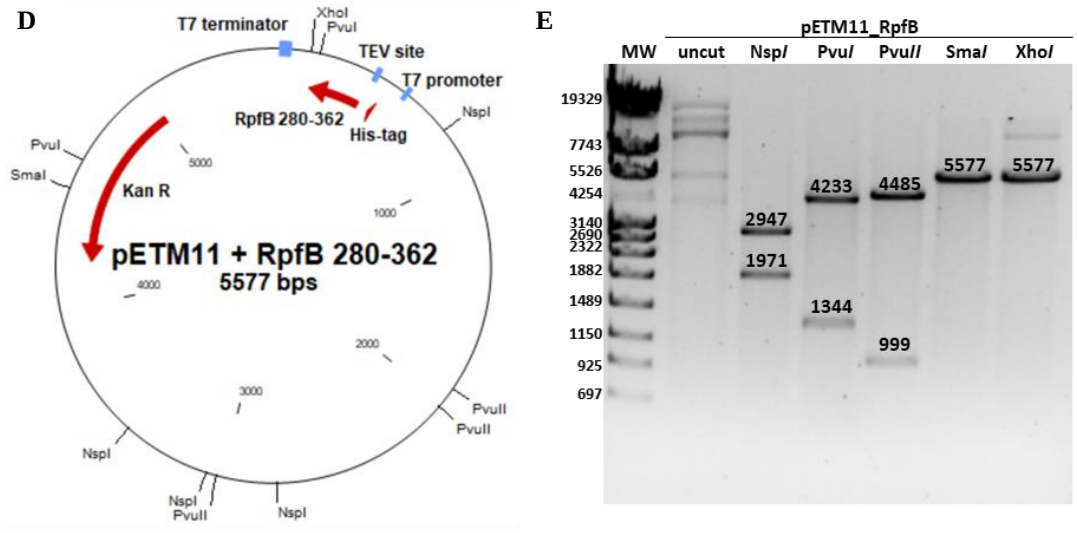
3.2.1. Western blots to confirm the presence of His-affinity tags

The vectors, pETM20_RipA$_{332-472}$ and pETM11_RpfB$_{280-362}$, both contain regions encoding histidine tags (his-tags) downstream of the inserted genes of interest. These tags can be used for affinity chromatography to isolate his-tagged proteins. To confirm expression of each protein, as well as the presence of the his-tag, a time course induction was performed over 22 hours. Cultures of RipA and RpfB were induced with 1 mM IPTG at 22°C, as described in section 2.6.1. Aliquots were taken at varying time points and the cells were harvested and lysed by re-suspension in BPER and protease inhibitor, as described in section 2.6.1 and 2.6.2. These aliquots were analysed on duplicate 12% SDS-PAGE gels, as described in section 2.6.11. One gel was stained with Coomassie R250, as described in section 2.6.12, and



C

Vector	Enzyme	No. of bands	Band sizes
pETM20_RipA	Nsp*I*	5	3038, 1971, 762, 367, 292
	Pvu*I*	1	6430
	Pvu*II*	3	5338, 999, 93
	Sca*I*	2	5126, 1304
	Xho*I*	2	6106, 324



F

Vector	Enzyme	No. of bands	Band sizes
pETM11_RpfB	Nsp*I*	4	2947, 1971, 367, 292
	Pvu*I*	2	4233, 1344
	Pvu*II*	3	4485, 999, 93
	Sma*I*	1	5577
	Xho*I*	1	5577

Figure 3.1. Confirmation of pETM20_RipA$_{332\text{-}472}$ and pETM11_RpfB$_{280\text{-}362}$ vectors by restriction digest. One microgram of vector DNA was digested with the appropriate enzyme at 37°C for 1 hour and analysed on a 1% (w/v) agarose gel. Both vectors mapped correctly (B and E) to their respective annotated maps (A and D), producing bands of the expected sizes respectively (C and F).

the other transferred to a PVDF membrane for Western blotting, as described in section 2.6.13.

Increasing expression of tagged-RipA (25 kDa protein), was observed over the 22-hour time course as seen on the SDS-PAGE gel (Figure 3.2a). The 25 kDa protein was also detected by western blot when probed with an anti-his antibody thus confirming the presence of the his-tagged protein (Figure 3.2a). Similarly, increasing expression of tagged-RpfB (12 kDa) was seen over the 22-hour time course by SDS-PAGE (Figure 3.2b). This protein was also detected when probed with an anti-his antibody during the western blot thus further confirming the presence of the his-tagged protein (Figure 3.2b). A decrease in the size of the band, indicative of the amount of protein, was observed at the last time-point for tagged-RipA due to a technical error, with some of the sample floating out of the well during protein loading. From these results, the induced his-tagged RipA and his-tagged RpfB could be used going forward for isolation of these two proteins.

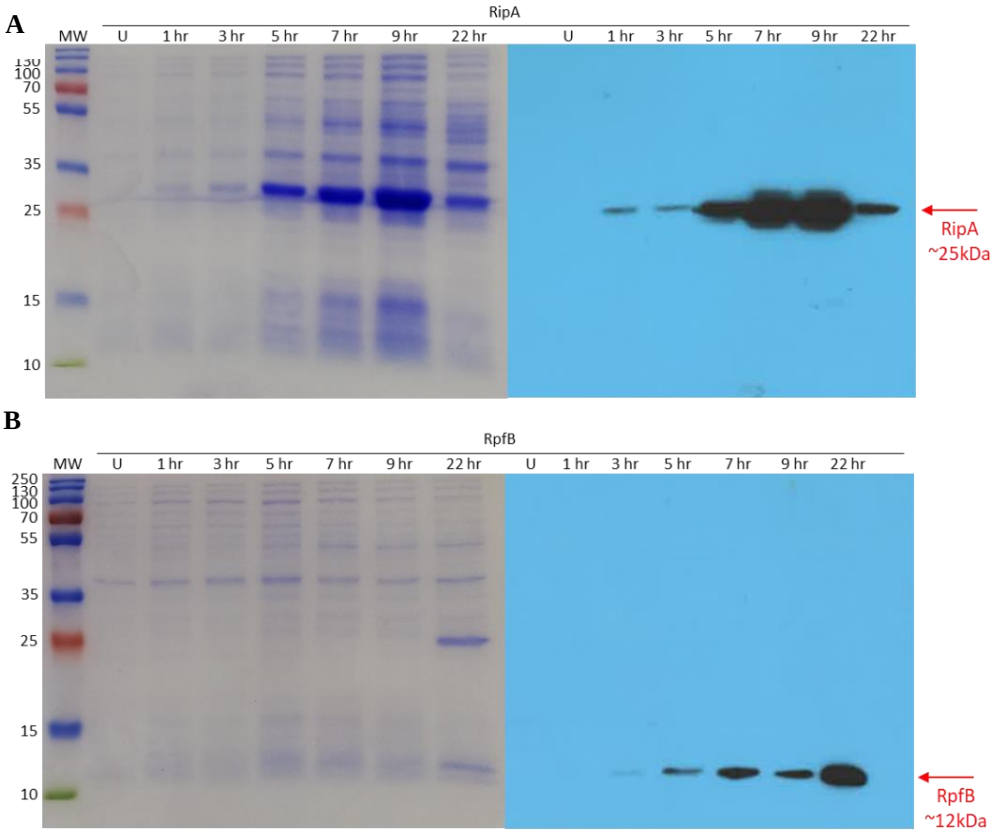


Figure 3.2. Time-course induction of his-tagged RipA (25 kDa) and his-tagged RpfB (12 kDa) protein expression. RipA (A) and RpfB (B) expression strains were induced with 1 mM IPTG at 22°C. Protein expression in both strains occurred in a time-dependent manner, producing visible protein bands of the correct sizes, compared to the uninduced control (U). Western blots with an anti-his conjugate antibody confirmed the presence of his-tags on both proteins.

3.2.2. Small scale purification using the His-affinity tags

To purify the his-tagged proteins, affinity chromatography was used to isolate his-tagged RipA and his-tagged RpfB from the small-scale protein extractions using 3 methods: the Zymo His-spin Protein Mini-prep kit (Zymo research), Qiagen Ni-NTA Spin Kit (Qiagen), and a small-scale His-select Affinity gel purification (Sigma), as described in sections 2.6.6, 2.6.7 and 2.6.8. Protein expression was induced overnight at 22°C and cells were harvested and lysed using B-PER, as described in sections 2.6.1 and 2.6.2. The soluble fractions were used for protein isolation. Protein purification using the Zymo His-Spin Mini-prep kit was successful for the purification of his-tagged RipA, as seen by the large amounts of clean RipA, at approximately 25 kDa, from the eluent without any non-specific protein bands (Figure 3.3a). However, the Zymo His-Spin kit was unsuccessful in isolating any his-tagged RpfB proteins (Figure 3.3a). Tagged-RpfB was expressed, as seen by the 12 kDa band in the soluble cell lysate fraction (Figure3.3a); however, it was not eluted off the column. As washes and flow through were not saved for SDS-PAGE analysis, it is unknown whether the expressed protein was unable to bind to the his-select membrane and was lost in the flow through. Purification by the Qiagen Ni-NTA Spin kit was successful in isolating small amounts of both tagged-RipA and tagged-RpfB as seen in the elution fractions (Figure 3.3b). A large amount of tagged-protein, both tagged RipA and tagged-RpfB, was lost in the flow through (Figure 3.3b). The elution of tagged-RipA and tagged-RpfB was also not very clean using this method, as evidenced by the presence of other non-specific proteins eluting off the column with the desired proteins of interest (Figure 3.3b). Protein purification in small scale using the His-Select Nickel Affinity gel (Sigma) was also successful when evaluated for isolating tagged-RipA and tagged-RpfB and generated the largest yield of the respective proteins of interest (Figure 3.3c). Therefore, the his-select nickel affinity gel method was used in all subsequent experiments for upscaling RipA and RpfB expression and purification.

3.3. Optimization of the conditions for RipA expression and purification

3.3.1. pH optimization

The cleanliness and specificity of protein purification is pH dependent. pH can affect the binding affinity of other proteins to the isolation medium, and by doing so allow non-specific proteins, which are less tightly bound, to be eluted off the medium during washing steps. This results in cleaner elutions of the desired protein, which is usually more tightly bound to the isolation medium (Bornhorst and Falke, 2000; Adhikari *et al.*, 2010). A range of pHs were

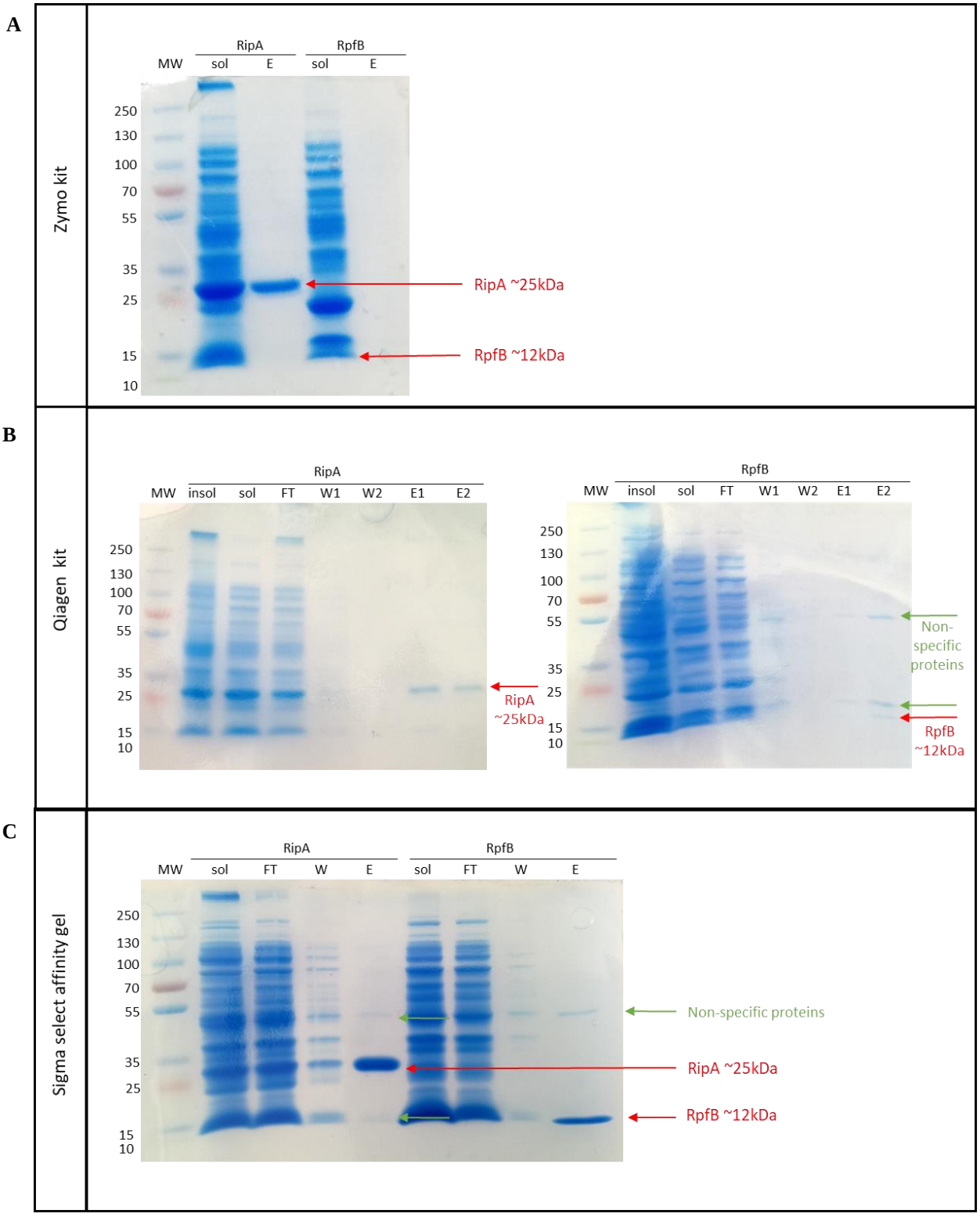


Figure 3.3. The small-scale purification of his-tagged RipA and his-tagged RpfB from the soluble lysate of RipA and RpfB strains. Three methods were evaluated: Zymo his-spin protein mini-prep kit (A), Qiagen Ni-NTA spin kit (B) and small-scale purification on Sigma his-select nickel affinity gel (C). The soluble lysate (sol) flow through (FT), washes (W) and elutions (E) were analysed on SDS-PAGE gels. The Sigma small scale purification on his-select nickel affinity gel was the most efficient at binding the his-tagged proteins of interest. Non-specific proteins were also purified on the his-selecting mediums and are indicated by the green arrows.

evaluated for their effects on the binding and elution of tagged-RipA and tagged RpfB. Protein expression was induced overnight at 22°C and cells were harvested and lysed using B-PER, as described in sections 2.6.1 and 2.6.2. The soluble fractions were applied to the his-select nickel affinity gel (Sigma) for small scale protein purification, as described in section 2.6.8. The amount of protein lost in the flow through, as well as the purity and the yield of the elution of his-tagged RipA and RpfB proteins, was evaluated for pH's ranging between 7.6 and 8.6.

Tagged-RipA was observed to bind optimally at lower pH, as seen by less tagged-RipA being lost in the flow through at lower pHs (Figure 3.4a and b). RipA eluted best at higher pHs, generating a cleaner, higher yield of tagged-RipA (Figure 3.4e and f). From these results, it was determined that the best pH to bind and wash tagged-RipA was pH 7.6 and the best pH to elute with was pH 8.6.

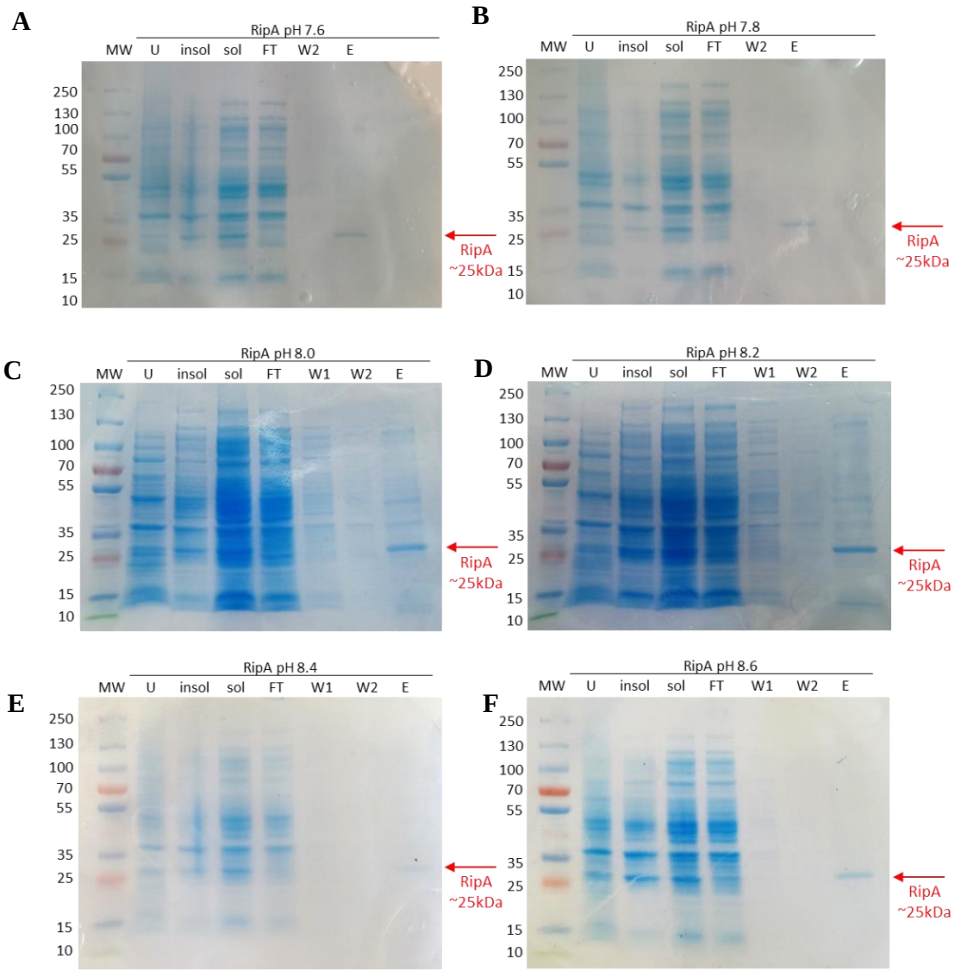


Figure 3.4. The pH optimisation of tagged-RipA purification on his-select nickel affinity gel. pHs ranging from pH 7.6 to pH 8.6 (A to F) were evaluated for their binding ability of his-tagged RipA (25 kDa) and the cleanliness of the elution of his-tagged RipA. The uninduced control (U), soluble (sol) and insoluble (insol) lysates, flow through (FT), washes (W1 and W2) and the elution (E) were analysed on SDS-PAGE gels. Tagged RipA bound more efficiently to the gel at lower pHs and eluted more cleanly at higher pHs.

3.3.2. Imidazole optimization

Imidazole competes with his-tagged proteins to bind to his-selecting resins. High imidazole concentrations outcompete weakly bound proteins, resulting in their elution from the his-selecting gel (Bornhorst and Falke, 2000). An increase in the imidazole concentration in wash buffers decreases the binding capabilities of weakly-binding non-specific proteins, resulting in a cleaner elution of the stronger bound protein of interest. To minimise the presence of non-specific proteins in the RipA elutions, a higher concentration of imidazole was evaluated for its ability to decrease the amount of non-specific binding to the affinity gel. The imidazole concentration in the binding and wash buffer was increased from 5 mM to 20 mM imidazole. For tagged-RipA, increasing the imidazole concentration improved the cleanliness of the elutions, reducing the amount of non-specific proteins in these fractions (Figure 3.5b). It was concluded that for future experiments, a higher concentration of imidazole, 20 mM, should be used for binding and washing of the his-tagged RipA on the his-select nickel affinity gel.

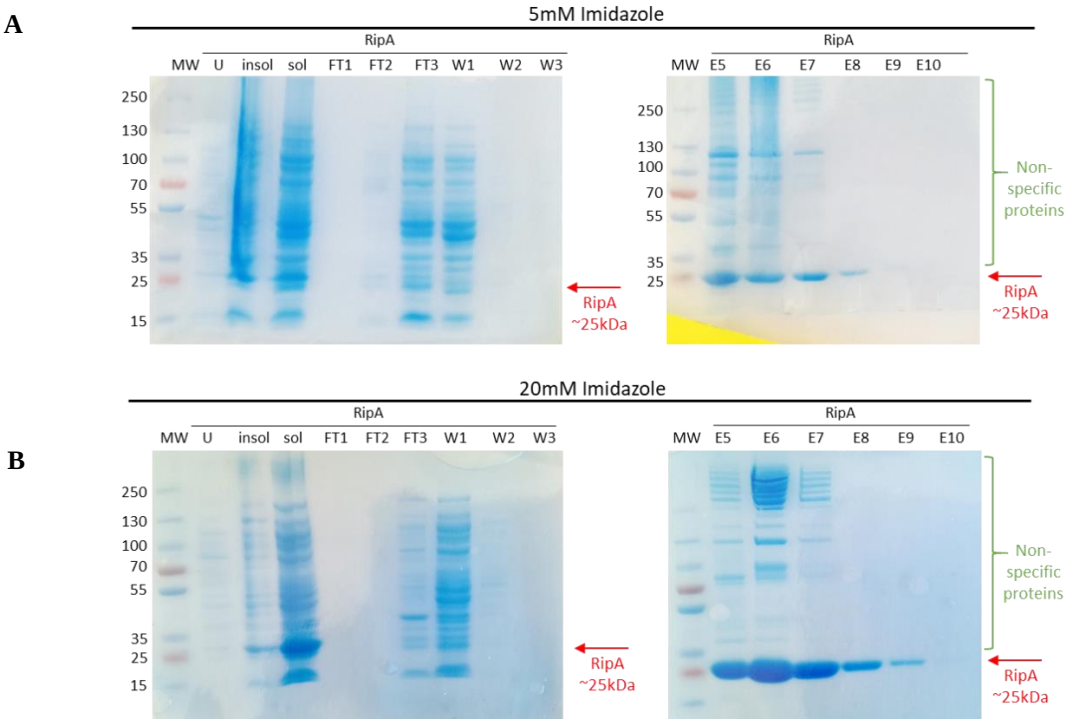


Figure 3.5. Imidazole concentration optimization for his tagged-RipA purification on his-select nickel affinity gel. The uninduced control (U), soluble (sol) and insoluble (insol) lysates, flow through (FT1 and FT2), washes (W1 and W2) and the elution (E) were analysed on SDS-PAGE gels. An increased imidazole concentration, from 5 mM (A) to 20 mM (B), decreased the amount of non-specific proteins (indicated by the green brackets) in the elution of tagged-RipA (E5 to E10).

3.3.3. Small scale RipA purification at the optimised conditions

Using the optimised pH and imidazole conditions, a small scale tagged-RipA purification was performed to validate these conditions. A 5 ml RipA pre-culture was grown overnight at 37°C with shaking at 100 rpm. This pre-culture was used to inoculate a 50 ml culture, which was grown to an OD_{600} of approximately 0.8 at 37°C with shaking at 100 rpm. The 50 ml culture was induced at 22°C overnight and lysed by French press, as described in sections 2.6.1 and 2.6.3. His-tagged RipA was isolated by running the soluble lysate on an 8 ml his-select nickel affinity gel column, as described in section 2.6.9. The protein concentrations of the elutions were measured by Nanodrop at 280 nm, as described in section 2.4.1. Protein concentrations peaked in elutions 5 to 10 (Figure 3.6a) and were analysed on an SDS-PAGE gel, along with the uninduced control, soluble and insoluble lysate, flow through and washes, as described in section 2.6.11. The elutions contained a significant amount of tagged-RipA (25 kDa) (Figure 3.6c). Some tagged-RipA did not bind to the column and was lost in the flow through and subsequent wash steps (Figure 3.6b). Elutions 5 to 8 contained other loosely bound, non-specific proteins; however, these elutions were considered clean enough for upscaling the extraction process to batch purify large quantities of tagged-RipA. A western blot of the SDS-PAGE gels was also performed, as described in section 2.6.13, and confirmed the presence of the his-tag on RipA at 25 kDa (Figure 3.6d and e). Due to the thickness of the protein band in elutions 5 to 8, transfer of these bands to the PVDF membrane during the western blot was not efficient, resulting in clear zones at the centre of each band.

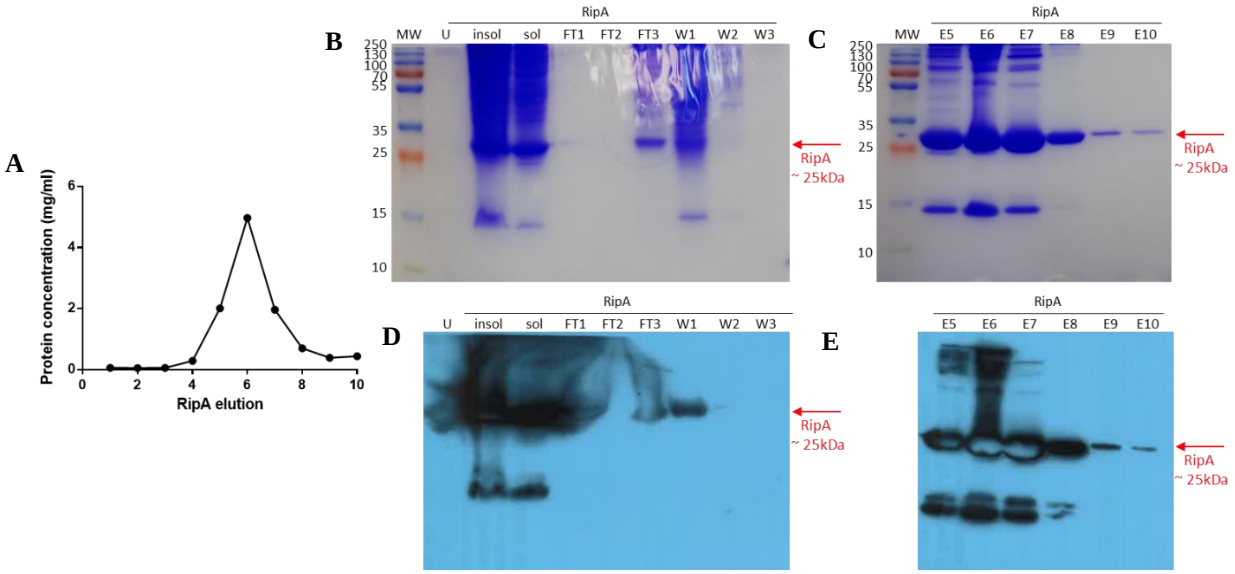


Figure 3.6. Small scale purification if his-tagged RipA on his-select nickel affinity gel at optimal pH and imidazole concentration. Tagged RipA was bound and washed at pH 7.8, in the presence of 20 mM imidazole, and eluted at pH 8.6. Protein concentrations peaked from elutions 5 to 10 (A) and were analysed on a 12% SDS-PAGE gel with the uninduced control (U), insoluble (insol) and soluble lysate (sol) (B and C). Western blot of the SDS-PAGE gels confirmed the maintenance of the his-tag used for the affinity purification (D and E).

3.4. Batch expression of RipA

3.4.1. Purification binding at pH 7.6 and eluting at pH 8.6

RipA was batch purified to maximise the amount of protein for downstream experiments. A 1L culture of RipA was induced overnight at 22°C and lysed by French press, as described in sections 2.6.1 and 2.6.3. His-tagged RipA was purified on an 8 ml His-select nickel affinity gel column, as described in section 2.6.12, using the optimised purification parameters in section 3.3.3. The protein concentrations of the elutions were determined by Nanodrop at 280 nm (Section 2.4.1). The protein concentrations peaked between elutions 4 and 10 (Figure 3.7a) and were visualised on an SDS-PAGE gel, as described in sections 2.6.11 and 2.6.12. A large amount of tagged-RipA was purified and collected in elutions 6 to 10 (Figure 3.7b and c). Despite the optimised purification conditions, other non-specific proteins were still present in the tagged-RipA elutions (Figure 3.7c). Further washing steps were required to minimise the quantity of these unwanted proteins in the elutions.

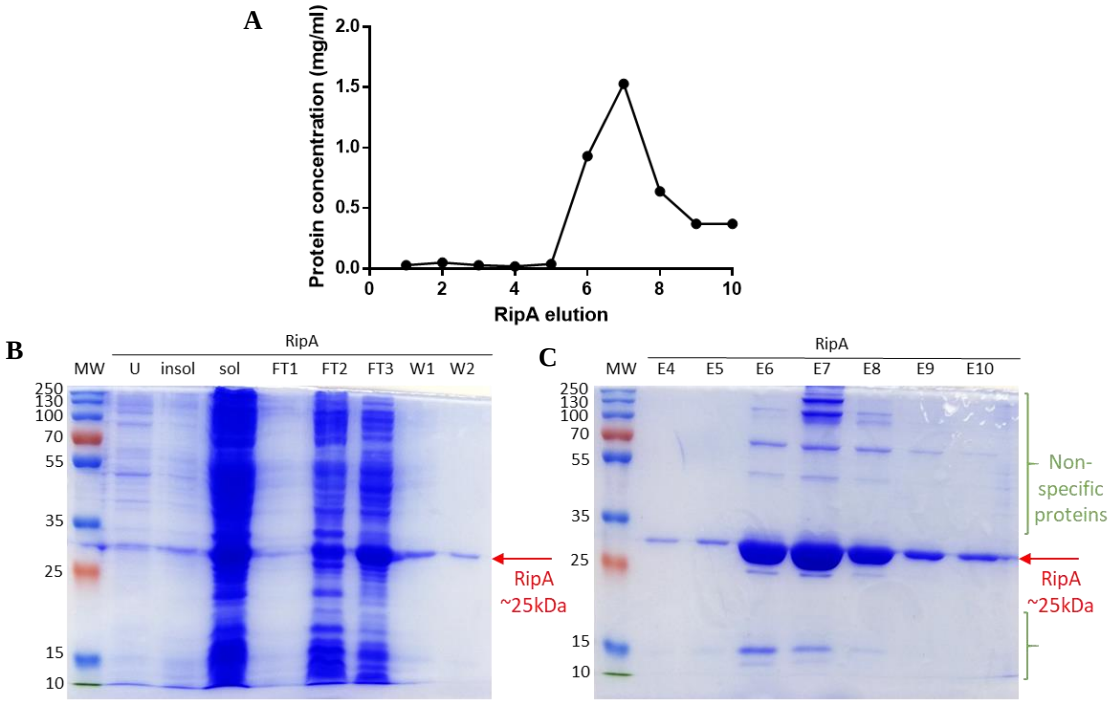


Figure 3.7. Batch purification of his-tagged RipA on his-select nickel affinity gel, binding at pH 7.6 and eluting at pH 8.6. Protein concentration of the elutions was determined by Nanodrop (A). The uninduced control (U), soluble (sol) and insoluble (insol) lysates, flow through (FT 1 to FT3), washes (W1 and W2) and the elution fractions containing the highest concentration of protein (E4 to E10) were analysed on an SDS-PAGE gel (B and C). A large amount of tagged-RipA bound the affinity gel column and was eluted in elutions 6 to 10. Some non-specific proteins were also eluted off the column at these optimised conditions (indicated by the green brackets).

3.4.2. Salt wash to remove non-specific binding proteins and aggregates

To minimise the presence of non-specific proteins and aggregated proteins in the purification elutions, a high salt wash was performed, as described in section 2.6.10. The high salt concentration weakens the binding of non-his tagged proteins, resulting in their elution from the column during the washing step (Bornhorst and Falke, 2000). More tightly bound his-tagged RipA will continue to bind to the column during the salt wash and will only be eluted during the imidazole elution gradient. Elutions 6 to 10 of the batch purification (Figure 3.7), containing the most tagged-RipA, were pooled and used for the high salt wash. The protein concentrations of the elutions from the salt wash was determined by Nanodrop (Figure 3.8a) and separated on a 12% SDS-PAGE gel, along with the pooled elutions, flow through and wash. Although a substantial amount of his-tagged RipA dissociated from the column during the high salt wash, the remaining tagged-RipA eluted off the column with fewer aggregates and less non-specific binding proteins (Figure 3.8b). Elution 5 from the salt wash contained relatively small amounts of non-specific proteins and aggregates and a substantial amount of tagged-RipA, as expected (Figure 3.8b). This elution, containing the most tagged-RipA, was used for subsequent experiments for tag removal.

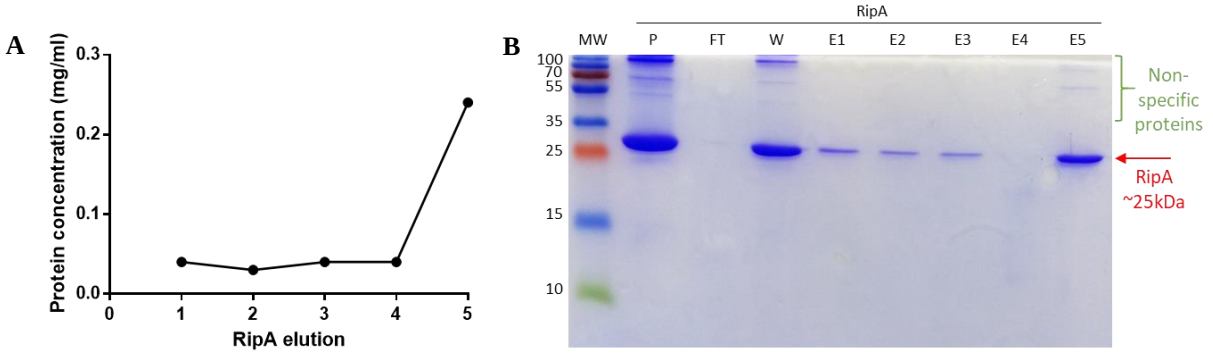


Figure 3.8. High salt wash of his-tagged RipA purification elutions to minimise non-specific binding proteins and aggregates. Pooled purification elutions were loaded onto his-select nickel affinity gel and washed with a high salt buffer before eluting off the gel column. The protein concentration of the elutions was determined by Nanodrop (A). The pooled elutions (P), flow through (FT), wash (W) and elutions (E1 to E5) were analysed on an SDS-PAGE gel (B). The salt wash removed most of the non-specific proteins and aggregates (indicated by the green brackets).

3.4.3. Affinity tag removal

Tag-removal was performed to minimise any inhibitory effects the purification tag may have on protein activity. The inhibitory effects were of particular concern for RipA, where the TrxA-His tag (approximately 10 kDa) was almost as large as the protein of interest (15 kDa).

Tag removal was performed on elution 5 of the salt wash by TEV digestion, as described in section 2.6.4. A time-course of the digestion was performed to observe the cleavage of the tag. Aliquots of the digestion reaction were collected every hour over 5 hours. The collected time-course aliquots were analysed on a 15% SDS-PAGE gel. Over time, the quantity of the 25 kDa tagged-RipA protein decreased while that of the tagless 10 kDa RipA protein increased (Figure 3.9).

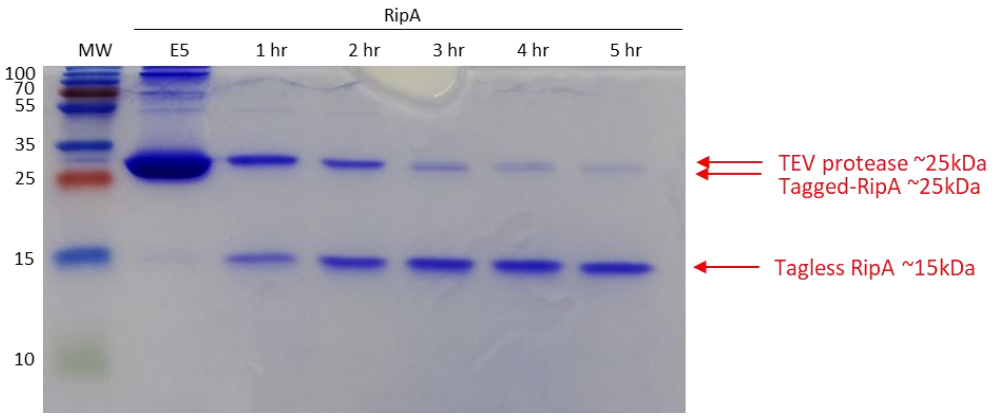


Figure 3.9. Time course digestion of his-tagged RipA by TEV protease at 37°C for the removal of the TxA-His tag. Cleavage of the tag from the his-tagged protein, from elution 5 of the salt wash (E5), resulted in more of the tagless 15 kDa RipA protein being present in the reaction and less of the tagged, 25 kDa RipA protein in the reaction over 5 hours. The cleavage enzyme, TEV protease, was almost indistinguishable from the tagged protein, with a similar size of ~25 kDa.

To remove the EDTA and DTT from the digestion reaction, dialysis buffer exchange was performed as described in section 2.6.5. This was performed to prevent chelation of the his-select nickel affinity gel during the purification of tagless-RipA.

3.4.4. Purification of tagless-RipA

Purification of tagless-RipA was performed using small-scale batch purification on the his-select nickel affinity gel, as described in section 2.6.8. Uncleaved tagged-RipA and the his-tagged TEV enzyme that were bound to the his-select gel were only eluted off the resin during the imidazole elution (Figure 3.10). The digestion reaction (pre- and post-dialysis buffer exchange), the flow through, washes and elution were all analysed on an SDS-PAGE gel. Tagless-RipA, lacking the his-tag, did not bind to the his-select affinity gel and was collected in the flow through (Figure 3.10); however, some residual tagless-RipA was present in the washes and elution. The flow through, containing tagless-RipA, was used for subsequent protein activity assays.

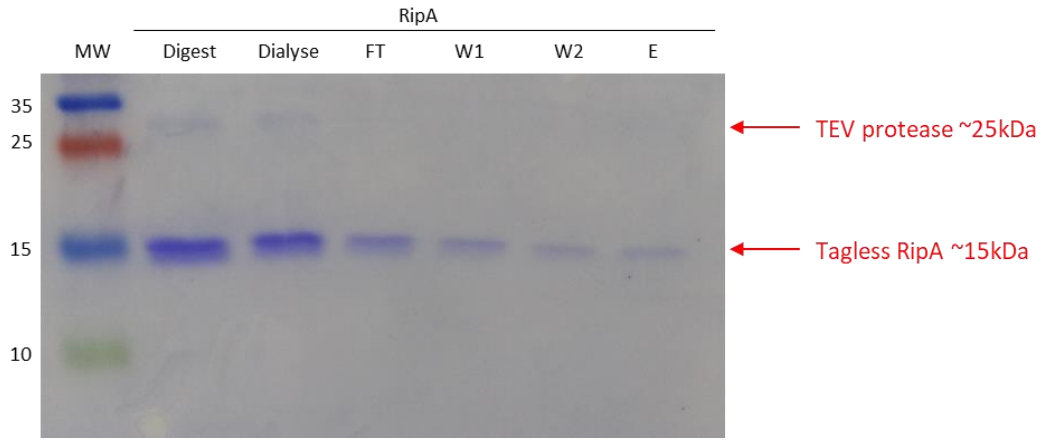


Figure 3.10. The purification of tagless-RipA on his-select nickel affinity gel. Tagless RipA was unable to bind to the his-select affinity gel and was collected in the flow through (FT). Undigested protein, still containing a his-tag, and the his-tagged digestion enzyme, TEV protease, bound to the affinity gel and were isolated from the tagless protein in the flow through. The digestion reaction (Digest), dialysed digestion reaction (Dialyse), the flow through, washes (W1 and W2) and the elution (E) were all analysed.

3.5. Optimization of the conditions for RpfB protein expression and purification

3.5.1. pH optimisation

Optimization of pH was also performed to determine the best pH at which to bind and elute pure his-tagged RpfB. A range of pHs from pH 7.6 to pH 8.6 were evaluated. Protein expression was induced overnight at 22°C and cells were harvested and lysed using B-PER as described in sections 2.6.1. and 2.6.2. The soluble fractions were applied to the his-select nickel affinity gel (Sigma) for small scale protein purification as described in section 2.6.8. The uninduced control, soluble and insoluble lysate, flow through, washes and elutions were visualised on an SDS-PAGE gel, as described in sections 2.6.11 and 2.6.12. Tagged-RpfB bound best at pH 8.0 and higher (Figure 3.11c to f) and at these pHs, very little variation in the amount of protein washing through the column in the flow through was observed (Figure 3.11c to f). No significant differences were observed in the yield and purity of the elutions between pH 8.0 and 8.6. (Figure 3.11c to f). As the tagged-proteins bind better at lower pHs, it was determined that the optimal pH to bind and elute tagged-RpfB, was pH 8.0, as recommended in the literature.

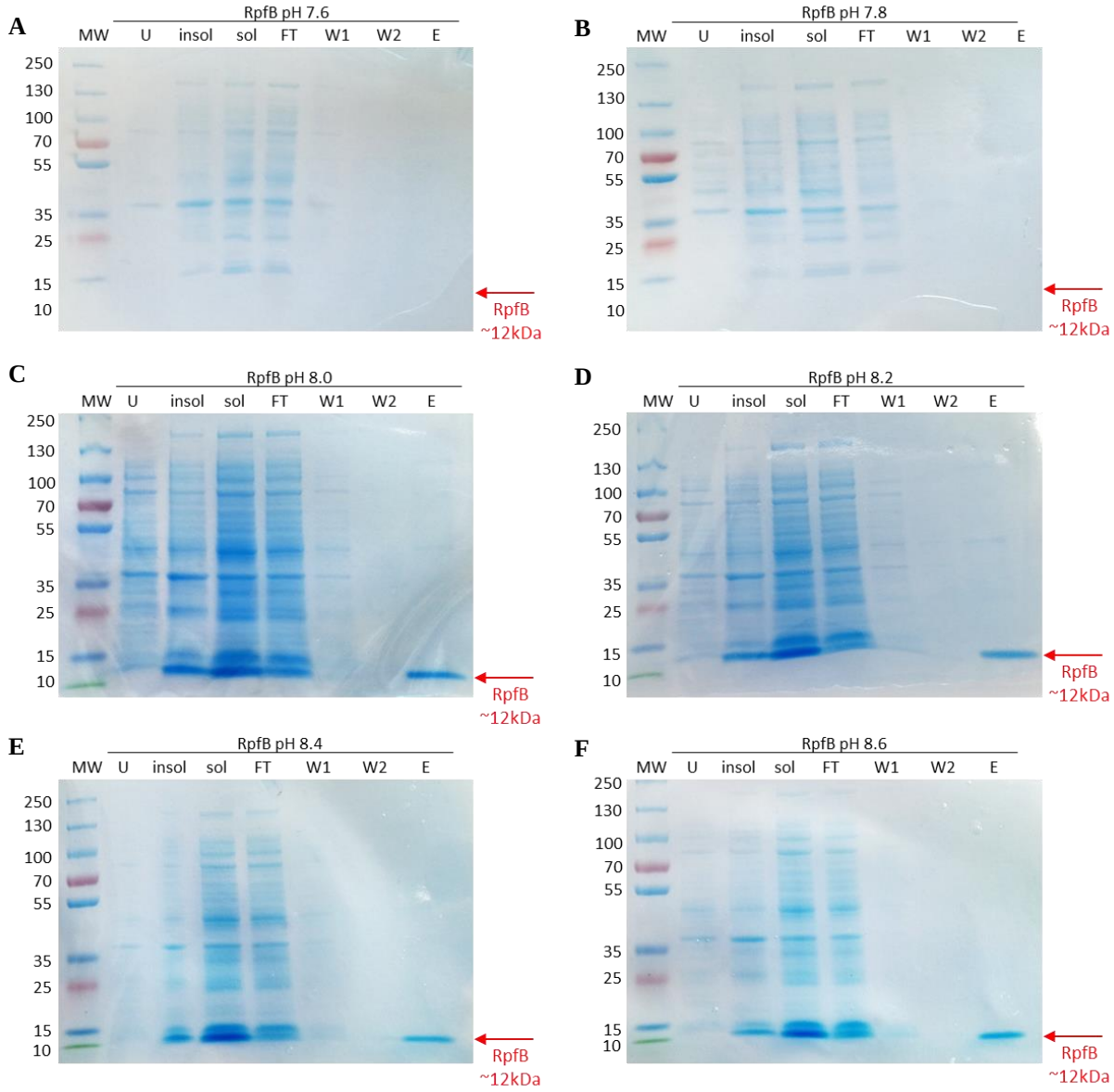


Figure 3.11. The pH optimisation of tagged-RpfB purification on his-select nickel affinity gel. pHs ranging from pH 7.6 to pH 8.6 were evaluated for their binding ability of his-tagged RpfB (12 kDa) and the cleanliness of the elution of his-tagged RpfB. The uninduced control (U), soluble (sol) and insoluble (insol) lysates, flow through (FT), washes (W1 and W2) and the elution (E) were analysed on SDS-PAGE gels for analysis (A to F). Tagged RpfB bound and eluted best at pHs 8.0 and above (C to F), with little variation in binding capability and elution cleanliness.

3.5.2. Imidazole optimization

To minimise the presence of non-specific binding proteins, different imidazole concentrations were evaluated for their effects on the cleanliness of tagged-RpfB purification. An increase in imidazole concentration in the wash buffer from 5 mM to 20 mM dramatically increased the cleanliness of RpfB elutions, with a noticeable reduction in the presence of non-specific proteins and aggregated tagged-RpfB in the elutions (Figure 3.12b). Therefore, 20 mM

imidazole in the wash buffer would be used in subsequent experiments for the purification of RpfB.

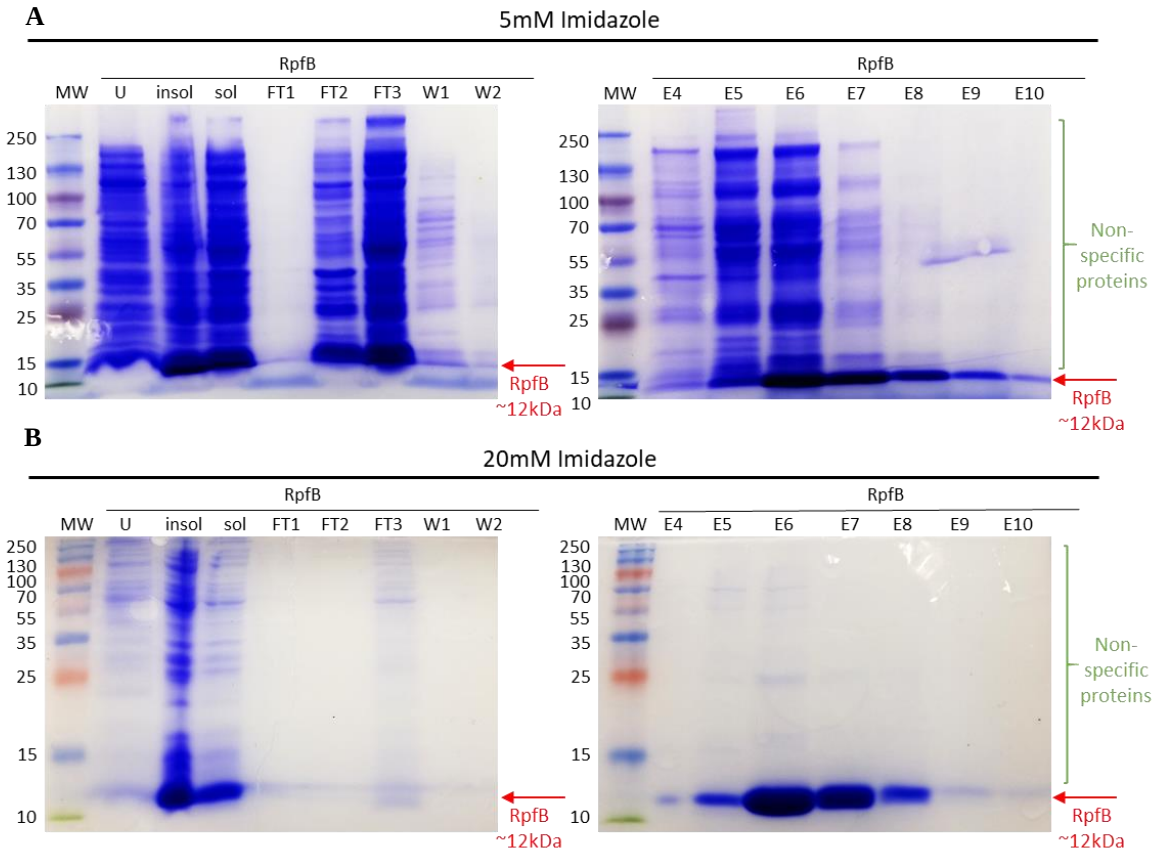


Figure 3.12. Imidazole concentration optimization for tagged-RpfB purification on his-select nickel affinity gel. The uninduced control (U), soluble (sol) and insoluble (insol) lysates, flow through (FT1 to FT3), washes (W1 and W2) and the elution (E) were analysed on SDS-PAGE gels. An increased imidazole concentration, from 5 mM (A) to 20 mM (B), decreased the quantity of non-specific proteins and RpfB aggregates (indicated by green brackets) in the elution of tagged-RpfB (E5 to E10).

3.5.3. Small scale RpfB purification at the optimised conditions

To validate the optimised purification conditions, a small-scale RpfB purification was performed on his-select nickel affinity gel, binding and eluting at pH 8.0 and washing with an imidazole concentration of 20 mM. A 50 ml RpfB culture was grown at 37°C, induced overnight at 22°C and lysed by French press as described in sections 2.6.1 and 2.6.3. The soluble lysate was purified on an 8 ml his-select column as described in section 2.6.9. The protein concentration of the elutions was determined by Nanodrop at 280 nm, as described in section 2.4.1. The protein concentrations were highest between elutions 5 and 10 (Figure 3.13a). These elutions were analysed on SDS-PAGE gels, along with the soluble and

insoluble lysate, flow through and washes. The lower molecular weight proteins (smaller than 15 kDa) did not stain well (Figure 3.13b and c); however, the western blot of the gels confirmed the presence of tagged-RpfB in the elutions (Figure 3.13d and e). The observation of non-specific proteins in the elutions was minimal, with a faint second band only seen in elution 6 by western blot (Figure 3.13e). These purification specifications were concluded to be clean enough for the upscaling of RpfB purification.

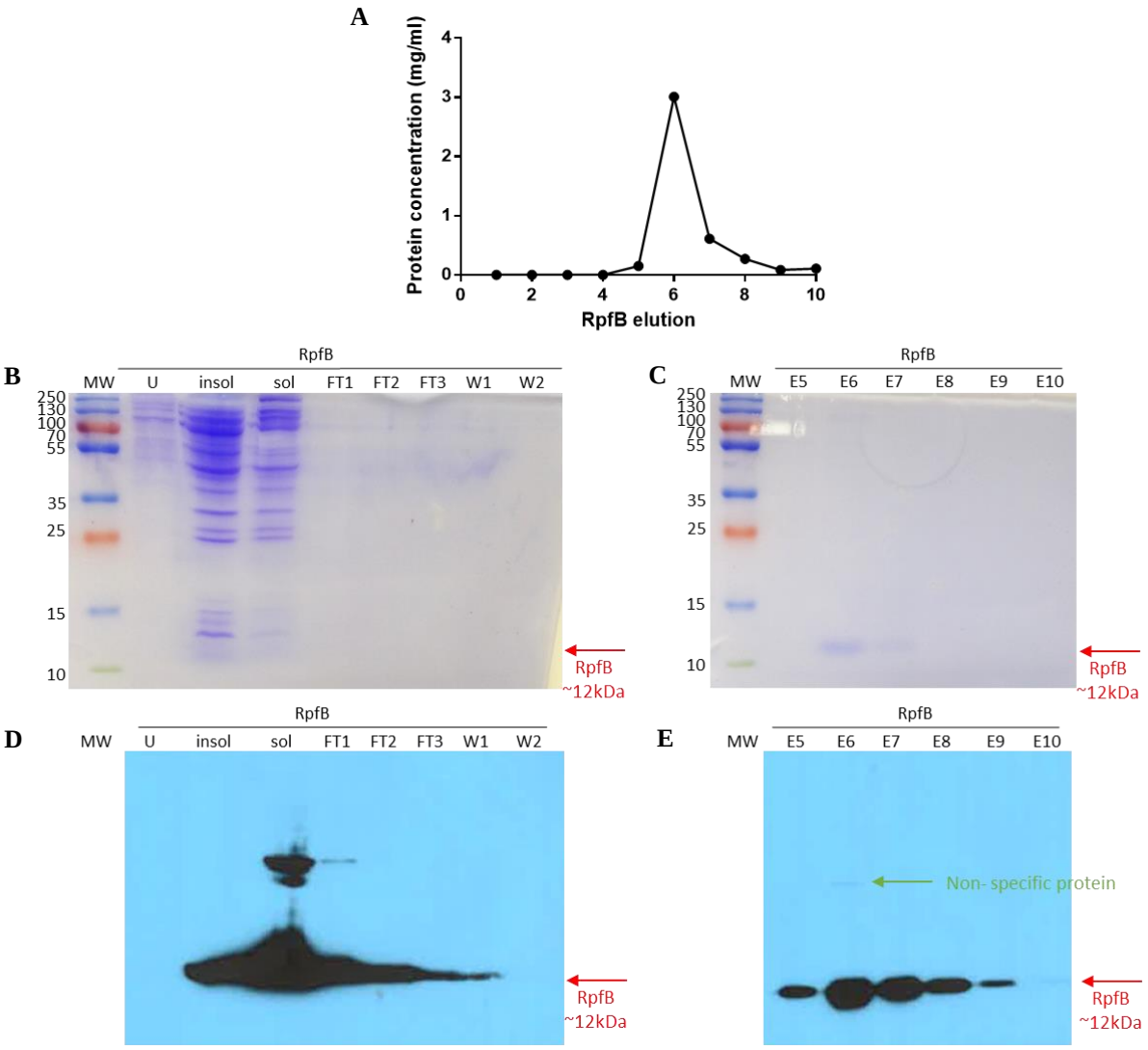


Figure 3.13. Small scale purification of his-tagged RpfB on his-select nickel affinity gel at optimal pH and imidazole concentration. Tagged-RpfB was bound and washed at pH 8.0, in the presence of 20 mM imidazole, and eluted at pH 8.0. Protein concentrations of the elutions were determined by Nanodrop (A) and the elutions with the highest protein concentrations (E5 to 10) along with the uninduced control (U), soluble (sol) and insoluble lysates (insol) were analysed on a 12% SDS-PAGE (B and C). Western blot confirmed the maintenance of the his-tag used for the affinity purification and the presence of tagged-RpfB in the elutions (D and E). A non-specific band of protein was present in elution 6 (indicated by the green arrow).

3.6. Batch expression of RpfB

3.6.1. Purification binding and eluting at pH 8.0

Like RipA, RpfB was batch purified to maximise the yield of protein for downstream experiments. A 1 L culture of RpfB was grown at 37°C, induced overnight at 22°C and lysed by French press, as described in sections 2.6.1 and 2.6.3. Tagged-RpfB was isolated on the his-select nickel affinity gel column at pH 8.0 for both binding and eluting, as described in section 2.6.9. Protein concentrations of the elutions were determined by Nanodrop at 280 nm and the elutions with the highest concentration of proteins, elutions 4 to 10 (Figure 3.14a), were visualised on a 12% SDS-PAGE gel with the lysate, flow through and washes, as described in sections 2.4.1 and 2.6.12. Some tagged-RpfB did not bind to the column and was lost in the flow through and washes; however, the majority of tagged-RpfB bound to the column and eluted off during the imidazole gradient elution (Figure 3.14b and c). Elutions 6 to 9 contained the highest concentrations of tagged-RpfB, but also contained some non-specific proteins (Figure 3.14c). To minimise the presence of these unwanted proteins, the respective elutions were pooled for a high salt wash.

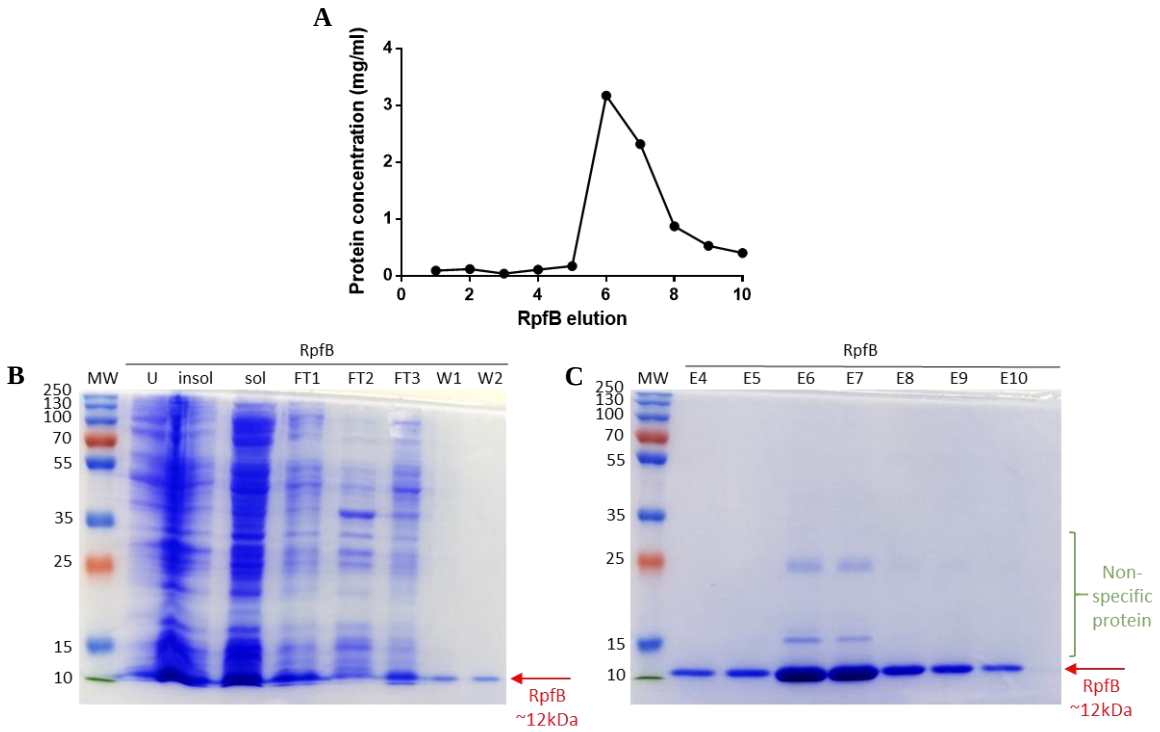


Figure 3.14. Batch purification of his-tagged RpfB on his-select nickel affinity gel, binding and eluting at pH 8.0. The protein concentrations of the elutions were determined by Nanodrop (A). The uninduced control (U), soluble (sol) and insoluble (insol) lysates, flow through (FT 1 to FT3), washes (W1 and W2) and the elution fractions with the highest concentrations of protein (E4 to E10) were analysed on a 12% SDS-PAGE gel (B and C). A large amount of tagged-RpfB bound the affinity gel column and was eluted in elutions 4 to 10. Some non-specific proteins were also eluted off the column during the imidazole gradient, indicated by the green bracket.

3.6.2. Salt wash to remove non-specific binding proteins and aggregates

A high salt wash was performed to remove some of the non-specific proteins and any RpfB aggregates in the elutions. The pooled elutions were run on the 8 ml his-select affinity gel column and washed with the high salt buffer as described in section 2.6.10. The protein concentrations of the salt wash elutions were determined by Nanodrop at 280 nm (Figure 3.15a) and analysed on a 12% SDS-PAGE gel, along with the pooled elutions, flow through and wash, as described in sections 2.4.1 and 2.6.12. A large amount of tagged-RpfB was lost during the high salt wash along with a small amount of non-specific proteins (Figure 3.15b). The salt wash produced two very clean elutions of tagged-RpfB (E4 and E5 in figure 3.15b), with no visible aggregates or non-specific proteins. These elutions were pooled and subsequently used for tag removal.

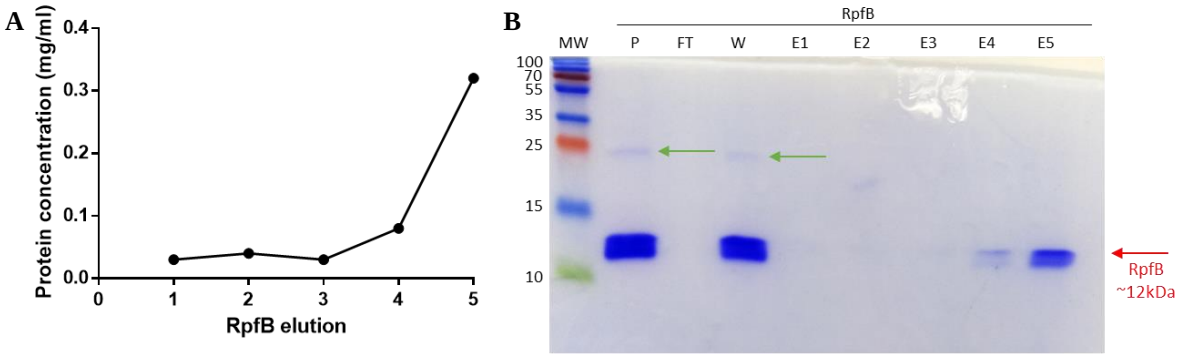


Figure 3.15. High salt wash of his-tagged RpfB purification elutions to minimise non-specific binding proteins and aggregates. Pooled purification elutions were re-loaded onto his-select nickel affinity gel and washed with a high salt buffer before re-eluting off the gel column. The protein concentration of the elutions were determined by Nanodrop (A). The pooled elutions (P), flow through (FT), wash (W) and elutions (E1 to E5) were analysed on a 12% SDS-PAGE gel (B). The salt wash removed most of the non-specific proteins and aggregates (indicated by the green arrows).

3.6.3. Affinity tag removal

To exclude any possible interference of the his-tag in protein activity, the his-tag was removed by TEV digestion as described in section 2.6.4. The pooled elutions from the salt wash (E4 and 5) were digested overnight in a time-course digestion, with aliquots being sampled every 2 hours for the first 8 hours. These aliquots were analysed on an SDS-PAGE gel to visualise the cleavage of the his-tag, as described in section 2.6.11. Over time, less of the tagged 12 kDa RpfB protein was seen in the digestion reaction and more tagless 10 kDa RpfB protein is observed (Figure 3.16). At the end of the digestion, almost no tagged-RpfB was present in the digestion reaction (Figure 3.16), and the reaction was dialysed overnight to

remove the EDTA and DTT from the reaction mixture, as described in section 2.6.5. The removal of these chelating agents was in preparation for the purification of any undigested protein and the his-tagged TEV enzyme on the his-select nickel affinity gel.

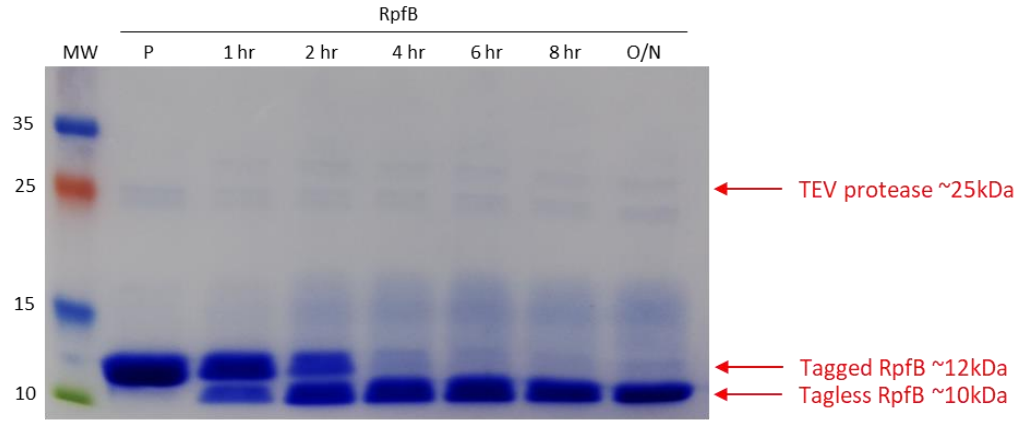


Figure 3.16. Time course digestion of his-tagged RpfB by TEV protease at 37°C for the removal of the his-tag. Elutions 4 and 5 of the high salt wash were pooled for tag removal. Cleavage of the tag from the pooled his-tagged protein (P) resulted in more of the tagless 10 kDa RpfB protein being present in the reaction and less of the tagged, 12 kDa protein in the reaction over time. The reaction proceeded overnight (O/N).

3.6.4. Purification of tagless RpfB

To purify tagless-RpfB and remove the his-tagged TEV enzyme and any remnant tagged-RpfB, the reaction mixture was dialysed and batch purified on his-select nickel affinity gel, as described in section 2.6.5 and 2.6.9. The flow through, which should contain tagless-RpfB which is unable to bind to the affinity gel, as well as the washes and elutions, were visualised on a SDS-PAGE gel as described in section 2.6.11. No protein was lost during the dialysis buffer exchange (Figure 3.17). Tagless RpfB (10 kDa) did not bind the affinity gel, as expected, and was aspirated off the gel in the flow through. The TEV enzyme and any non-specific proteins bound to the column and were eluted off the affinity gel during the imidazole elution (Figure 3.17). A small amount of tagless RpfB was present in the wash; however, most of the desired protein was present in the flow through (Figure 3.17). The protein concentration of RpfB in the flow through was determined by Nanodrop at 280 nm and the flow through was subsequently used for activity assays.

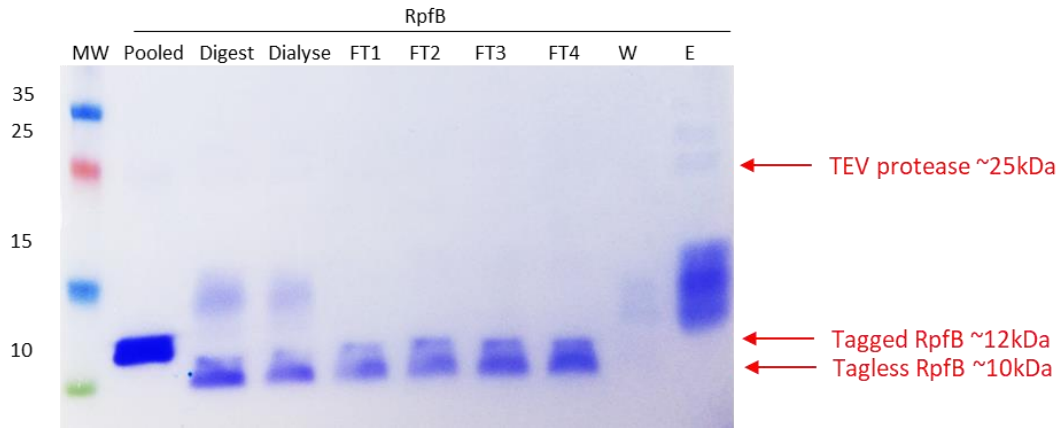


Figure 3.17. The purification of tagless-RpfB on his-select nickel affinity gel. Tagless RpfB was unable to bind to the his-select affinity gel and was collected in the flow through (FT). Undigested protein, still containing a his-tag and the his-tagged digestion enzyme, TEV protease, bound to the affinity gel and were isolated from the tagless protein in the flow through. The pooled protein elutions (pooled), digestion reaction (Digest), dialysed digestion reaction (Dialyse), the flow through (FT1 to FT4), washes (W1 and W2) and the elution (E) were all analysed.

3.7. Protein activity assays

Purified recombinant RipA and RpfB were tested for muralytic activity. These proteins act on the peptidoglycan of the mycobacterial cell wall, releasing products which promote resuscitation from dormancy and mycobacterial cell growth. To test the activity of the purified proteins, four different assays were used: the MUF-triNAG assay, FITC assay, the Remazol dye release assay and zymography.

3.7.1. MUF-triNAG assay

The first assay used to evaluate protein muralytic activity was the MUF-triNAG assay. Cleavage of the MUF-triNAG substrate produces a florescent emission, which can be measured at 450 nm. The assay was first set up, as described in section 2.7.1, with varying concentrations of lysozyme, an enzyme known to cleave the MUF-triNAG substrate, to validate the functionality of the assay. Over time, the fluorescent emission at 450 nm increased, indicating the cleavage of more MUF-triNAG substrate with time (Figure 3.18a). The intensity of the signal was also seen to be lysozyme concentration dependent, with a faster increase in fluorescent emission observed with higher concentrations of lysozyme, and overall a greater change in florescence with higher concentrations of lysozyme (figure 3.18a and b). Once it was verified that the assay worked, purified recombinant RipA and RpfB cleavage activity was evaluated. Over 3 hours, no significant change in emission at 450 nm was observed (Figure 3.18c), hence the muralytic capabilities of these proteins was not be established using this assay.

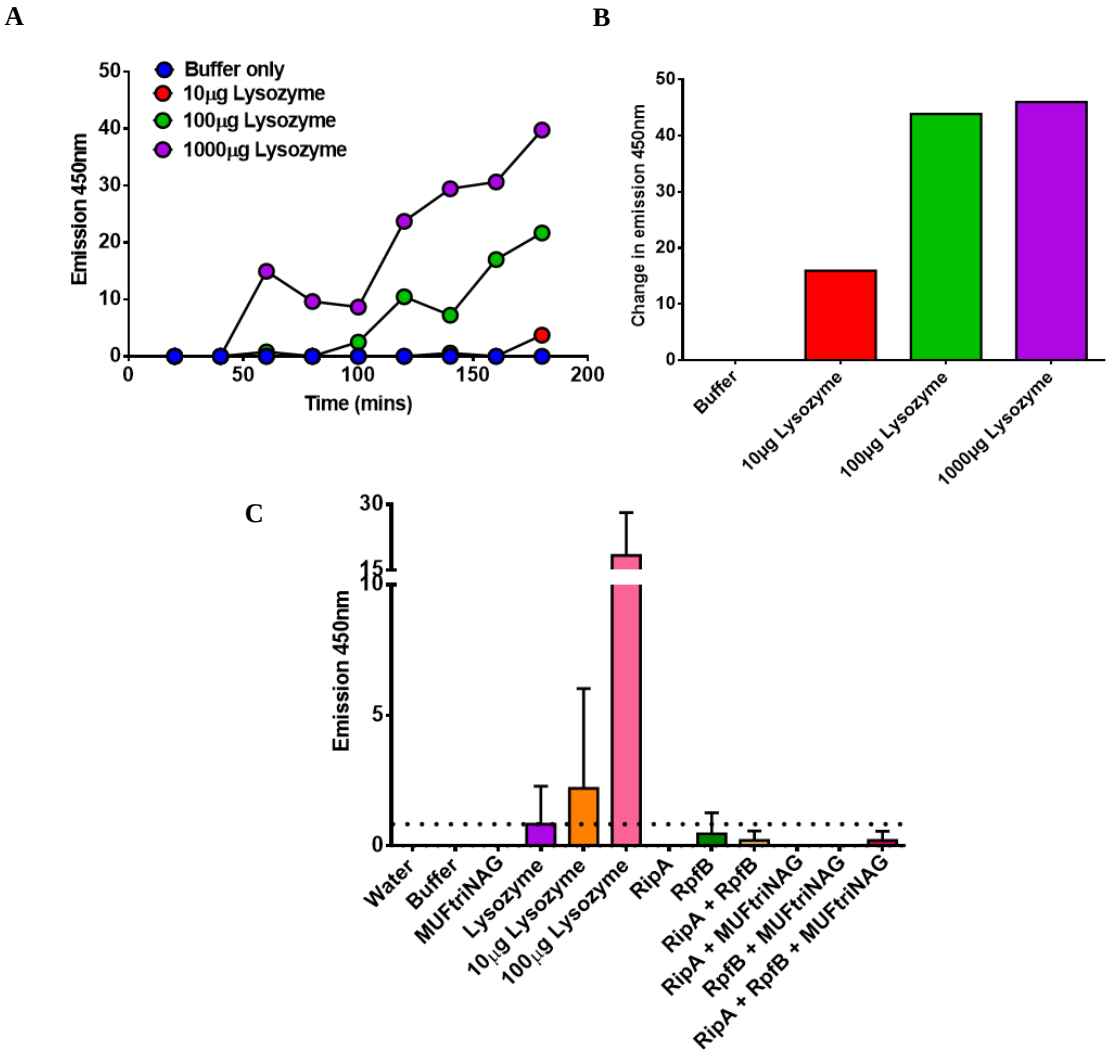


Figure 3.18. MUF-triNAG assay was inconclusive in establishing recombinant RipA and RpfB muralytic activity. The functionality of the assay was established with a lysozyme gradient in which increasing fluorescent emission at 450 nm was observed over 3 hours, in a lysozyme-concentration dependent manner (A and B). No fluorescent emission, indicative of the cleavage of the fluorescent MUF-triNAG substrate by active muralytic enzymes, was observed for RipA and RpfB (B). Statistical analysis was performed using a one-way ANOVA adjusted for multiple comparisons (Graphpad Prism 6). Error bars indicate the standard error of the mean.

3.7.2. FITC assay

Because the activity of recombinant RipA and RpfB was not established using the MUF-triNAG assay, an alternative fluorescent assay, the FITC assay was used to test muralytic activity of the recombinant proteins. The FITC assay utilises the cleavage and release of a fluorescent molecule from a substrate as an indication of muralytic activity. The FITC assay was conducted, as described in Section 2.7.2. with varying concentrations of lysozyme, to verify the functionality of the assay. Lysozyme cleaved the substrate, resulting in the release of the fluorescent molecule which was detected at 515 nm (Figure 3.19a). The fluorescent emission at 515 nm was dependent on the concentration of lysozyme, with a greater

fluorescent emission as the concentration of lysozyme increased, which is indicative of increased substrate cleavage (Figure 3.19a). When recombinant RipA and RpfB muralytic activities were tested using the FITC assay, RipA displayed no significant muralytic activity on its own, but in combination with RpfB, significant cleavage of the substrate was observed (Figure 3.19b). This is indicative of the reported synergism between these two enzymes for cleavage of the peptidoglycan substrate (Hett *et al.*, 2008). The positive control, lysosome, in this particular assay did not display any significant muralytic activity. It was concluded that an alternative assay, which was not reliant on fluorescence should be utilised to validate the synergistic protein activity observed during the FITC assay.

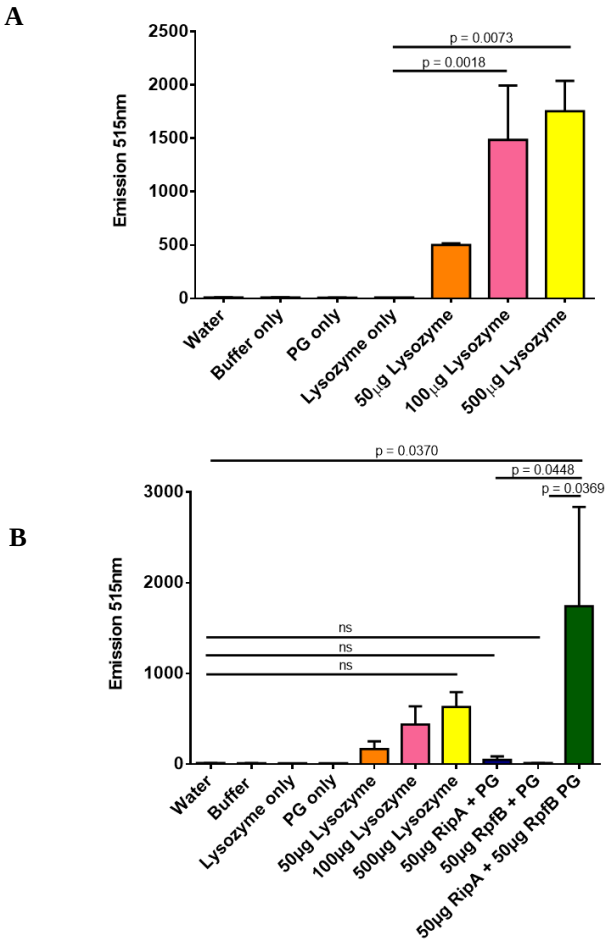


Figure 3.19. Recombinant RipA and RpfB synergistic muralytic activity was established by FITC assay. The functionality of the assay was established with a lysozyme gradient (A) in which a positive fluorescent emission at 515 nm was observed after 3 to 5 days, in a lysozyme-concentration dependent manner. No significant fluorescent emission at 515 nm, indicative of the cleavage of the fluorescent FITC-labelled peptidoglycan substrate by active muralytic enzymes, was observed for RipA and RpfB alone. However, in combination, significant cleavage of the substrate was observed, indicative of a synergism between these two enzymes during muralytic cleavage (B). Statistical analysis was performed using a one-way ANOVA adjusted for multiple comparisons (Graphpad Prism 6). Error bars indicate the standard error of the mean.

3.7.3. Remazol brilliant blue dye release assay

The remazol brilliant blue dye release assay was performed as an alternative protein activity assay to validate the observed synergism between RipA and RpfB in the FITC assay (section 2.7.3). Both RipA and RpfB displayed significant cleavage activity on the labelled cell wall material (Figure 3.20), resulting in an observable change in optical density at 595 nm compared to the cell wall substrate alone. The synergism between these two enzymes that was seen previously in the FITC assay was not confirmed, with the muralytic activity of these two proteins decreasing when they were used in combination (Figure 3.20). The lysozyme control in this assay did not produce a significant change in optical density at 595 nm compared to the substrate alone.

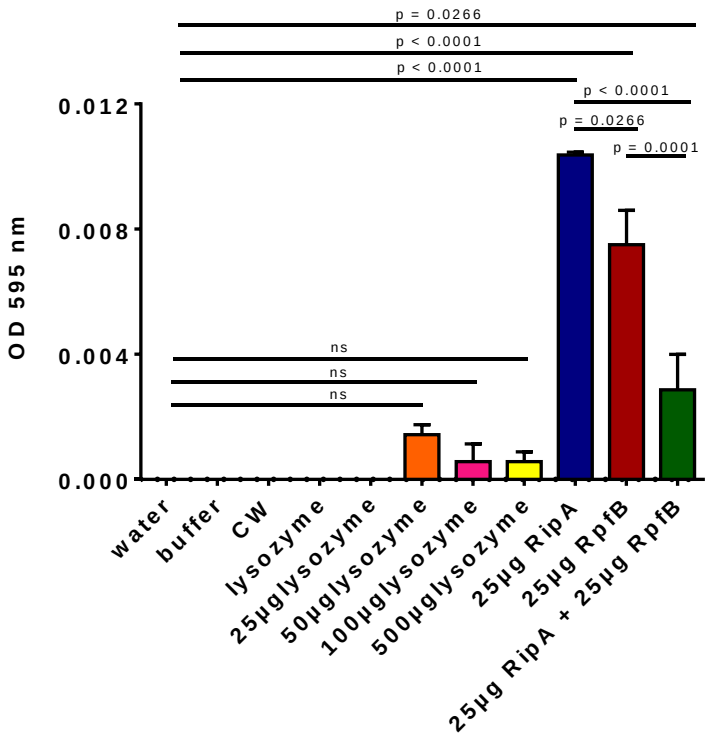


Figure 3.20. Recombinant RipA and RpfB display antagonistic muralytic activity in the remazol brilliant blue protein activity assay. RipA and RpfB both display significant muralytic activity, cleaving the remazol brilliant blue-labelled cell wall substrate, producing an observable change in optical density at 595 nm, compared to the substrate on its own. In combination, RipA and RpfB muralytic activity is hindered and decreases compared to the two enzymes alone, indicative of an antagonistic interaction between these two enzymes. Statistical analysis was performed using a one-way ANOVA adjusted for multiple comparisons (Graphpad Prism 6). Error bars indicate the standard error of the mean.

3.7.4. Zymography

To evaluate the activity of recombinant RipA and RpfB alone, zymography was used, as an alternative assay to the fluorescent and optical density assays previously tested. The proteins

of interest were separated on a peptidoglycan-SDS-PAGE gel and incubated in renaturation buffer at 37°C, as described in section 2.7.4. If the protein is active, it is expected to digest the peptidoglycan in the gel surrounding itself hence creating zones of clearance in the gel. Bovine serum albumin (BSA) and lysozyme were used as negative and positive controls respectively. RipA displayed lytic activity, creating visible clearance zones, similar to that of the lysozyme positive control (Figure 3.21a and b). RipA's lytic activity was proven to be very robust, as both heat denatured (Figure 3.21a) and chemically denatured protein (Figure 3.21b) were able to refold and digest the peptidoglycan. RpfB did not create any zones of clearance. From the zymogram the activity of RipA was confirmed; however, the synergistic effect of RpfB on RipA activity, as well as the lytic activity of RpfB alone, could not be determined. Because the cleavage activity of RpfB was confirmed in the remazol brilliant blue release assay, both proteins were carried forward into the *in vitro* assays. As the synergy of RipA and RpfB could not be proven in atleast two muralytic activity assays, the proteins were evaluated individually and in combination in the *in vitro* resuscitation experiments.

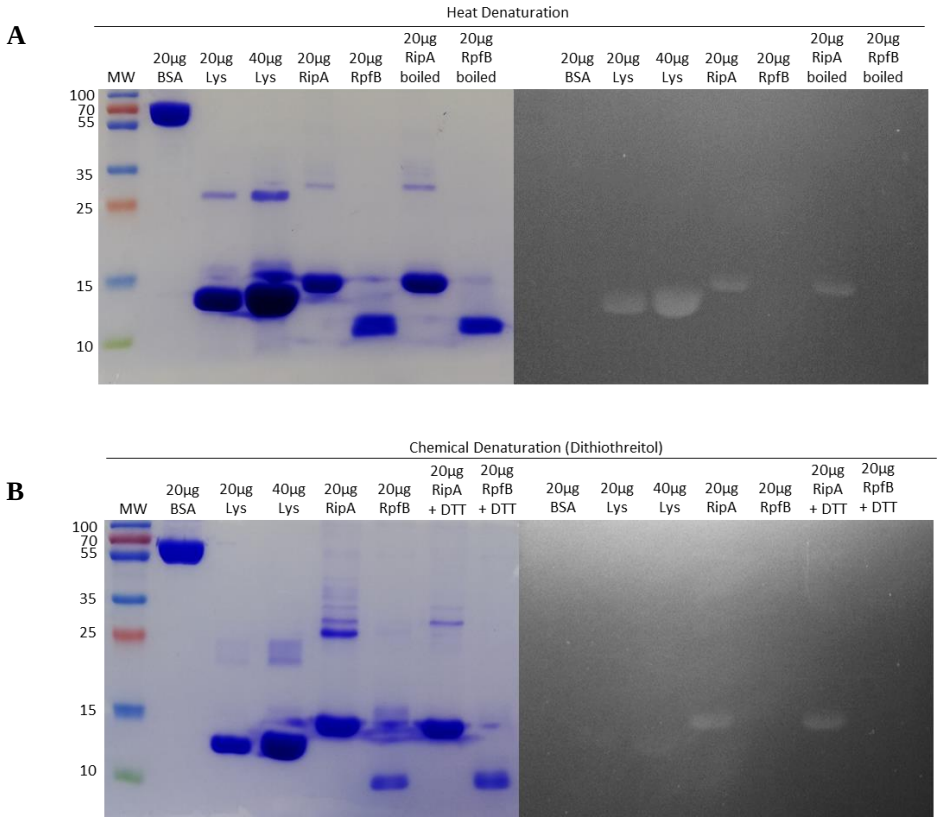


Figure 3.21. Zymogram demonstrating the lytic activity of recombinant RipA. Recombinant RipA displayed muralytic activity digesting the peptidoglycan of the SDS-PAGE gel, in a similar fashion to the positive lysozyme control (Lys). This activity was shown to be robust, as RipA was able to renature and retain activity after both heat denaturation (A) and chemical denaturation (B). RpfB, as in previous literature, displayed no significant lytic activity on the peptidoglycan-SDS-PAGE gel. Bovine serum albumin (BSA), a protein with no muralytic activity, was used as a negative control.

3.8. *In vitro* assays

3.8.1. Resuscitation of starved H37Rv in liquid media with recombinant RipA and RpfB

RipA and RpfB are hypothesised to have resuscitation and growth stimulatory capabilities. To evaluate their ability to resuscitate and promote the growth of non-culturable *Mtb*, purified recombinant RipA and RpfB were added to MGIT assays and MPNs, as described in sections 2.9.1 and 2.9.3. It was expected that the addition of the recombinant proteins would enhance the growth and resuscitation of the inoculated bacterial cells, shortening the TTP in MGIT assays and increasing the number of organisms detected by MPN assays. Non-culturable cells were prepared by carbon starvation, as described in section 2.8. H37Rv CF, containing endogenous secreted Rpfs, was also evaluated in this assay for resuscitation capabilities. The addition of 20 ng/ml RipA and 20 ng/ml RpfB to MGIT cultures significantly decreased the TTP of starved H37Rv cultures compared to cells cultured with just 7H9 MGIT media and cells cultured with CF supplemented MGIT media (Figure 3.22a). The decrease in MGIT TTP was RipA and RpfB concentration dependent. Higher concentrations of RipA and RpfB (50 ng/ml), negated the positive effect by increasing the TTP to values comparable to media alone (Figure 3.22a). The positive effect observed with MGIT cultures was not reflected in MPN assays, where the supplementation of media with RipA and RpfB had no significant effect on the resuscitation and enumeration of H37Rv cells quantified by resuscitation index (Figure 3.22b).

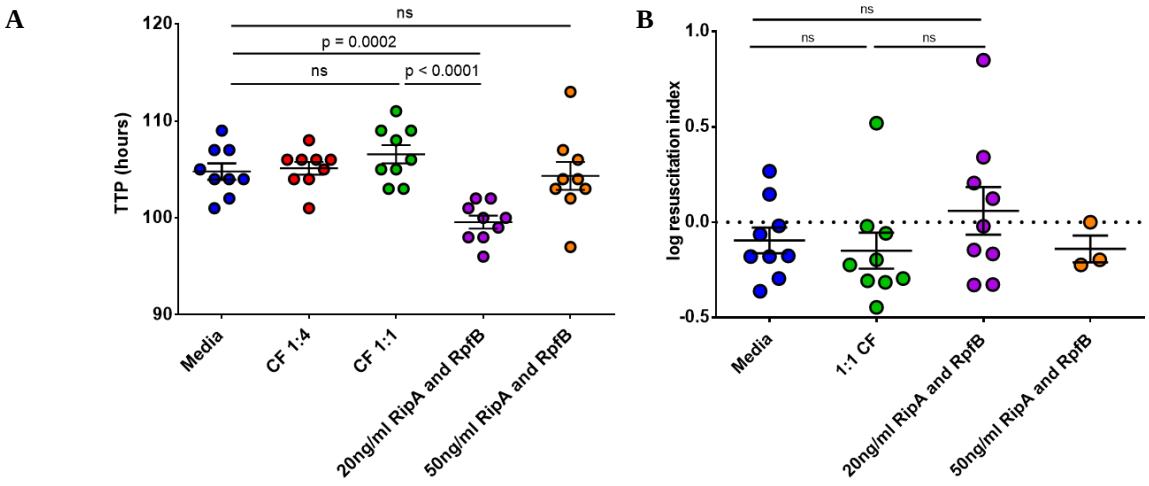


Figure 3.22. Supplementation of recombinant RipA and RpfB to MGIT cultures decreased the time to positivity of starved H37Rv. Supplementation of 20 ng/ml of RipA and 20 ng/ml RpfB significantly decreased the TTP compared to normal MGIT media and MGIT media supplemented with CF (A). Increasing the concentration of recombinant protein negated this effect. The growth stimulatory properties in the MGIT assay were not conserved in other liquid cultures assays, such as the MPN assay, where recombinant protein supplementation had no significant impact of resuscitation index (B). Experiments were performed as 3 3 technical replicates of 3 biological replicates. Statistical analysis was performed using a one-way ANOVA adjusted for multiple comparisons (Graphpad Prism 6). Error bards indicate the standard error of the mean.

3.8.2. Resuscitation of starved H37Rv on solid media with recombinant RipA and RpfB

To evaluate whether resuscitation of carbon starved H37Rv with recombinant RipA and RpfB could also be achieved on solid media, starved H37Rv was plated on un-supplemented solid media and solid media supplemented with 20 ng/ml recombinant RipA and RpfB, as described in section 2.9.2. As the decrease in TTP was only observed for the lower concentrations of supplemented proteins in the liquid assay (Figure 3.23), this assay was performed with the lower concentration of supplemented RipA and RpfB, 20ng/ml. No significant differences were observed in the number of CFUs/ml, indicative of resuscitated cells, between the un-supplemented media and RipA and RpfB supplemented media (Figure 3.23).

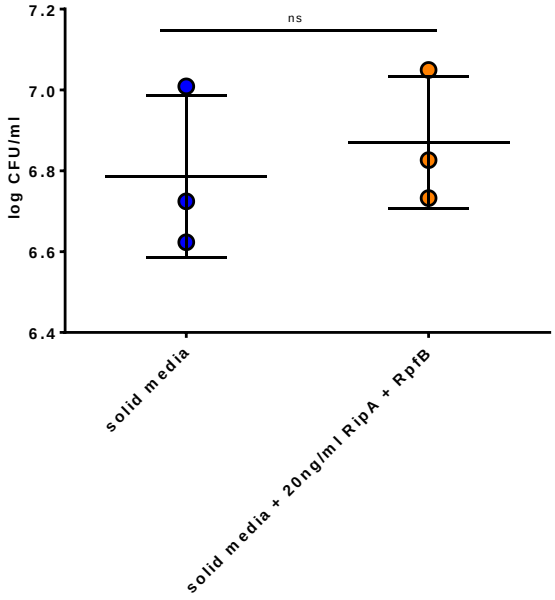


Figure 3.23. Supplementation of recombinant RipA and RpfB did not increase the number of resuscitated H37Rv bacilli on solid media. Carbon starved H37Rv cells were plated on solid media supplemented with 20 ng/ml RipA and RpfB displayed no significant difference in the number of resuscitated organisms, indicated by CFUs/ml, compared to cells plated on un-supplemented solid media. Experiments were performed as 3 technical replicates. Statistical analysis was performed using a paired student t-test (Graphpad Prism 6). Error bars indicate the standard error of the mean.

3.8.3. Resuscitation of starved H37RV, Beijing and LAM strains with recombinant RipA and RpfB

To investigate whether RipA and RpfB supplemented resuscitation and growth stimulation was strain dependent, non-culturable, starved H37Rv, Beijing and LAM isolates were resuscitated. Non-culturable cells were generated by the modified carbon starvation model, as described in section 2.8, and resuscitated in supplemented MGIT assays, as described in

section 2.9.3. In agreement with previous experiments (Section 3.8.1), supplementation of MGIT assays with RipA and RpfB improved the TTP of starved H37Rv (Figure 3.24a). In contrast to observations seen in section 3.8.1, supplementation with H37Rv CF improved MGIT TTP for H37Rv cells (Figure 3.24a). RipA and RpfB supplementation and H37Rv CF supplementation had no significant effect on MGIT TTP for Beijing and LAM isolates (Figure 3.24b and c).

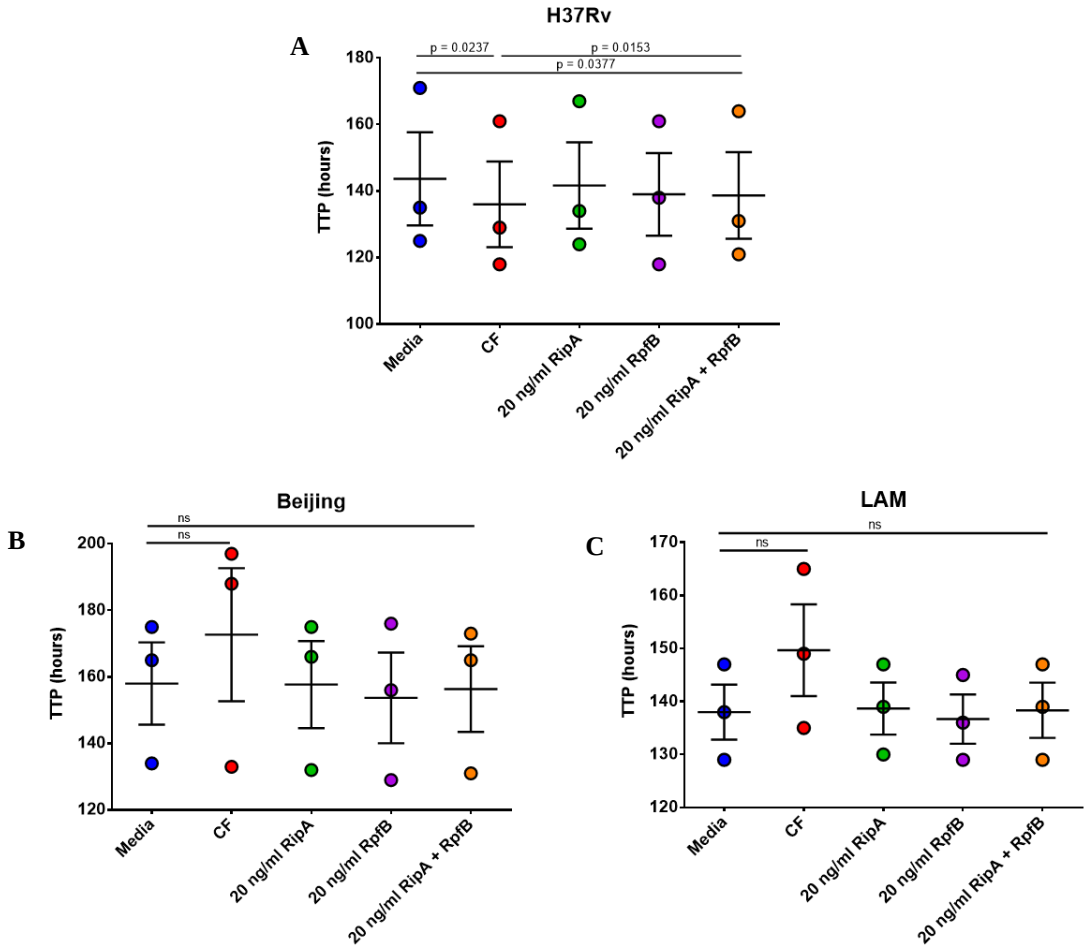


Figure 3.24. Improved resuscitation of carbon starved *Mtb* in MGIT assays with recombinant RipA and RpfB supplementation is strain dependent. Supplementation of MGIT assays with 20 ng/ml recombinant RipA and RpfB decreases the TTP of carbon-starved H37Rv (A) but has no significant effect on carbon-starved Beijing isolates (B) and carbon-starved LAM isolates (C). Experiments were performed as 3 biological replicates. Statistical analysis was performed using a one-way ANOVA adjusted for multiple comparisons (Graphpad Prism 6). Error bars indicate the standard error of the mean.

3.8.4. Resuscitation of clinical *Mtb* strains with recombinant RipA and RpfB

The effect of recombinant RipA and RpfB on clinical isolates of *Mtb* in decontaminated sputum was evaluated to determine whether supplementation with recombinant resuscitation factors could decrease the TTP in MGIT cultures. MGIT cultures were performed as described in section 2.9.3. The supplemented MGIT assays were tested on 30 clinical isolates

that were collected for a previous study in our laboratory and stored at -80°C for approximately 1 year (Ethics certificate M200164 – Appendix A). The demographics, immunology and the original diagnostic data of the specimens is listed in table 4 below. The demographics and immunology of 4 specimens were unknown, and therefore excluded from the table.

Table 4. The demographics, immunology and original diagnostic data of the 30 clinical specimens utilised in this study, categorised by HIV status and CD4 cell count.

Variable	Overall (n = 26)	HIV negative (n = 4)	HIV positive (n = 22)	CD4 count <200 (n = 17)	CD4 count >200 (n = 5)
Demographics and Immunology					
Male, n (%)	16 (53.3)	3 (10)	13 (43.3)	10 (33.3)	3 (10)
Female, n (%)	10 (33.3)	1 (3.3)	9 (30)	7 (23.30	2 (6.7)
Median Age, years (IQR)	37 (33-48.5)	50.5 (26-51)	36 (33-46.5)	36 (33.5-43)	34 (30-48)
Median CD4 count, cells/mm3			151.5 (83-177.5)	149 (52.5-159.5)	418 (213-617)
Clinical diagnostic for TB -					
Negative, n (%)	11 (36.70)	1 (3.3)	10 (33.3)	8 (26.7)	2 (6.7)
Positive, n (%)	15 (50)	3 (10)	12 (40)	9 (30)	3 (10)
Scanty, n (%)	0	0	0	0	0
+, n (%)	4 (13.3)	0	4 (13.3.)	4 (13.3)	0
++, n (%)	3 (10)	0	3 (10)	1 (3.3)	2 (16.7)
+++, n (%)	8 (26.70	3 (10)	5 (16.7)	4 (13.3)	1 (3.3)
Clinical diagnostic for TB -					
High, n (%)	7 (23.3)	2 (6.7)	5 (16.7)	4 (13.3)	1 (3.3)
Medium, n (%)	8 (26.7)	1 (3.3)	7 (23.3)	5 (16.7)	2 (6.7)
Low, n (%)	2 (6.7)	0	2 (6.7)	1 (3.3)	1 (3.3)
Very low, n (%)	5 (16.7)	0	5 (16.7)	4 (13.3)	1 (3.3)
Not detected, n (%)	4 (13.3)	1 (3.3)	3 (10)	3 (10)	0
Median GeneXpert threshold (CT), cycles (IQR)	16.8 (13.6-24.2)	14 (3.1-16.4)	20 (15-25.2)	16.9 (13.2-26)	22.3 (18-27.7)
MGIT					
Media, hours (IQR)	271.5 (184-421)	200.5 (186.5-801.8)	301.5 (179.8-421)	323 (192.5-422)	252 (133-398.5)
H37Rv CF, hours (IQR)	269 (146.8-401.3)	202.5 (171.3-218.8)	315.5 (97-415.3)	336 (149.5-419.5)	270 (77.5-653.5)
20ng/ml RipA, hours (IQR)	267 (188.8-397.5)	203.5 (186.3-802)	298.5 (183.2-397.5)	314 (196-400)	250 (122.5-346.5)
20ng/ml RpfB, hours (IQR)	282.5 (190-392.5)	206.5 (189.3-802)	317 (186.3-397.5)	324 (197.5-375)	254 (140-542.5)
20ng/ml RipA and RpfB, hours (IQR)	240.5 (191.5-402.5)	204 (187.5-389.3)	269.5 (187.3-402.5)	317 (198-407)	252 (129.5-643.5)

Of the 30 clinical samples tested, 10 were shown to have high initial bacterial load by CFU assay during the previous study, 10 were shown to have low initial bacterial load by CFU assay and 10 were shown to have no culturable bacterial load by CFU assay (data from previous study, not shown). Overall, in the clinical specimens of the cohort examined, the addition of recombinant RipA and RpfB had no significant effect on TTP compared to normal MGIT culture, regardless of original bacterial load determined by CFU (Figure 3.25a and supplementary figure 1). Four of the specimens under normal MGIT conditions were negative and yielded the maximum TTP of 1000 hours (specimens 2248 and 2299 in Supplementary figure 2 and specimens 2205 and 2461 in Supplementary figure 4). Two of the four specimens (specimens 2248 and 2461) when supplemented with CF and both RipA and RpfB had a decreased TTP and became positive (Figure 3.25b). Although the decrease in TTP was not as large with RipA and RpfB supplementation compared to CF supplementation, a reduction in TTP to less than 500 hours was observed (Supplementary figure 2 and 4). However, the addition of RipA and RpfB and CF to the four negative MGIT specimens overall had no statistically significant effect on TTP (Figure 3.25b).

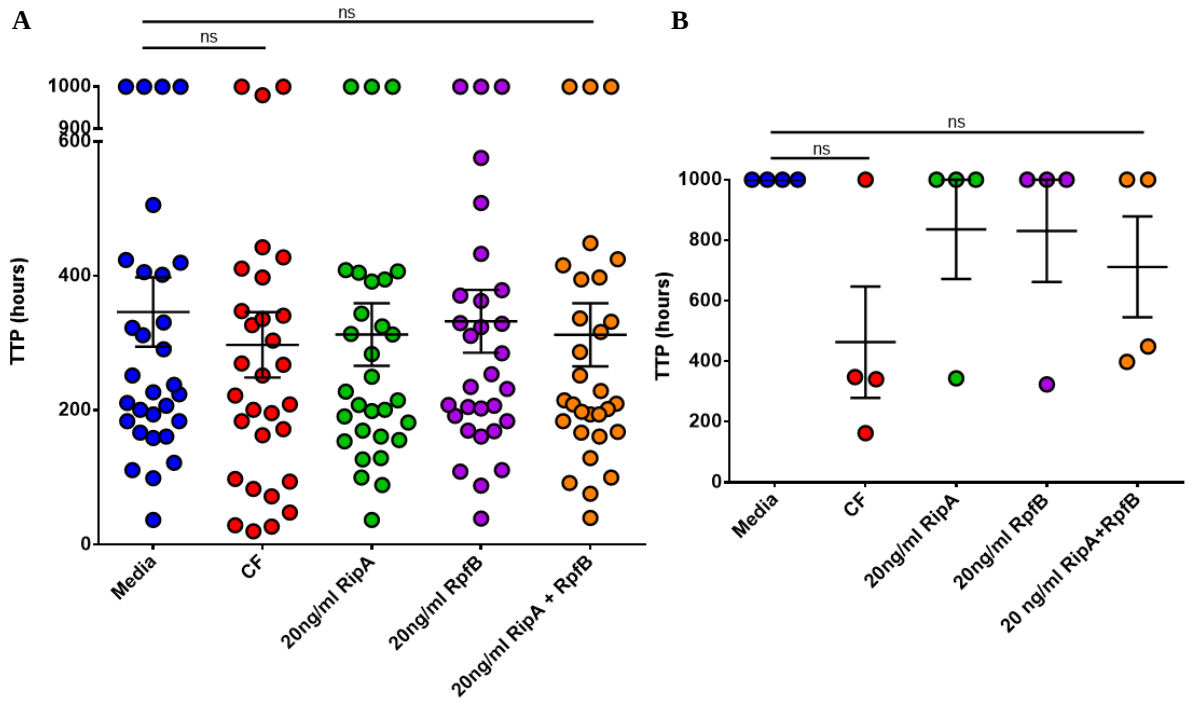


Figure 3.25. Supplementation of recombinant RipA and RpfB to MGIT cultures had no significant effect on the time to positivity of clinical isolates of *M. tuberculosis*. (A) Supplementation of 20 ng of RipA and 20 ng RpfB individually and together had no significant effect on MGIT TTP compared to normal MGIT media and MGIT media supplemented with CF. (B) Two of the four specimens which are negative in normal MGIT media had a decreased TTP and became positive when supplemented with both RipA and RpfB. Statistical analysis was performed using a one-way ANOVA adjusted for multiple comparisons (Graphpad Prism 6). The error bars indicate the standard error of the mean.

When examining the MGIT results of individual specimens, supplementation with both RipA and RpfB improved the TTP in 20% of the examined specimens (specimens 2248, 2315, 2372, 2309, 2461, 2380 in Supplementary figures 2, 3 and 4). An increased TTP was observed in a single specimen (3.3%) when supplementing MGIT assays with both RipA and RpfB (2371 in Supplementary figure 4). The benefit of RipA and RpfB supplementation overall outweighs the negative effect seen in only 3% of the tested specimens.

An investigation into whether demographics, immunology and initial diagnostic data (summarized in table 4) influenced RipA and RpfB supplementation of MGIT assays was performed next. It was observed that gender (Figure 3.26a), HIV-status (Figure 3.26b), CD4 count in HIV positive specimens (Figure 3.26c), initial smear microscopy result (Figure 3.26d) and initial GeneXpert grading (Figure 3.26e) had no significant effect on RipA and RpfB supplementation of MGIT assays.

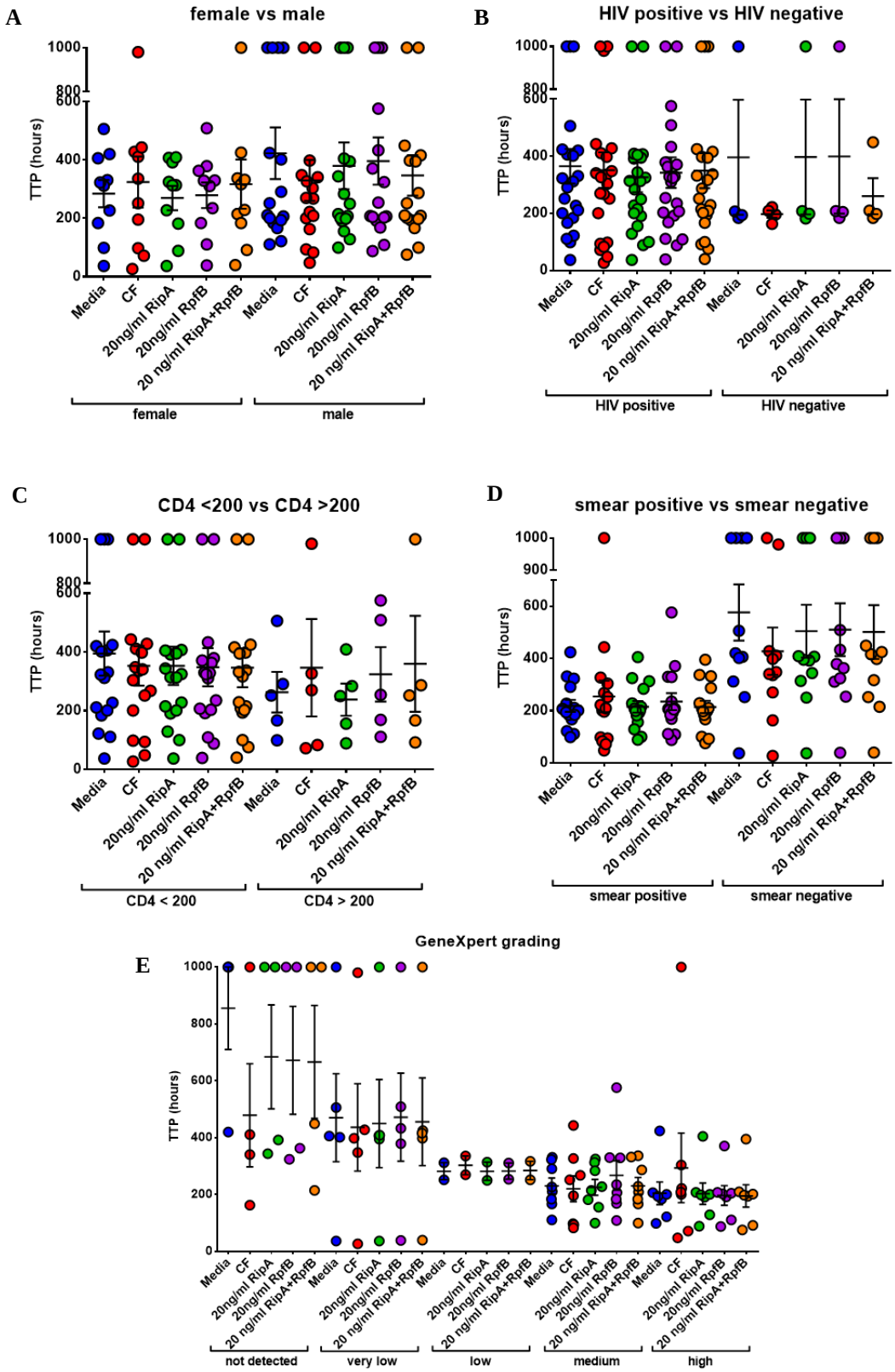


Figure 3.26. Supplementation of MGIT assays with recombinant RipA and RpfB had no significant effect on MGIT time-to-positivity regardless of specimen demographics, immunology and diagnostic data. Supplementation of 20 ng/ml recombinant RipA and RpfB, alone and in combination, did not significantly change the MGIT TTP, compared to normal MGIT media and CF, regardless of gender (A), HIV-status (B), CD4 count (C) and diagnostic smear (D) and GeneXpert result (E). Error bars indicate the standard error of the mean.

4. Discussion

Mtb is considered to be one of the most successful pathogens worldwide. Its success can be largely attributed to its ability to evade various stresses. A key mechanism utilised in this evasion is the adoption of non-culturable states, in which the bacterium is more tolerant of stresses that would normally be detrimental to survival. Once permissive conditions resume, the bacteria exit these less culturable states, often termed dormancy, and resume active replication (Kell and Young, 2000; Jones and Lennon, 2010; Lennon and Jones, 2011). Rpfs and their interacting partner, RipA, have been identified as key partners in the re-emergence of *Mtb* from the non-culturable state leading to the re-establishment of active infection (Mukamolova, Turapov, Kazarian, *et al.*, 2002). This study aimed to investigate whether supplementation of MGIT cultures with RpfB and RipA, could improve the detection and diagnosis of *Mtb*.

Vectors expressing the catalytic regions of these two proteins were obtained and transformed into BL21 DE3. The catalytic region of RipA encompassing residues 355 to 472, forms a NlpC/P60 domain and houses the cysteine-histidine-glutamate catalytic triad (Ruggiero, Marasco, *et al.*, 2010). This catalytic domain has been shown previously to be folded and fully functional as an endopetidase in the absence of the N-terminal auto-inhibitory domain (Ruggiero, Marasco, *et al.*, 2010). The catalytic region of RpfB encompassing residues 280 to 362, folds into a c-type lysozyme structure, suggesting a lysozyme-like mechanism of activity. (Cohen-Gonsaud *et al.*, 2004; Ruggiero *et al.*, 2009). The enzyme however lacks the critical aspartate residue of c-type lysozymes, replacing it with tyrosine. This change in catalytic residues has proven RpfB to be functionally distinct from c-type lysozyme but instead possessing the structure for lytic transglycoslase activity that is similar to that of soluble lytic transglycosylase SLT70 from *E. coli* (Thunnissen *et al.*, 1995; Cohen-Gonsaud *et al.*, 2004; Ruggiero *et al.*, 2009). The catalytic C-terminal domains of both RipA and RpfB have also been identified as the regions of interaction for these two proteins (Hett *et al.*, 2007). It was demonstrated that the expression of these two interacting catalytic domains, $RipA_{332-472}$ and $RpfB_{280-362}$, and not the full-length proteins, are sufficient for mycobacterial resuscitation and growth stimulation (Ruggiero, Marasco, *et al.*, 2010; Nikitushkin *et al.*, 2015).

Three different small scale purification methods were evaluated for the purification of recombinant RipA and RpfB. No recombinant RpfB was recovered from the small scale

purification using the Zymo His-spin kit. It is unknown whether induced RpfB, seen in the soluble lysate, was lost in the flow through or washing steps, as these elutions were discarded and not analysed on the SDS-PAGE gel (Figure 3.3a). The elution buffer for this kit contains 250 mM imidazole which is the starting concentration of imidazole for the elution of RpfB off the his-select nickel affinity gel (Sigma) (Figure 3.13a and Figure 3.14a). It is possible that RpfB may have not eluted off the Zymo kit column and still be bound to the gel, hence going undetected in the final elution. The recovery of both proteins was poor using the Qiagen Ni-NTA spin columns, where a large amount of recombinant RipA and RpfB was lost in the flow through, as seen in figure 3.3b. The best purification method for the isolation of both proteins was the small scale purification using his-select nickel affinity gel (Sigma) (Figure 3.3c). As this method was successful in isolating both proteins of interest with a substantial yield, it was carried forward for optimisation and upscaling.

The purification of RipA and RpfB was optimised to maximise the yield and purity of the recombinant proteins. Very little variation was seen during the purification of RpfB under different pH conditions; however, binding and eluting of RipA differed under different pH conditions. It was therefore decided to alter pH conditions for the purification of RipA from those previously reported (Ruggiero, Squeglia, *et al.,* 2010). It is unknown whether pH optimisation for the purification of both proteins was performed previously; however, in our hands, RipA bound best to the nickel purification gel at pH 7.6 and eluted best at pH 8.6., maximising our yield and purity of recombinant protein.

To test the muralytic activity of the recombinant proteins, four assays were used. The MUF-triNAG assay measures lytic activity on the peptidoglycan-like substrate by the release of a fluorescent dye. MUF-triNAG has previously been used to demonstrate the cleavage activity of RpfB on peptidoglycan-like substrates, due to its lysozyme-like fold (Mukamolova *et al.*, 2006; Telkov *et al.,* 2006). Lysozyme, which was used as the positive control, displayed muralytic activity using this assay; however, neither of the recombinant proteins produced a significant fluorescent signal (Figure 3.18). This observation may be due to the fact that MUF-triNAG is specifically a lysozyme substrate and hence the substrate may be inappropriate for the evaluation of endopeptidase activity by RipA. The MUF-triNAG assay has only been reported twice in the evaluation of muralytic activity (Mukamolova *et al.*, 2006; Telkov *et al.,* 2006), therefore cleavage activity was assessed using an alternative, and more widely used assay - the FITC assay.

The FITC assay also relies on the release of a fluorescent substrate from fluorescently labelled peptidoglycan as an indication of muralytic activity. The FITC assay has been used previously to evaluate both recombinant RipA and RpfB activity (Mukamolova *et al.*, 2006; Hett *et al.*, 2008; Ruggiero, Marasco, *et al.*, 2010; Nikitushkin *et al.*, 2015). The cleavage of the FITC-labelled peptidoglycan by RipA was observed by Hett et al. (2008) and Ruggiero et al. (2010), but no muralytic activity by RpfB alone was observed in these studies. This is contradictory to observations by Nikitushkin et al. (2015), where muralytic activity by both RipA and RpfB alone in the FITC assay was observed (Hett *et al.*, 2008; Nikitushkin *et al.*, 2015). Interestingly, a synergistic effect was observed by adding both RipA and RpfB to the FITC assay, resulting in a larger fluorescent signal than RipA and RpfB alone (Hett *et al.*, 2008; Nikitushkin *et al.*, 2015). These observations in the FITC assay mimicked those seen by Hett et al. (2008) and Ruggiero et al. (2010), showing synergistic muralytic activity for RipA and RpfB (Figure 3.19). To validate this observation, the remazol brilliant blue dye release assay was performed. Contrast to the observations in the FITC assay, an antagonistic interaction was observed between RipA and RpfB in this assay, with muralytic activity decreasing when both enzymes were present (Figure 3.20). RpfB displayed muralytic activity against the peptidoglycan substrate on its own (Figure 3.20), similar to observations by Nikituskin et al. (2015). It could not be concluded from these experiments whether the relationship between RipA and RpfB is synergistic or antagonistic, therefore in later *in vitro* experiments, both proteins were assessed individually and together for resuscitation capabilities.

Zymography was used as a non-florescent assay to evaluate the lytic activity of recombinant RipA and RpfB. Recombinant RipA displayed muralytic activity, creating clearance zones in the peptidoglycan-SDS-PAGE gel thus confirming the activity of our recombinant protein (Figure 3.21). RpfB did not create any zones of clearance. In an effort to understand this, a literature search to determine possible reasons for this unexpected result was undertaken. Zymography to test the activity of *Mtb* RpfB has not been reported in literature; however, the essential *Mi. luteus* Rpf protein has previously been shown to create lytic clearance zones in zymography assays (Mukamolova *et al.*, 2006; Telkov *et al.*, 2006). It is possible that recombinant *Mtb* RpfB, which is non-essential, may be distinct to that of *Mi. luteus*, which is an essential gene, thus resulting in the apparent discrepancy in zymography assays.

The ability of recombinant RipA and RpfB to resuscitate non-culturable *Mtb* in *in vitro* assays was investigated. Previous studies have investigated the effect of Rpfs and Rpf-containing CF on the growth and resuscitation of mycobacteria (Sun and Zhang, 1999; Shleeva *et al.*, 2002; Wu *et al.*, 2008; Mukamolova *et al.*, 2010; Huang *et al.*, 2014; Kolwijck *et al.*, 2014; Nikitushkin *et al.*, 2015; O'Connor *et al.*, 2015; Chengalroyen *et al.*, 2016). Shleeva et al. (2002 and 2004) showed that the addition of recombinant Rpf from *Mi. luteus*, as well as *Mi. luteus* CF, to *M. smegmatis* and *Mtb* cultures improved viability and culturability on solid media (Shleeva *et al.*, 2002, 2004). Co-cultivation of *Mi. luteus* and *M. smegmatis*, allowing the release of *Mi. luteus* Rpf into the culturing media, also increased the viability of *M. smegmatis* cells (Shleeva *et al.*, 2004). Supplementation with *Mtb* CF has repeatedly been shown to improve the culturability of *Mtb* cultures (Sun and Zhang, 1999; Shleeva *et al.*, 2002; Kolwijck *et al.*, 2014; O'Connor *et al.*, 2015; Dusthackeer *et al.*, 2019). CF from a number mycobacterial species, both virulent and avirulent, has also been shown to have resuscitation capabilities on sputum-derived *Mtb* (Sun and Zhang, 1999; Dusthackeer *et al.*, 2019). The resuscitation capabilities of CF on dormant tubercle bacteria generally outweigh that of recombinant Rpfs, in most cases in terms of the number of resuscitated organisms. However, there are advantages to the use of recombinant proteins over CF, for example, recombinant Rpfs are more stable when stored correctly and do not require continuous fresh culturing of *Mtb.* Heterogeneity in bacterial infections has been displayed in a previous study by Chengalroyen et al (2016). This study demonstrated variability in the dependence on Rpfs for resuscitation and growth stimulation, with some mycobacterial populations in sputum being completely dependent on the presence of Rpfs in CF for growth stimulation and detection, while others were able to resuscitate and grow in the absence of Rpf in the CF (Mukamolova *et al.*, 2010; Chengalroyen *et al.*, 2016). The resuscitation capabilities of RipA has only been revealed in recent years, where supplementation of RipA into non-culturable *M. smegmatis* cultures, promoted growth and the emergence from this state (Nikitushkin *et al.*, 2015). The synergy of RipA and RpfB seen in *in vitro* assays was also displayed in this study, with the combination of RipA and RpfB being more potent in growth stimulation than each protein individually (Nikitushkin *et al.*, 2015). From this observation, it was expected that supplementation of *Mtb* cultures with a combination of RipA and RpfB would enhance the growth and emergence of mycobacteria.

A reduction in TTP was observed when non-culturable *Mtb* H37Rv MGIT assays were supplemented with recombinant RipA and RpfB, compared to normal MGIT media and

H37Rv CF (Figure 3.22a). The growth stimulatory proteins promoted the emergence from the non-culturable state and the resumption of exponential growth at 20 ng/ml. A dose-dependent stimulatory effect on non-culturable cells was observed, where increasing the concentration of RipA and RpfB, from 20 ng/ml to 50 ng/ml, negated the reduction in the time to detection (Figure 3.22a). This result correlates with observations by Nikitushkin et al. (2015), where growth stimulation and resuscitation are dependent on protein concentration, forming a bell curve (Nikitushkin *et al.*, 2015). The observed optimal protein concentration at the top of the bell curve were approximately 10 ng/ml for both RipA and RpfB. RpfB in these experiments was shown to have a substantial reduction in resuscitation capabilities at 50 ng/ml (Nikitushkin *et al.*, 2015). Cell wall hydrolytic enzymes, such as RipA and RpfB, require strict regulation to prevent cell lysis, therefore excessive amounts of these enzymes may result in cell lysis instead of resuscitation. This has been seen previously, where supplementation of lysozyme, RipA and RpfE, causes cell wall weakening, enhancing the activity of cell wall targeting antibiotics (Gustine *et al.*, 2019). Despite reducing the TTP, the overall number of bacteria resuming active growth, measured by resuscitation index in the MPN assay, did not change with RipA and RpfB supplementation (Figure 3.22b). It appears that RipA and RpfB are able to speed up reactivation from the non-culturable state but have minimal effect on enhancing growth once a cell count threshold has been reached after resuscitation. After this, overall growth mimics growth in normal media. This has been eluded to in previous studies by Wu et al. (2008), where RpfB stimulation was only effective on low inoculum cultures (Wu *et al.*, 2008). This correlates with the observation that RipA and RpfB supplementation does not increase the number resuscitated organisms on solid media (Figure 3.23). As the time of emergence of resuscitated bacteria in the solid media resuscitation assays (Section 3.8.2) was not monitored, it is unclear whether resuscitation on solid media was accelerated when supplemented with recombinant RipA and RpfB. Interestingly, a reduction in TTP when MGIT cultures were supplemented with H37Rv CF was not observed in this experiment, which is contradictory to previous studies showing improved TTP and detection of *Mtb* with CF supplementation (Sun and Zhang, 1999; Shleeva *et al.*, 2002; Kolwijck *et al.*, 2013; O'Connor *et al.*, 2015; Chengalroyen *et al.*, 2016; Dusthackeer *et al.*, 2019). This may be due to the fact that the MGIT is a different system to previously studied assays and therefore may present a unique micro-environment. As variation in the dependence on CF and resuscitation promoting agents is seen between different bacterial populations (Chengalroyen *et al.*, 2016), it is possible that the non-culturable cells generated in our model are not responsive to CF for resuscitation, resulting in

no observable stimulation of growth and no improvement in the time to detection. As CF contains a range of excreted factors, both growth stimulatory and inhibitory factors, it is also possible that an unidentified inhibitory factor may be inhibiting the growth stimulatory properties of the CF. This would need to be investigated further in future work, by investigating the components of CF by mass spectrometry. Small variations in the OD_{600} of *Mtb* cultures from which the CF is derived were also observed to impact the resuscitation and growth stimulatory effects of CF on non-culturable H37Rv (Supplementary figure 5). Variation in OD_{600} from previous studies may also be accountable for the opposing result.

It was observed that H37Rv CF and the recombinant proteins did not stimulate the resuscitation of Beijing and LAM strains of *Mtb*. Ongoing studies our laboratory have also noted this finding (Padarath, unpublished). It was observed by Padarath (unpublished) that CF from Beijing strains was able to stimulate resuscitation of Beijing strains more successfully than media and CF from H37Rv. This suggests that the stimulation of growth and resuscitation of different *Mtb* strains is dependent on the components of the CF of that particular strain. Further investigation into the components and Rpf ratios in the CF of different *Mtb* strains requires further investigation.

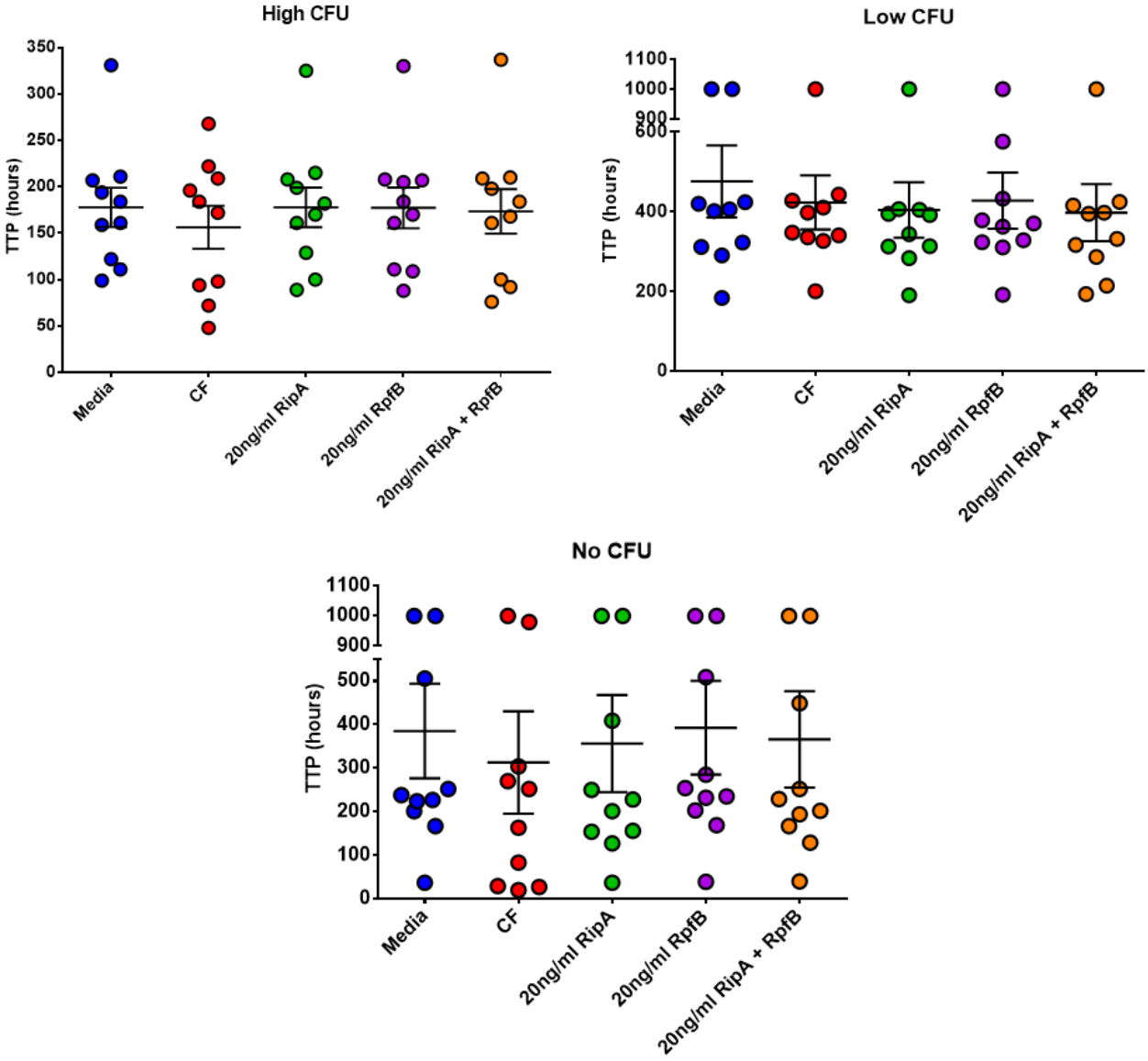
A reduction in TTP will positively impact the speed of a confirmed diagnosis for TB-infected individuals thus allowing for a faster initiation of treatment. An investigation into whether the reduction in TTP seen in the detection of H37Rv with RipA and RpfB supplementation, would also be seen in a cohort of South African TB-infected individuals was performed. Previous studies have shown that supplementation of BACTEC 960 and BacT/ALERT MP MGIT systems with CF and recombinant RpfB, improves the TTP of *Mtb* from sputum samples (Huang *et al.*, 2014; Kolwijck *et al.*, 2014). It should be noted that Huang et al. (2014) found the supplementation to only be beneficial in patients whose normal MGITs were only positive after ~480 hours (20 days). The effect of RipA and RpfB supplementation in MGITs on 30 patient specimens which had varied initial CFUs, indicative of starting culturable bacterial load, was investigated. Overall, no reduction in TTP when MGIT cultures were supplemented with RipA alone, RpfB alone and RipA and RpfB in combination was observed, which was in stark contrast with the axenic experiments that were carried out on H37Rv. There was a large range of variability between patients, which would skew any possible significant effect, hence presenting a limitation to this experiment. Looking at patients individually, a reduction in TTP with the supplementation of RipA and RpfB, is seen

in a handful of patients (~20%) (Supplementary figure 2, 3 and 4). Supplementation with RipA and RpfB only hindered detection in a single patient (~3%), and in the remaining patients in this cohort (77%), supplementation of RipA and RpfB into MGIT cultures neither enhanced or hindered detection, with no significant change in TTP observed. The addition of recombinant RipA and RpfB to MGIT assays may therefore be beneficial in enhancing the detection of *Mtb* in some sputum samples, while causing minimal inhibitory effect on others. This requires further investigation in a larger cohort going forward.

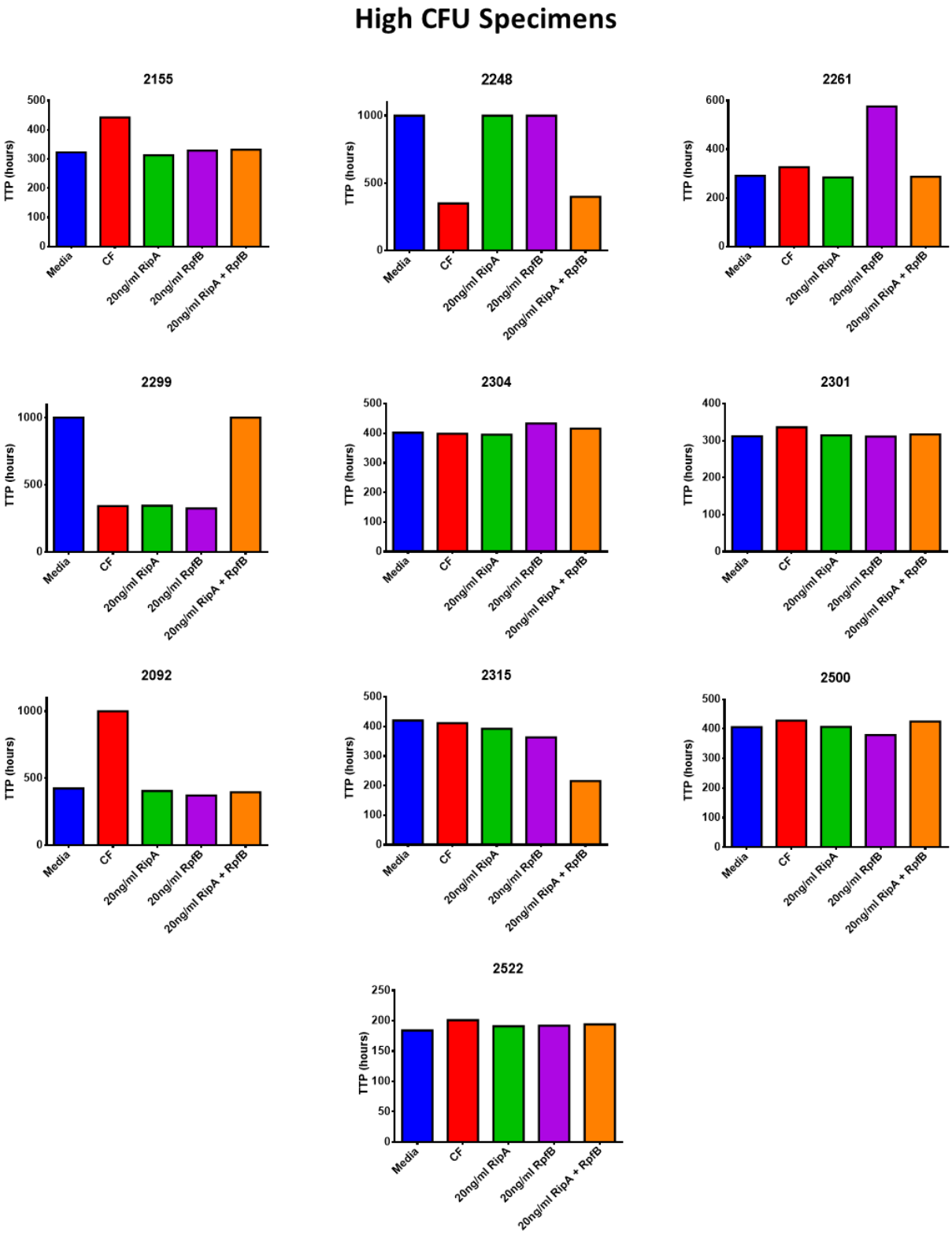
4.1. Conclusion

The catalytic regions of two *Mtb* proteins, RipA and RpfB, which are involved in the resuscitation and growth stimulation of *Mtb*, were successfully expressed and purified. The muralytic activity of recombinant RipA and RpfB was evaluated by zymography and florescent and optical density-based protein activity assays, where both proteins displayed muralytic activity. The resuscitation capabilities of recombinant RipA and RpfB were assessed in MGIT assays on non-culturable *Mtb* H37Rv generated using a modified published carbon starvation model. In this regard, a reduction in TTP compared to normal MGIT media and CF was observed, suggesting that RipA and RpfB are able to promote the growth and resuscitation of non-culturable *Mtb*. An investigation into whether this reduction in MGIT TTP would be observed in clinical samples derived from a South African cohort of patients was conducted. To this end, no significant alteration in the TTP overall following supplementation with RipA and RpfB was reported. Looking at individual patients however, some specimens benefited from the supplementation, as observed by a decrease in the time to detection. For the remaining patients, addition of recombinant proteins did not affect the TTP, hence posing no detriment to diagnostic speed. Future work will focus on investigating these effects on a larger cohort, as well as a study of the other components of CF which may display resuscitation capabilities. The supplementation of MGIT assays with RipA and RpfB may enhance MGIT assays and provide faster diagnosis and detection of *Mtb* and better treatment monitoring, key areas of interest in the fight to eliminate this epidemic causing pathogen.

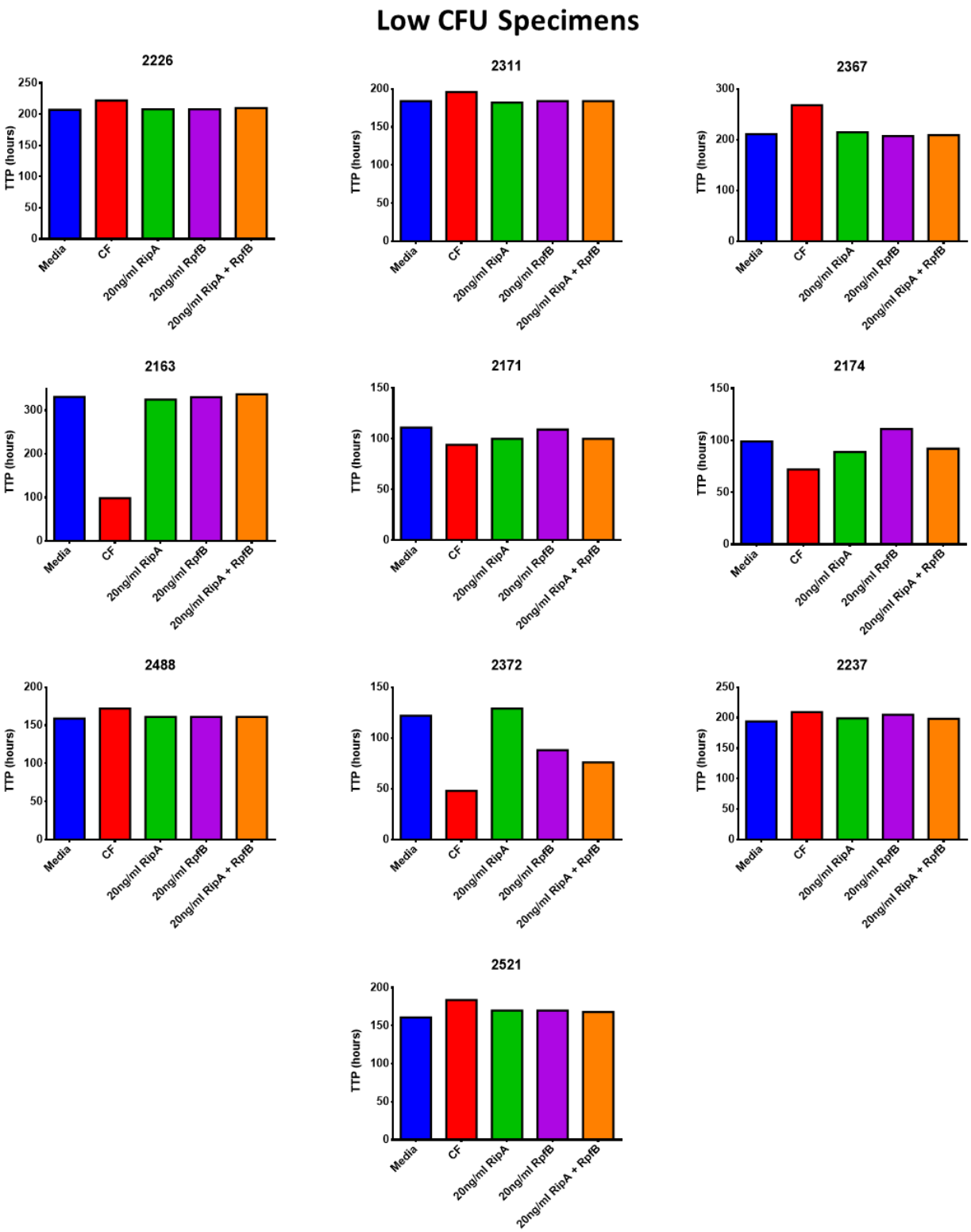
5. Supplementary Figures



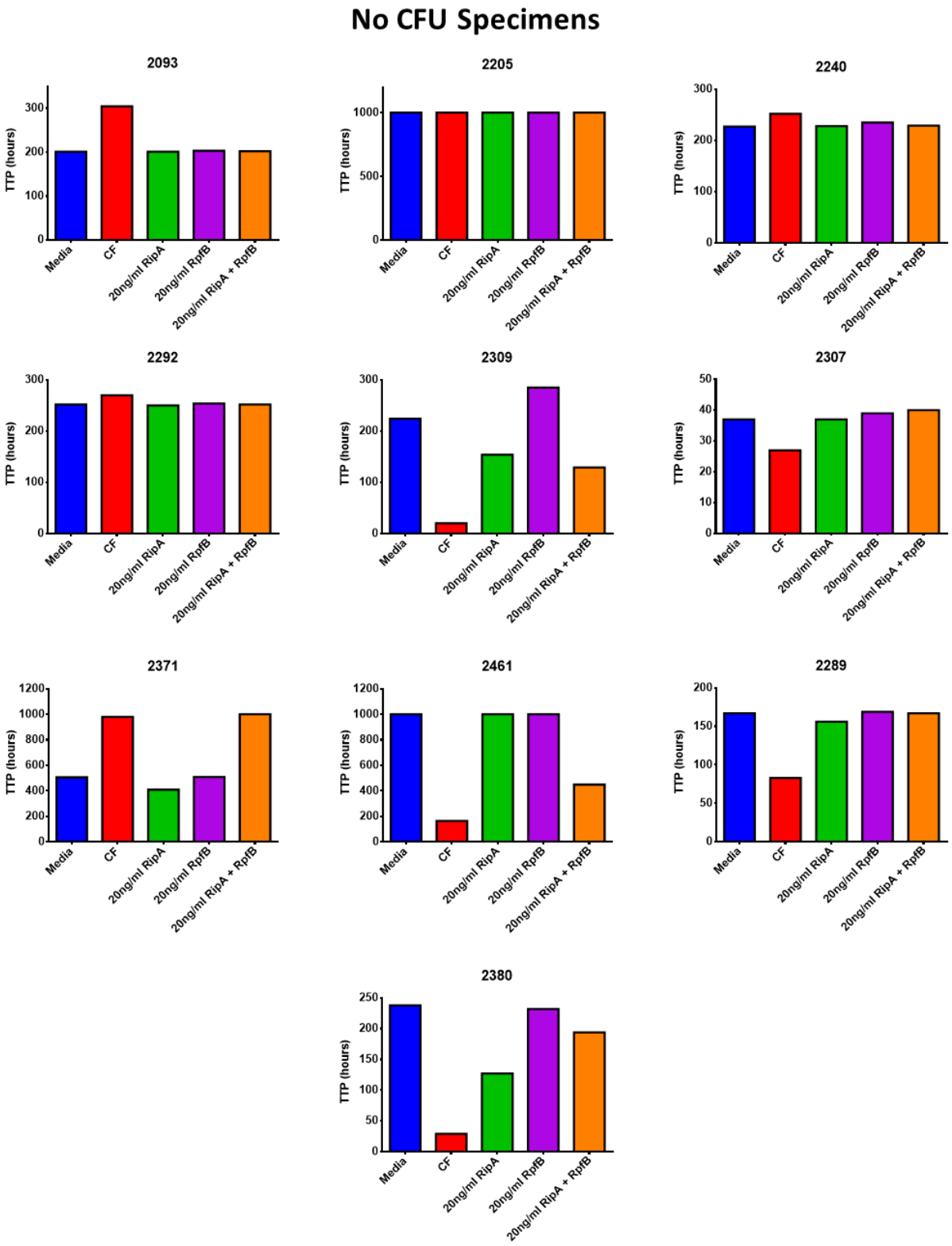
Supplementary figure 1. Growth and resuscitation of *Mtb* from patient specimens in MGIT assays by initial bacterial load. Specimens were grown and resuscitated in normal MGIT media, CF supplemented media (CF), media supplemented with 20 ng/ml RipA, media supplemented with 20 ng/ml RpfB and media supplemented with 20 ng/ml RipA and RpfB. Growth and resuscitation were indicated by positivity of the MGIT tube. Specimens were categorized by their respective initial culturable bacterial load, indicated by CFUs/ml No significant difference in TTP is observed in supplemented MGITs, regardless of initial bacterial load. Error bars indicate the standard error of the mean.



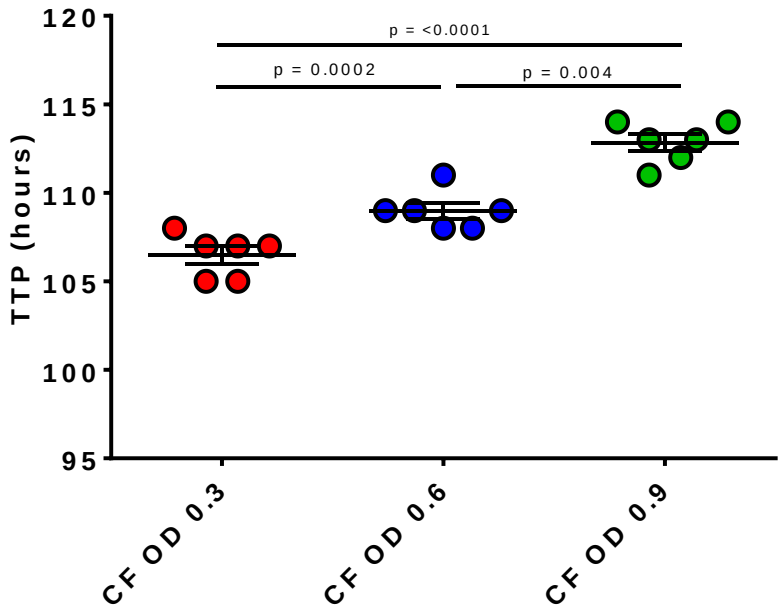
Supplementary figure 2. Growth and resuscitation of *Mtb* from individual patient specimens with high initial colony forming units (CFUs) in MGIT assays. Specimens were grown and resuscitated in normal MGIT media, CF supplemented media (CF), media supplemented with 20 ng/ml RipA, media supplemented with 20 ng/ml RpfB and media supplemented with 20 ng/ml RipA and RpfB. Growth and resuscitation were indicated by positivity if the MGIT tube.



Supplementary figure 3. Growth and resuscitation of *Mtb* from individual patient specimens with low initial colony forming units (CFUs) in MGIT assays. Specimens were grown and resuscitated in normal MGIT media, CF supplemented media (CF), media supplemented with 20 ng/ml RipA, media supplemented with 20 ng/ml RpfB and media supplemented with 20 ng/ml RipA and RpfB. Growth and resuscitation were indicated by positivity if the MGIT tube.



Supplementary figure 4. Growth and resuscitation of *Mtb* from individual patient specimens with no initial colony forming units (CFUs) in MGIT assays. Specimens were grown and resuscitated in normal MGIT media, CF supplemented media (CF), media supplemented with 20 ng/ml RipA, media supplemented with 20 ng/ml RpfB and media supplemented with 20 ng/ml RipA and RpfB. Growth and resuscitation were indicated by positivity if the MGIT tube.



Supplementary figure 5. Resuscitation of carbon starved H37Rv is dependent on the optical density of the culture filtrate used during MGIT assays. Carbon starved H37Rv was resuscitated in MGIT assays with CF extracted from cultures with optical density of 0.3, 0.6 and 0.9 at 600 nm. Better resuscitation, indicated by the faster TTP, is achieved with CF from lower density cultures. Experiments were performed as 3 technical replicates of 2 biological replicates. Error bars indicate the standard error of the mean.

Appendix A: Ethics clearance certificate

UNIVERSITY OF THE WITWATERSRAND JOHANNESBURG

R14/49 Dr Z Waja and Professor B Kana

HUMAN RESEARCH ETHICS COMMITTEE (MEDICAL)
CLEARANCE CERTIFICATE NO. M200164

NAME: (Principal Investigator)	Dr Z Waja and Professor B Kana
DEPARTMENT:	Schools of Clinical Medicine (Waja) and Pathology (Kana) Perinatal HIV RU (Waja) & CoE in Biomedical TB Res (Kana) CHBAH (Waja) and NHLS (Kana)
PROJECT TITLE:	Sputum and oral swab collection for novel mycobacteriology testing techniques (SNT study)
DATE CONSIDERED:	Ad hoc
DECISION:	Approved unconditionally
CONDITIONS:	
SUPERVISOR:	Not applicable
APPROVED BY:	Dr CB Penny, Chairperson HREC (Medical)
DATE OF APPROVAL:	2020/03/18

This clearance certificate is valid for 5 years from date of approval. Extension may be applied for.

DECLARATION OF INVESTIGATORS

To be completed in duplicate and **ONE COPY** returned to the Research Office Secretary on the 3rd Floor, Phillip Tobias Building, Parktown, University of the Witwatersrand, Johannesburg.
I/we fully understand the conditions under which I am/we are authorized to carry out the above-mentioned research and I/we undertake to ensure compliance with these conditions. Should any departure be contemplated, from the research protocol as approved, I/we undertake to submit details to the Committee. I agree to submit a yearly progress report. When a funder requires annual re-certification, the application date will be one year after the date when the study was initially reviewed. In this case, the study was initially reviewed in **January** and will therefore reports and re-certification will be due early in the month of **January** each year. Unreported changes to the application may invalidate the clearance given by the HREC (Medical).

Principal Investigator Signature Date

PLEASE QUOTE THE CLEARANCE CERTIFICATE NUMBER IN ALL ENQUIRIES

6. References

Aagaard, C. *et al.* (2009) 'TB vaccines: current status and future perspectives', *Immunology and Cell Biology*, 87, pp. 279–286. doi: 10.1038/icb.2009.14.

Abubakar, I. *et al.* (2013) 'Systematic review and meta-analysis of the current evidence on the duration of protection by bacillus Calmette-Guérin vaccination against tuberculosis', *Health Technology Assessment*, pp. 1–4. doi: 10.3310/hta17370.

Adhikari, S. *et al.* (2010) 'A unified method for purification of basic proteins', *Analytical Biochemistry*. Academic Press, 400(2), pp. 203–206. doi: 10.1016/j.ab.2010.01.011.

Ahmad, S. (2011) 'Pathogenesis, immunology, and diagnosis of latent *Mycobacterium tuberculosis* infection', *Clinical and Developmental Immunology*, 2011. doi: 10.1155/2011/814943.

Ai, J.-W. *et al.* (2016) 'Updates on the risk factors for latent tuberculosis reactivation and their managements', *Emerging Microbes & Infections*, 5(1), pp. 1–8. doi: 10.1038/emi.2016.10.

Anantharaman, V. and Aravind, L. (2003) 'Evolutionary history, structural features and biochemical diversity of the NlpC/P60 superfamily of enzymes.', *Genome biology*, 4(2). doi: 10.1186/gb-2003-4-2-r11.

Anochie, P. I. *et al.* (2012) 'Recent advances in the diagnosis of *Mycobacterium tuberculosis*', *GERMS*, pp. 110–120. doi: 10.11599/germs.2012.1021.

Aronson, N. E. *et al.* (2004) 'Long-term Efficacy of BCG Vaccine in American Indians and Alaska Natives: A 60-Year Follow-up Study', *Journal of the American Medical Association*, pp. 2086–2091. doi: 10.1001/jama.291.17.2086.

Avery, S. V. (2006) 'Microbial cell individuality and the underlying sources of heterogeneity', *Nature Reviews Microbiology*, 4(8), pp. 577–587. doi: 10.1038/nrmicro1460.

Ayrapetyan, M. *et al.* (2015) 'Viable but Nonculturable and Persister Cells Coexist Stochastically and Are Induced by Human Serum.', *Infection and immunity*. American Society for Microbiology, 83(11), pp. 4194–203. doi: 10.1128/IAI.00404-15.

Ayrapetyan, M., Williams, T. C. and Oliver, J. D. (2015) 'Bridging the gap between viable but non-culturable and antibiotic persistent bacteria', *Trends in Microbiology*, 23(1), pp. 7–13. doi: 10.1016/j.tim.2014.09.004.

Barreto, M. L. *et al.* (2005) 'Neonatal BCG protection against tuberculosis lasts for 20 years in Brazil', *International Journal of Tuberculosis and Lung Disease*, 9(10), pp. 1171–1173.

Boehme, C. C. *et al.* (2010) 'Rapid Molecular Detection of Tuberculosis and Rifampin Resistance', *New England Journal of Medicine*, 363(11), pp. 1005–1015. doi: 10.1056/NEJMoa0907847.

Bornhorst, J. A. and Falke, J. J. (2000) 'Purification of proteins using polyhistidine affinity tags', *Methods in Enzymology*. Academic Press Inc., pp. 245–254. doi: 10.1016/s0076-6879(00)26058-8.

Brandt, L. *et al.* (2002) 'Failure of the *Mycobacterium bovis* BCG vaccine: Some species of environmental mycobacteria block multiplication of BCG and induction of protective immunity to tuberculosis', *Infection and Immunity*, 70(2), pp. 672–678. doi: 10.1128/IAI.70.2.672-678.2002.

Brennan, P. J. (2003) 'Structure, function, and biogenesis of the cell wall of *Mycobacterium tuberculosis*', *Tuberculosis*, 83(1–3), pp. 91–97. doi: 10.1016/S1472-9792(02)00089-6.

Buerger, S. *et al.* (2012a) 'Microbial scout hypothesis, stochastic exit from dormancy, and the nature of slow growers', *Applied and Environmental Microbiology*, 78(9), pp. 3221–3228. doi: 10.1128/AEM.07307-11.

Buerger, S. *et al.* (2012b) 'Microbial scout hypothesis and microbial discovery', *Applied and Environmental Microbiology*, 78(9), pp. 3229–3233. doi: 10.1128/AEM.07308-11.

Caulfield, A. J. and Wengenack, N. L. (2016) 'Diagnosis of active tuberculosis disease: From microscopy to molecular techniques', *Journal of Clinical Tuberculosis and Other Mycobacterial Diseases*. Elsevier, 4, pp. 33–43. doi: 10.1016/J.JCTUBE.2016.05.005.

Ceyssens, P. J. *et al.* (2017) 'Matrix-assisted laser desorption ionization-time of flight mass spectrometry for combined species identification and drug sensitivity testing in mycobacteria', *Journal of Clinical Microbiology*. American Society for Microbiology, 55(2), pp. 624–634. doi: 10.1128/JCM.02089-16.

Chakravorty, S., Roh, S. S., *et al.* (2017) 'Detection of Isoniazid-, Fluoroquinolone-, Amikacin-, and Kanamycin-Resistant Tuberculosis in an Automated, Multiplexed 10-Color Assay Suitable for Point-of-Care Use', *Journal of Clinical Microbiology*. Edited by G. A. Land. American Society for Microbiology Journals, 55(1), pp. 183–198. doi: 10.1128/JCM.01771-16.

Chakravorty, S., Simmons, A. M., *et al.* (2017) 'The new Xpert MTB/RIF ultra: Improving detection of *Mycobacterium tuberculosis* and resistance to Rifampin in an assay suitable for point-of-care testing', *mBio*, 8(4), pp. 1–12. doi: 10.1128/mBio.00812-17.

Chengalroyen, M. D. *et al.* (2016) 'Detection and quantification of differentially culturable tubercle bacteria in sputum from patients with tuberculosis', *American Journal of*

Respiratory and Critical Care Medicine, 194(12), pp. 1532–1540. doi: 10.1164/rccm.201604-0769OC.

Churchyard, G. *et al.* (2017) 'What We Know About Tuberculosis Transmission: An Overview', *The Journal of Infectious Diseases*. Oxford University Press, 216(suppl_6), pp. S629–S635. doi: 10.1093/infdis/jix362.

Cohen-Gonsaud, M. *et al.* (2004) 'Resuscitation-promoting factors possess a lysozyme-like domain', *Trends in Biochemical Sciences*. Elsevier Ltd, pp. 7–10. doi: 10.1016/j.tibs.2003.10.009.

Cohen-Gonsaud, M. *et al.* (2005) 'The structure of a resuscitation-promoting factor domain from *Mycobacterium tuberculosis* shows homology to lysozymes', *Nature Structural and Molecular Biology*, 12(3), pp. 270–273. doi: 10.1038/nsmb905.

Colebunders, R. and Bastian, I. (2000) 'A review of the diagnosis and treatment of smear-negative pulmonary tuberculosis', *International Journal of Tuberculosis and Lung Disease*, pp. 97–107.

Dheda, K. *et al.* (2017) 'Clinical management of adults and children with multidrug-resistant and extensively drug-resistant tuberculosis', *Clinical Microbiology and Infection*. Elsevier B.V., pp. 131–140. doi: 10.1016/j.cmi.2016.10.008.

Dheda, K., Barry, C. E. and Maartens, G. (2016) 'Tuberculosis', *The Lancet*, 387(10024), pp. 1211–1226. doi: 10.1016/S0140-6736(15)00151-8.

Dowdy, D. W., Basu, S. and Andrews, J. R. (2013) 'Is passive diagnosis enough? The impact of subclinical disease on diagnostic strategies for tuberculosis', *American Journal of Respiratory and Critical Care Medicine*, 187(5), pp. 543–551. doi: 10.1164/rccm.201207-1217OC.

Downing, K. J. *et al.* (2004) 'Global expression profiling of strains harbouring null mutations reveals that the five rpf-like genes of *Mycobacterium tuberculosis* show functional redundancy', *Tuberculosis*, 84(3–4), pp. 167–179. doi: 10.1016/j.tube.2003.12.004.

Downing, K. J. *et al.* (2005) 'Mutants of *Mycobacterium tuberculosis* Lacking Three of the Five rpf -Like Genes Are Defective for Growth In Vivo and for Resuscitation In Vitro', 73(5), pp. 3038–3043. doi: 10.1128/IAI.73.5.3038.

Drain, P. K. *et al.* (2018) 'Incipient and subclinical tuberculosis: A clinical review of early stages and progression of infection', *Clinical Microbiology Reviews*, 31(4), pp. 1–24. doi: 10.1128/CMR.00021-18.

Dusthackeer, A. *et al.* (2019) 'Differential Culturability of *Mycobacterium tuberculosis* in Culture-Negative Sputum of Patients With Pulmonary Tuberculosis and in a Simulated

Model of Dormancy', *Frontiers in Microbiology*, 10. doi: 10.3389/fmicb.2019.02381.

Dworkin, J. and Shah, I. M. (2010) 'Exit from dormancy in microbial organisms', *Nature Reviews Microbiology*, 8(12), pp. 890–896. doi: 10.1038/nrmicro2453.

Ealand, C. *et al.* (2018) 'Resuscitation-promoting factors are required for *Mycobacterium smegmatis* biofilm formation', *Applied and Environmental Microbiology*. American Society for Microbiology, 84(17). doi: 10.1128/AEM.00687-18.

Epstein, S. S. (2009) 'Microbial awakenings', *Nature*, 457(7233), p. 1083. doi: 10.1038/4571083a.

Farer, L. S., Lowell, A. M. and Meador, M. P. (1979) 'Extrapulmonary tuberculosis in the united states', *American Journal of Epidemiology*. Oxford University Press, 109(2), pp. 205–217. doi: 10.1093/oxfordjournals.aje.a112675.

Farhat, M. *et al.* (2006) 'False-positive tuberculin skin tests: What is the absolute effect of BCG and non-tuberculous mycobacteria?', *International Journal of Tuberculosis and Lung Disease*, pp. 1192–1204.

Fernandez-Soto, P. *et al.* (2019) 'Mechanism of catalysis and inhibition of *Mycobacterium tuberculosis* SapM, implications for the development of novel antivirulence drugs', *Scientific Reports*. Springer US, 9(1), pp. 1–14. doi: 10.1038/s41598-019-46731-6.

Frieden, T. R. *et al.* (2003) 'Tuberculosis', 362, pp. 887–899.

Gardner, A., West, S. A. and Griffin, A. S. (2007) 'Is Bacterial Persistence a Social Trait?', *PLoS ONE*. Edited by W. Getz, 2(8), p. e752. doi: 10.1371/journal.pone.0000752.

Gengenbacher, M. and Kaufmann, S. H. E. (2012) '*Mycobacterium tuberculosis*: Success through dormancy', *FEMS Microbiology Reviews*, 36(3), pp. 514–532. doi: 10.1111/j.1574-6976.2012.00331.x.

Getahun, H. *et al.* (2007) 'Diagnosis of smear-negative pulmonary tuberculosis in people with HIV infection or AIDS in resource-constrained settings: informing urgent policy changes', *Lancet*, 369(9578), pp. 2042–2049. doi: 10.1016/S0140-6736(07)60284-0.

Gomes, M., Saad, R. and Stirbulov, R. (2003) 'Pulmonary tuberculosis: Relationship between sputum bacilloscopy and radiological lesions', *Revista do Instituto de Medicina Tropical de Sao Paulo*, 45(5), pp. 275–281. doi: 10.1590/S0036-46652003000500007.

Gupta, R. K., Srivastava, B. S. and Srivastava, R. (2010) 'Comparative expression analysis of rpf-like genes of *Mycobacterium tuberculosis* H37Rv under different physiological stress and growth conditions', *Microbiology*, 156(9), pp. 2714–2722. doi: 10.1099/mic.0.037622-0.

Gustine, J. N. *et al.* (2019) 'Cell Wall Hydrolytic Enzymes Enhance Antimicrobial Drug

Activity Against *Mycobacterium*', *Current Microbiology*. Springer US, 76(4), pp. 398–409. doi: 10.1007/s00284-018-1620-z.

Hänscheid, T. *et al.* (2007) 'Fluorescence microscopy for tuberculosis diagnosis.', *The Lancet. Infectious diseases*. Elsevier, 7(4), pp. 236–7. doi: 10.1016/S1473-3099(07)70058-0.

Helb, D. *et al.* (2010) 'Rapid detection of *Mycobacterium tuberculosis* and rifampin resistance by use of on-demand, near-patient technology', *Journal of Clinical Microbiology*, 48(1), pp. 229–237. doi: 10.1128/JCM.01463-09.

Hett, E. C. *et al.* (2007) 'A partner for the resuscitation-promoting factors of *Mycobacterium tuberculosis*', *Molecular Microbiology*, 66(3), pp. 658–668. doi: 10.1111/j.1365-2958.2007.05945.x.

Hett, E. C. *et al.* (2008) 'A Mycobacterial Enzyme Essential for Cell Division Synergizes with Resuscitation-Promoting Factor', *PLoS Pathog*, 4(2), p. 1000001. doi: 10.1371/journal.ppat.1000001.

Huang, W. *et al.* (2014) 'Use of Resuscitation-Promoting Factor Proteins Improves the Sensitivity of Culture-based Tuberculosis Testing in Special Samples', *American Journal of Respiratory and Critical Care Medicine*, 189(5), pp. 612–614. doi: 10.1164/rccm.201310-1899LE.

Hunter, R. L. *et al.* (2014) 'Pathogenesis of post primary tuberculosis: Immunity and hypersensitivity in the development of cavities', *Annals of Clinical and Laboratory Science*. Association of Clinical Scientists, 44(4), pp. 365–387.

Isaeva, Y. *et al.* (2013) 'Determination of critical concentrations of moxifloxacin and gatifloxacin for drug susceptibility testing of *Mycobacterium tuberculosis* in the BACTEC MGIT 960 system', *Journal of Antimicrobial Chemotherapy*. doi: 10.1093/jac/dkt202.

Johnson, J. L. *et al.* (1998) 'Impact of human immunodeficiency virus type-1 infection on the initial bacteriologic and radiographic manifestations of pulmonary tuberculosis in Uganda', *The International Journal of Tuberculosis and Lung Disease*. International Union Against Tuberculosis and Lung Disease, 2(5).

Jones, S. E. and Lennon, J. T. (2010) 'Dormancy contributes to the maintenance of microbial diversity', *Proceedings of the National Academy of Sciences of the United States of America*, 107(13), pp. 5881–5886. doi: 10.1073/pnas.0912765107.

Kagina, B. M. N. *et al.* (2009) 'Delaying BCG vaccination from birth to 10 weeks of age may result in an enhanced memory CD4 T cell response'. doi:

10.1016/j.vaccine.2009.06.103.

Kana, B. D. *et al.* (2008) 'The resuscitation-promoting factors of *Mycobacterium tuberculosis* are required for virulence and resuscitation from dormancy but are collectively dispensable for growth in vitro', *Molecular Microbiology*, 67(3), pp. 672–684. doi: 10.1111/j.1365-2958.2007.06078.x.

Kana, B. D. and Mizrahi, V. (2010) 'Resuscitation-promoting factros as lytic enzymes for bacterial growth and signalling', *FEMS Immunolohy and Medical Microbiology*, 58(April), pp. 39–50. doi: 10.1111/j.1574-695X.2009.00606.x.

Kandola, P. and Meena, L. S. (2014) 'Extra pulmonary tuberculosis: Overview, manifestations, diagnostic and treatment techniques', *ADVANCED MATERIALS Reviews Adv. Mater. Rev*, 2014(1), pp. 13–19. doi: 10.5185/amr.2014.1003.

Karumbi, J. and Garner, P. (2015) 'Directly observed therapy for treating tuberculosis', *Cochrane Database of Systematic Reviews*. John Wiley and Sons Ltd. doi: 10.1002/14651858.CD003343.pub4.

Kell, D. B. and Young, M. (2000) 'Bacterial dormancy and culturability', *Current Opinion in Microbiology*, 3, pp. 238–243. Available at: http://www.sanger.ac.uk/Projects/Microbes/] (Accessed: 11 December 2019).

Kerantzas, C. A. and Jacobs, W. R. (2017) 'Origins of Combination Therapy for Tuberculosis: Lessons for Future Antimicrobial Development and Application', *American Society for Microbiology*, 8(2), pp. e01586-16. doi: 10.1128/mBio.01586-16.

Kim, H. *et al.* (2013) ' Evaluation of MGIT 960 System for the Second-Line Drugs Susceptibility Testing of *Mycobacterium tuberculosis* ', *Tuberculosis Research and Treatment*. Hindawi Limited, 2013, pp. 1–6. doi: 10.1155/2013/108401.

Kolwijck, E. *et al.* (2013) 'Short-Term Storage Does Not Affect the Quantitative Yield of *Mycobacterium tuberculosis* in Sputum in Early-Bactericidal-Activity Studies'. doi: 10.1128/JCM.02751-12.

Kolwijck, E. *et al.* (2014) 'Early stationary phase culture supernatant accelerates growth of sputum cultures collected after initiation of anti-tuberculosis treatment', *Clinical Microbiology and Infection*. doi: 10.1111/1469-0691.12441.

Lawn, S. D. and Nicol, M. P. (2011) 'Xpert® MTB/RIF assay: Development, evaluation and implementation of a new rapid molecular diagnostic for tuberculosis and rifampicin resistance', *Future Microbiology*, pp. 1067–1082. doi: 10.2217/fmb.11.84.

Lennon, J. T. and Jones, S. E. (2011) 'Microbial seed banks: the ecological and evolutionary implications of dormancy', *Nature Reviews Microbiology*, 9(2), pp. 119–130. doi:

10.1038/nrmicro2504.

Lewis, K. (2007) ‘Persister cells, dormancy and infectious disease’, *Nature Reviews Microbiology*, 5(1), pp. 48–56. doi: 10.1038/nrmicro1557.

Lewis, K. (2010) ‘Persister Cells’, *Annual Review of Microbiology*, 64(1), pp. 357–372. doi: 10.1146/annurev.micro.112408.134306.

Li, L. *et al.* (2014) ‘The importance of the viable but non-culturable state in human bacterial pathogens’, *Frontiers in Microbiology*, 5, p. 258. doi: 10.3389/fmicb.2014.00258.

Lönnroth, K. *et al.* (2010) ‘Tuberculosis control and elimination 2010–50: cure, care, and social development’, *The Lancet*. Elsevier, 375(9728), pp. 1814–1829. doi: 10.1016/S0140-6736(10)60483-7.

Mahomed, H. *et al.* (2011) ‘The Tuberculin Skin Test versus QuantiFERON TB Gold® in Predicting Tuberculosis Disease in an Adolescent Cohort Study in South Africa’, *PLoS ONE*. Edited by M. Pai. Public Library of Science, 6(3), p. e17984. doi: 10.1371/journal.pone.0017984.

Maisonneuve, E. and Gerdes, K. (2014) ‘Molecular Mechanisms Underlying Bacterial Persisters’, *Cell*, 157(3), pp. 539–548. doi: 10.1016/j.cell.2014.02.050.

Mangtani, P. *et al.* (2014) ‘Protection by BCG Vaccine Against Tuberculosis: A Systematic Review of Randomized Controlled Trials’, *Clinical Infectious Diseases*. Narnia, 58(4), pp. 470–480. doi: 10.1093/cid/cit790.

Mangtani, P. *et al.* (2018) ‘The duration of protection of school-aged BCG vaccination in England: a population-based case–control study’, *International Journal of Epidemiology*. Oxford University Press, 47(1), pp. 193–201. doi: 10.1093/ije/dyx141.

Marakalala, M. J. *et al.* (2016) ‘Inflammatory signaling in human tuberculosis granulomas is spatially organized.’, *Nature medicine*. NIH Public Access, 22(5), pp. 531–8. doi: 10.1038/nm.4073.

McCrady, M. H. (1915) ‘The numerical interpretation of fermentation-tube results’, *Journal of Infectious Diseases*, 17(1), pp. 183–212. doi: 10.1093/infdis/17.1.183.

McShane, H. (2011) ‘Tuberculosis vaccines: Beyond bacilli Calmette-Guérin’, *Philosophical Transactions of the Royal Society B: Biological Sciences*. Royal Society, pp. 2782–2789. doi: 10.1098/rstb.2011.0097.

Millet, J. P. *et al.* (2013) ‘Factors that influence current tuberculosis epidemiology’, *European Spine Journal*, 22(SUPPL.4). doi: 10.1007/s00586-012-2334-8.

Moore, D. F., Guzman, J. A. and Mikhail, L. T. (2005) ‘Reduction in turnaround time for laboratory diagnosis of pulmonary tuberculosis by routine use of a nucleic acid

amplification test', *Diagnostic Microbiology and Infectious Disease*, 52(3), pp. 247–254. doi: 10.1016/j.diagmicrobio.2005.02.014.

Mukamolova, G. V. *et al.* (1998) 'A bacterial cytokine', *Proceedings of the National Academy of Sciences of the United States of America*. National Academy of Sciences, 95(15), pp. 8916–8921. doi: 10.1073/pnas.95.15.8916.

Mukamolova, G. V., Turapov, O. A., Young, D. I., *et al.* (2002) 'A family of autocrine growth factors in *Mycobacterium tuberculosis*', *Molecular Microbiology*, 46(3), pp. 623–635. doi: 10.1046/j.1365-2958.2002.03184.x.

Mukamolova, G. V., Turapov, O. A., Kazarian, K., *et al.* (2002) 'The rpf gene of *Micrococcus luteus* encodes an essential secreted growth factor', *Molecular Microbiology*, 46(3), pp. 611–621. doi: 10.1046/j.1365-2958.2002.03183.x.

Mukamolova, G. V. *et al.* (2010) 'Resuscitation-promoting factors reveal an occult population of tubercle bacilli in sputum', *American Journal of Respiratory and Critical Care Medicine*, 181(2), pp. 174–180. doi: 10.1164/rccm.200905-0661OC.

Mukamolova, G. V *et al.* (2006) 'Muralytic activity of *Micrococcus luteus* Rpf and its relationship to physiological activity in promoting bacterial growth and resuscitation', 59, pp. 84–98. doi: 10.1111/j.1365-2958.2005.04930.x.

Nayak, S. and Acharjya, B. (2012) 'Mantoux test and its interpretation.', *Indian dermatology online journal*. Wolters Kluwer -- Medknow Publications, 3(1), pp. 2–6. doi: 10.4103/2229-5178.93479.

Nguipdop-Djomo, P. *et al.* (2015) 'Duration of BCG protection against tuberculosis and change in effectiveness with time since vaccination in Norway: A retrospective population-based cohort study', *The Lancet Infectious Diseases*. Elsevier Ltd, 16(2), pp. 219–226. doi: 10.1016/S1473-3099(15)00400-4.

Nikitushkin, V. D. *et al.* (2015) 'A product of RpfB and RipA joint enzymatic action promotes the resuscitation of dormant mycobacteria', 282, pp. 2500–2511. doi: 10.1111/febs.13292.

O'Connor, B. D. *et al.* (2015) 'Can resuscitation-promoting factors be used to improve culture rates of extra-pulmonary tuberculosis?', *International Journal of Tuberculosis and Lung Disease*. International Union against Tubercul. and Lung Dis., pp. 1556–1557. doi: 10.5588/ijtld.15.0682.

Pai, M. *et al.* (2014) 'Gamma interferon release assays for detection of *Mycobacterium tuberculosis* infection', *Clinical Microbiology Reviews*, 27(1), pp. 3–20. doi: 10.1128/CMR.00034-13.

Pai, M. *et al.* (2016) 'Tuberculosis', *Nature Reviews Disease Primers*, 2, pp. 1–23. doi: 10.1038/nrdp.2016.76.

Palaci, M. *et al.* (2007) 'Cavitary disease and quantitative sputum bacillary load in cases of pulmonary tuberculosis', *Journal of Clinical Microbiology*, 45(12), pp. 4064–4066. doi: 10.1128/JCM.01780-07.

Palomino, J. C., Leao, S. C. and Ritacco, V. (2007) *Tuberculosis 2007: from basic science to patient care*.

Pfyffer, G. E. and Edition, T. H. (2015) *Manual of Clinical Microbiology, Manual of Clinical Microbiology, 11th Edition*. doi: 10.1128/9781555817381.

Pilgrim, S. *et al.* (2003) 'Deletion of the gene encoding p60 in Listeria monocytogenes leads to abnormal cell division and loss of actin-based motility', *Infection and Immunity*, 71(6), pp. 3473–3484. doi: 10.1128/IAI.71.6.3473-3484.2003.

Ramakrishnan, L. (2012) 'Revisiting the role of the granuloma in tuberculosis', *Nature Reviews Immunology*, pp. 352–366. doi: 10.1038/nri3211.

Ramirez-Lapausa, M., Menendez-Saldana, A. and Noguerado-Asensio, A. (2015) 'Extrapulmonary tuberculosis: an overview', *Rev Esp Sanid Penit*, 17(1), pp. 3–11.

Rangaka, M. X. *et al.* (2014) 'Isoniazid plus antiretroviral therapy to prevent tuberculosis: a randomised double-blind placebo-controlled trial', *Lancet*, 384(9944), pp. 682–690. doi: 10.1016/S0140-6736(14)60162-8.

Rezwan, M. *et al.* (2007) 'Breaking down the wall: Fractionation of mycobacteria', *Journal of Microbiological Methods*, 68(1), pp. 32–39. doi: 10.1016/j.mimet.2006.05.016.

Ruggiero, A. *et al.* (2009) 'Crystal Structure of the Resuscitation-Promoting Factor Δ DUF RpfB from M . tuberculosis', *Journal of Molecular Biology*. Elsevier Ltd, 385(1), pp. 153–162. doi: 10.1016/j.jmb.2008.10.042.

Ruggiero, A., Squeglia, F., *et al.* (2010) 'Expression , Purification , Crystallization and Preliminary X-Ray Crystallographic Analysis of the Resuscitation Promoting Factor Interacting Protein RipA from M . tuberculosis', *Protein and Peptide Letters*, 17, pp. 70–73.

Ruggiero, A., Marasco, D., *et al.* (2010) 'Structure and Functional Regulation of RipA , a Mycobacterial Enzyme Essential for Daughter Cell Separation', *Structure/Folding and Design*. Elsevier Ltd, 18(9), pp. 1184–1190. doi: 10.1016/j.str.2010.06.007.

Russel, D. (2011) *'Mycobacterium tuberculosis* and the intimate discourse of a chronic infection', *Immunological Reviews*, 240(1), pp. 252–268. doi: 10.1111/j.1600-065X.2010.00984.x.

Ryu, Y. J. (2015) ‘Diagnosis of pulmonary tuberculosis: Recent advances and diagnostic algorithms’, *Tuberculosis and Respiratory Diseases*, 78(2), pp. 64–71. doi: 10.4046/trd.2015.78.2.64.

Said, H. M. *et al.* (2012) ‘Comparison between the BACTEC MGIT 960 system and the agar proportion method for susceptibility testing of multidrug resistant tuberculosis strains in a high burden setting of South Africa’, *BMC Infectious Diseases*, 12(1), p. 369. doi: 10.1186/1471-2334-12-369.

Saito, K. *et al.* (2017) ‘Rifamycin action on RNA polymerase in antibiotic-tolerant *Mycobacterium tuberculosis* results in differentially detectable populations’, *Proceedings of the National Academy of Sciences*, 114(24), pp. E4832–E4840. doi: 10.1073/pnas.1705385114.

Sassetti, C. M., Boyd, D. H. and Rubin, E. J. (2003) ‘Genes required for mycobacterial growth defined by high density mutagenesis’, *Molecular Microbiology*, 48(1), pp. 77–84. doi: 10.1046/j.1365-2958.2003.03425.x.

Schluger, N. W. and Rom, W. N. (1998) ‘State of the Art The host: Immune response to tuberculosis’, *Am J Respir Crit Care Med*, 157(19), pp. 679–691.

Scriba, T. J. *et al.* (2017) ‘Sequential inflammatory processes define human progression from M. tuberculosis infection to tuberculosis disease’, *PLoS Pathogens*, 13(11), pp. 1–24. doi: 10.1371/journal.ppat.1006687.

Setlow, P. (2007) ‘I will survive: DNA protection in bacterial spores’, *Trends in Microbiology*, 15(4), pp. 172–180. doi: 10.1016/j.tim.2007.02.004.

Setlow, P. (2014) ‘Resistance of Bacterial Spores’, in *Bacterial Stress Responses, Second Edition*. American Society of Microbiology, pp. 319–332. doi: 10.1128/9781555816841.ch18.

Shleeva, M. *et al.* (2004) ‘Formation of “non-culturable” cells of *Mycobacterium smegmatis* in stationary phase in response to growth under suboptimal conditions and their Rpf-mediated resuscitation’, *Microbiology*. Society for General Microbiology, 150(6), pp. 1687–1697. doi: 10.1099/mic.0.26893-0.

Shleeva, M. O. *et al.* (2002) 'Formation and resuscitation of ’ non-culturable ’ cells of *Rhodococcus rhodochrous* and *Mycobacterium tuberculosis* in prolonged stationary phase ', *Microbiology*, 148 (1), pp. 1581-91.

Siddiqi, S. *et al.* (2012) ‘Direct drug susceptibility testing of Mycobacterium tuberculosis for rapid detection of multidrug resistance using the bactec MGIT 960 system: A multicenter study’, *Journal of Clinical Microbiology*, 50(2), pp. 435–440. doi:

10.1128/JCM.05188-11.

Simmons, J. D. *et al.* (2018) 'Immunological mechanisms of human resistance to persistent *Mycobacterium tuberculosis* infection', *Nature Reviews Immunology*. Nature Publishing Group, pp. 575–589. doi: 10.1038/s41577-018-0025-3.

Smith, I. (2003) '*Mycobacterium tuberculosis* pathogenesis and molecular determinants of virulence.', *Clinical microbiology reviews*. American Society for Microbiology (ASM), 16(3), pp. 463–96. doi: 10.1128/CMR.16.3.463-496.2003.

Sohn, H. *et al.* (2014) 'Xpert MTB/RIF testing in a low tuberculosis incidence, high-resource setting: Limitations in accuracy and clinical impact', *Clinical Infectious Diseases*. Oxford University Press, 58(7), pp. 970–976. doi: 10.1093/cid/ciu022.

Squeglia, F. *et al.* (2013) 'Carbohydrate recognition by RpfB from *Mycobacterium tuberculosis* unveiled by crystallographic and molecular dynamics analyses', *Biophysical Journal*. Elsevier Ltd, 104(11), pp. 2530–2539. doi: 10.1016/j.bpj.2013.04.040.

Sun, J. *et al.* (2010) 'Mycobacterial Nucleoside Diphosphate Kinase Blocks Phagosome Maturation in Murine Raw 264.7 Macrophages', *PLoS ONE*. Edited by A. K. Tyagi. Public Library of Science, 5(1), p. e8769. doi: 10.1371/journal.pone.0008769.

Sun, Z. and Zhang, Y. (1999) 'Spent culture supernatant of *Mycobacterium tuberculosis* H37Ra improves viability of aged cultures of this strain and allows small inocula to initiate growth', *Journal of Bacteriology*, 181(24), pp. 7626–7628.

Telkov, M. V. *et al.* (2006) 'Proteins of the Rpf (resuscitation promoting factor) family are peptidoglycan hydrolases', *Biochemistry (Moscow)*, 71(4), pp. 414–422. doi: 10.1134/S0006297906040092.

Theron, G. *et al.* (2011) 'Evaluation of the Xpert MTB/RIF Assay for the Diagnosis of Pulmonary Tuberculosis in a High HIV Prevalence Setting', *American Journal of Respiratory and Critical Care Medicine*, 184(1), pp. 132–140. doi: 10.1164/rccm.201101-0056OC.

Thunnissen, A. M. W. H. *et al.* (1995) 'Structure of the 70-kDa Soluble Lytic Transglycosylase Complexed with Bulgecin A. Implications for the Enzymatic Mechanism', *Biochemistry*, 34(39), pp. 12729–12737. doi: 10.1021/bi00039a032.

Trunz, B. B., Fine, P. and Dye, C. (2006) 'Effect of BCG vaccination on childhood tuberculous meningitis and miliary tuberculosis worldwide: a meta-analysis and assessment of cost-effectiveness', *Lancet*. doi: 10.1016/S0140-6736(06)68507-3.

Tufariello, J. M., Jacobs, W. R. and Chan, J. (2004) 'Individual *Mycobacterium tuberculosis*

resuscitation-promoting factor homologues are dispensable for growth in vitro and in vivo.', *Infection and immunity*, 72(1), pp. 515–26. doi: 10.1128/iai.72.1.515-526.2004.

Volmink, J. and Garner, P. (2007) 'Directly observed therapy for treating tuberculosis', in Volmink, J. (ed.) *Cochrane Database of Systematic Reviews*. Chichester, UK: John Wiley & Sons, Ltd. doi: 10.1002/14651858.CD003343.pub3.

Vynnycky, E. and Fine, P. E. (1997) 'The natural history of tuberculosis: the implications of age-dependent risks of disease and the role of reinfection.', *Epidemiology and infection*. Cambridge University Press, 119(2), pp. 183–201. Available at: http://www.ncbi.nlm.nih.gov/pubmed/9363017 (Accessed: 28 March 2018).

WHO (2019a) *Global Tuberculosis Report 2019*.

WHO (2019b) *WHO consolidation guidelines on drug-resistant tuberculosiis treatment*. doi: 10.4103/ijmr.IJMR_579_19.

Wu, X. *et al.* (2008) 'Effect of recombinant Rv1009 protein on promoting the growth of *Mycobacterium tuberculosis*', *Journal of Applied Microbiology*, 105(4), pp. 1121–1127. doi: 10.1111/j.1365-2672.2008.03850.x.

Zak, D. E. *et al.* (2017) 'A prospective blood RNA signature for tuberculosis disease risk', *The Lancet*, 387(10035), pp. 2312–2322. doi: 10.1016/S0140-6736(15)01316-1.This.

Zhao, P. *et al.* (2014) 'Evaluation of BACTEC MGIT 960 system for testing susceptibility of *Mycobacterium tuberculosis* to first-line drugs in China', *PLoS ONE*, 9(9), pp. 1–5. doi: 10.1371/journal.pone.0099659.

Zhou, R., Chen, S. and Recsei, P. (1988) 'A dye release assay for determination of lysostaphin activity', *Analytical Biochemistry*, 171(1), pp. 141–144. doi: 10.1016/0003-2697(88)90134-0.

van Zyl-Smit, R. N. *et al.* (2011) 'Comparison of quantitative techniques including Xpert MTB/RIF to evaluate mycobacterial burden', *PLoS ONE*, 6(12). doi: 10.1371/journal.pone.0028815.